ANALYSIS OF LONG-TERM DURABILITY OF PRESTRESSED TENDONS IN SWEDISH NUCLEAR REACTOR CONTAINMENTS 2021

REPORT 2026:1207

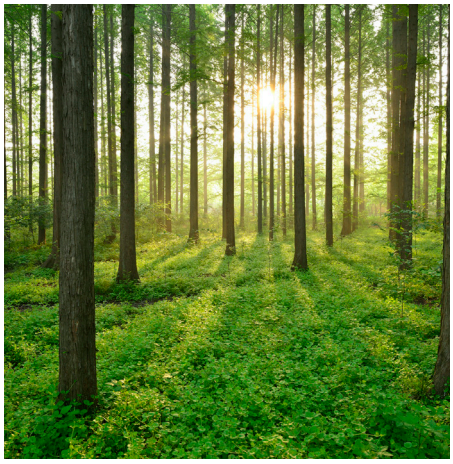

NUCLEAR POWER CONCRETE TECHNOLOGY

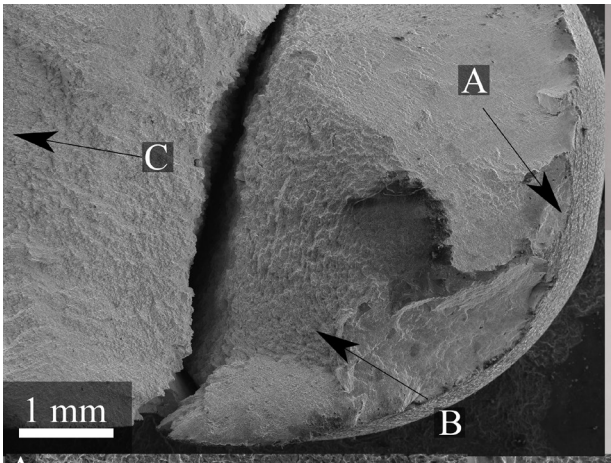

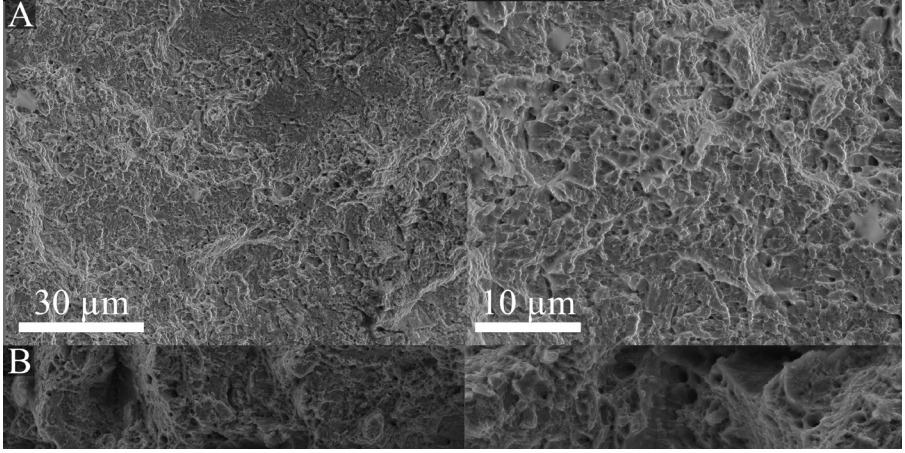

Energiforsk

Analysis of long-term durability of prestressed tendons

in Swedish nuclear reactor containments

JAN SUCHORZEWSKI, KONRAD TARKA, DIMITRIOS BOUBITSAS

ISBN 978-91-89917-50-7 | © Energiforsk July 2026

Energiforsk AB | Phone: 08-677 25 30 | E-mail: kontakt@energiforsk.se | www.energiforsk.se

Foreword

Prestressed tendons are essential load-bearing components in many nuclear power plant structures, contributing to structural integrity and safety over long service lives. Understanding their long-term durability is critical to ensure continued safe operation, ageing management, and compliance with regulatory requirements.

The purpose of this study is to investigate the long-term degradation mechanisms affecting prestressed tendons and to assess their performance under relevant environmental and operational conditions. The work aims to support improved evaluation methods and inform maintenance and inspection strategies for nuclear facilities.

The results show that tendon durability is influenced by a combination of material properties, environmental exposure, and protective system performance. The study concludes that with appropriate monitoring and maintenance, long-term functionality can be maintained, while highlighting key factors requiring particular attention to mitigate degradation risks.

This report forms the results of a project performed within the Energiforsk Nuclear Power Concrete Program, which is financed by Vattenfall, Uniper, Fortum, TVO, Skellefteå Kraft, Karlstads Energi, the Swedish Radiation Safety Authority and SKB. The Concrete Program aims to increase the knowledge of aspects affecting safety, maintenance and development of concrete structures in the Nordic nuclear power plants.

The study was carried out by Jan Suchorzewski, Konrad Tarka and Dimitrios Boubitsas, RISE.

Sammanfattning

Projektet analyserade en unik databas som samlats in i över 40 år av mekanisk provning av spännkablar, utförd inom ramen av fortlöpande inspektioner i svenska kärnreaktors inneslutningar. I det andra steget av projektet utfördes experiment av mekanisk prestanda, kemisk sammansättning och mikroskopisk analys av utvalda spännkablar för att validera resultaten från de statistisk analysen.

Arbetet i projektet omfattar följande:

• Statistisk analys av tillgängliga resultat från mekaniska provningar inklusive identifiering av trender för förändrade materialegenskaper.

• Bedömning av observerade trender beroende på spännkabelsystem, korrosionsskyddsteknik och trådorientering i strukturerna,

• Extrapolering av de observerade trenderna i ett försök att förutsäga framtida materialprestanda och jämföra med kraven på nytt stål,

• Litteraturstudie om åldringsprocessen av hårt kolstål
och nerbrytningsmekanismer som kan vara aktuella för spännarmeringen.

• Rekommendationer om utvidgad experimentellt program för att undersöka en del av de hypoteser som ställts fram inom projektets omfattning.

• Enaxiell dragprovning an spännkablar som togs ut 2020 och oanvända spännkablar,

• Analys av kemisk sammansättning av använda och oanvända spännkablar,

• Mikroskopanalys av brottytorna från dragprov och utmattningsprov samt tvärsnittsanalys med EDS av använt och oanvänt material.

Den statistiska analysen visade stor spridning i resultaten gällande stålets elasticitetsmodul. Detta gjorde det omöjligt att identifiera några tydliga trender. Resultaten för draghållfastheten *Fm* samt för 0,1%- och 0,2%-gränserna (F0,1 och F0,2), liksom gränstöjningen uppvisade små förändringar under den analyserade period och låg spridning. De enda tydliga trenderna som observerades var för sprödhet när man mätte brottöjning och omvänd dubbelbockningsprovning. Sprödhetsökningen var extremt signifikant för Forsmark 1 & 2 där VLS spännkablar används och torr luft son antikorrosiv åtgärd.

Jämförelse mellan aktuella resultat och resultat från tidigare Energiforsk-rapport visar att trenderna är de samma och därför kan extrapoleras.

Extrapolationen indikerar att den genomsnittliga brottförlängningen kommer att nå det ursprungliga standardkriteriet på 3% om 10 år för Ringhals och om 15 år för Forsmark 1 & 2.

Litteraturstudien indikerade att de möjliga fenomenen bakom den observerade sprödheten skulle kunna bero på olika typer av korrosion eller åldrande, såsom väteförsprödning eller försprödning p.g.a. strålning. Dessa processer sker mycket långsamt över tid och är därför svåra att upptäcka under naturliga förhållanden. Dessutom observerades några av dessa fenomen först efter byggnationen av de analyserade inneslutningarna och kan relateras till stålproduktionstekniken på 70-talet. Därför föreslogs ett experimentellt program som ett fortsättnings projekt för att klargöra vilka processer som kan ha orsakat den observerade sprödheten.

Av resultaten från den experimentella delen kunde inte den observerade trenden av ökat sprödhet förklaras. En resultatjämförelse mellan använda och oanvända spännkablar visade inga statistiskt säkerställda skillnader i materialprestanda. Kemiska- och mikroskopanalyser visade inga förändringar i materialets mikrostruktur eller kemiska sammansättning. Brottytorna karaktäriserades av typiska duktila brottmönster. Några mindre defekter (mikrosprickor och inneslutningar) upptäcktes både i de använda och oanvända spännkablar. Både den kemiskanalysen och SEM / EDS-analysen visade högt fosfor- och svavelinnehåll.

Rapporten avslutades med slutsatser, kommentarer och rekommendationer för eventuell framtida forskning inom området och praktiska råd för den framtida destruktiva provningen vid inspektioner.

Nyckelord

Spännkablar, statistisk analys, säkerhet, åldrande, sprödhet, reaktorinneslutningar, SEM, EDS,

Summary

The project analysed a unique database gathered over 40 years of destructive testing of prestressing tendons performed within interval technical evaluations in Swedish nuclear reactors containments. In the second stage of the project experiments on mechanical performance, chemical composition and the microscopic analysis of selected used and unused wires was performed to validate the findings of statistical analysis.

The project scope covered:

- Statistical analysis of the available results of mechanical tests including identifying trends of changing material properties and confidence intervals for the trends,
- Assessment of observed trends dependency on prestressing system, anti-corrosion protection technique and wires orientation in the structures,
- Extrapolation of the observed trends in attempt to predict future material performance and comparison with the requirements for new steel from original standards applied in Ringhals and Forsmark,
- Literature study on aging processes of hard carbon steel and the influencing factors, as well as similar degradation in other nuclear containments,
- Recommendations on an additional experimental programme to confirm or exclude some of the hypothesis built within the project scope,
- Uniaxial tensile test on wires extracted in 2020 and unused wires,
- Chemical composition analysis of used and unused steel,
- Microscopy analysis of the fracture surfaces from tensile test and reversed bend test as well as cross-section analysis with EDS of used and unused material.

The statistical analysis has demonstrated high results scatter within the steel modulus of elasticity which made it impossible to identify any clear trends. The results for tensile strength and elastic limits at 0,1 % and 0,2 % of elongation ($F_{0,1}$ and $F_{0,2}$), as well as, the elastic limit to ultimate tensile strength ratio exhibited minor and inconclusive changes over the analysed period with a low scatter. The only clear trends were observed for brittleness in ultimate elongation and in reverse bending test. The brittleness increase was extremely significant for Forsmark 1&2 where VLS tendons system was used, and dry air anti-corrosion system was applied.

Comparison between the current results with previous Energiforsk report[1] indicate that the trends are maintained and therefore could be extrapolated. The extrapolation indicates that in 10 years for Ringhals and in 15 years for Forsmark 1&2 the average ultimate elongation values will reach the original standard[2] criterium of 3%.

The literature study indicated that the possible phenomena behind the observed embrittlement could be related to different types of corrosion or ageing like hydrogen embrittlement or irradiation of steel. The overmentioned processes occur very slowly over time and therefore are difficult to capture in natural conditions. Moreover, some of them were first observed after construction of the analysed containments and could be related to the steel production technology in the 70'. Therefore, an experimental programme has been proposed as a subsequent project part to clarify which processes caused the observed embrittlement.

The results of the experimental part did not confirm the observed trends of increasing steel brittleness. The results obtained for used and unused wires did not indicate any statistically meaningful changes in material performance. Moreover, chemical and microscopy analysis did not indicate any changes in the material microstructure and chemical composition. The fracture surfaces were characterized with typical ductile failure pattern. Some minor defects (microcracks and inclusions) were detected both in the used and unused material. Secondly, both chemical and SEM/EDS analysis indicated high Phosphorus and Sulphur content.

The report was completed with conclusions, remarks and recommendations for possible future research within the area and practical implications concerning the future inspection destructive testing.

Keywords

Prestressing tendons, statistical analysis, safety, ageing, embrittlement, nuclear reactor containments, SEM, EDS,

[1] S.B. Westberg Long term stability of tendons and post tensioning wires - Effect on relaxation and mechanical properties, Energiforsk Report 2016:244.
[2] SS 14 17 57 Requirements for steel

List of content

1 Background and problem description 10

1.1 Background 10

1.2 Prestressing steel 10

1.3 Statistical anlysis methods 12

2 Sampling and testing procedures 13

2.1 Sampling procedure 13

2.2 Testing 13

3 Statistical data analysis 14

3.1 Uniaxial Tensile test 14

3.1.1 Modulus of elasticity E 15

3.1.2 Ultimate tensile strength F_m 15

3.1.3 Elastic-plastic ratio $F_{0.2}/F_m$ 17

3.1.4 Ultimate elongation ε_g 18

3.2 Reversed bend test 26

4 Literature study on hard steel degradation 31

4.1 Stressors Affecting the Prestressing Steel 31

4.1.1 Corrosion 31

4.1.2 Elevated temperature 34

4.1.3 Irradiation 34

5 New experimental results 35

5.1 Mechanical tests 35

5.1.1 Samples and methods 35

5.1.2 Results obtained by RISE 38

5.1.3 Results obtained by Vattenfall 42

5.1.4 Conclusions 44

5.2 Chemical analysis 44

5.2.1 Samples and method 44

5.2.2 Results 45

5.3 Microcsopic ANALYsis with SEM and EDS 46

5.3.1 Theoretical background 46

5.3.2 SEM investigation of samples 47

5.3.3 Investigation of corrosion indicators 47

5.3.4 Results 48

5.3.5 Cross sections and EDX analysis of same 53

5.3.6 Analysis after hydrogen exposure and bend test 55

6 Conclusions and future research 61

7 Appendix 1 – raw data used for the statistical analysis 65

7.1 Ringhals 2 – Tensile test 65

7.2	Ringhals 2 – reversed bend test	69
7.3	Ringhals 3 – tensile test	71
7.4	Ringhals 3 – Reversed bend test	74
7.5	Ringhals 4 – tensile test	76
7.6	Ringhals 4 – Reversed bend test	79
7.7	Forsmark 1 – tensile test	81
7.8	Forsmark 2 – tensile test	83
7.9	Forsmark 3 – tensile test	86
7.10	Forsmark 3 – Reversed bend test	90

1 Background and problem description

Sweden owns 7 nuclear reactors producing 34%[3] of country's electricity supply. The safety of nuclear containments under accidental load depends on the prestressing system confining concrete walls and domes. A monitoring method to ensure constant prestress level and detect corrosion based on measurements with hydraulic jacks during which samples analysed in this project are being extracted is used periodically. Nevertheless, the most reliable method of the tendons condition evaluation is destructive mechanical testing in lab environment. The testing has been performed constantly over 40 years in Swedish nuclear plants.

1.1 BACKGROUND

Safety and reliability are crucial requirements for all kinds of structures from single-family dwellings to large infrastructure objects. However, they are even more sensitive aspects for nuclear power plants due to high risk and pressure of public opinion. In case of a serious reactor core malfunction or breakdown the main barrier preventing the spread of radioactive substances is the reactor containment. In many nuclear power plants, all around the world[4,5,6] including those in Sweden[1] and Finland[7] the containments are made of prestressed concrete to ensure the high level of concrete confinement, prevent cracking, and grant the barriers tightness. Therefore, the critical element determining the resilience of the overmentioned solution are the prestressing tendons.

1.2 PRESTRESSING STEEL

Prestressing steel is a high-quality alloy with high carbon content increasing its tensile strength and brittleness[8,9,10] but also with aim of granting low relaxation and creep to diminish the prestressing force losses[11]. Also, special treatments in the

[3] https://pris.iaea.org/pris/CountryStatistics/CountryDetails.aspx?current=SE
[4] Naus D.J., Oland C.B., Ellingwood, B.R, (1996) Report on Aging of Nuclear Power Plant Reinforced Concrete Structures. The John Hopkins University.
[5] Kellet et al. U.S. Patent 3,935,062 (1976) Nuclear Power Plant with a Safety Enclosure.
[6] NEA/CSNI/R(2015)5 (2015) Bonded or Unbonded Technologies for Nuclear Reactor Prestressed Concrete Containments. Nuclear Energy Agency Committee on the Safety of Nuclear Installations.
[7] GUIDE YVL E.6 Building and Structures of a Nuclear Facility (2013) Finish Radiation and Nuclear Safety Authority (STUK)
[8] Münstermann, S., Feng, Y. and Bleck, & W. (2014) 'Influencing parameters on elastic modulus of steels', *Canadian Metallurgical Quarterly*, 53(3), pp. 264–273. doi: 10.1179/1879139514Y.0000000127.
[9] Youb Han, S. *et al.* (no date) 'Effect of Carbon Content on Cracking Phenomenon Occurring during Cold Rolling of Three Light-Weight Steel Plates'. doi: 10.1007/s11661-010-0456-3.
[10] Bae, C. M., Lee, C. S. and Nam, W. J. (2013) 'Materials Science and Technology Effect of carbon content on mechanical properties of fully pearlitic steels Effect of carbon content on mechanical properties of fully pearlitic steels'. doi: 10.1179/026708302225007556.
[11] Sundar, R. S. and Deevi, S. C. (2003) 'Effect of carbon addition on the strength and creep resistance of FeAl alloys', *Metallurgical and Materials Transactions A 2003 34:10*, 34(10), pp. 2233–2246. doi: 10.1007/S11661-003-0287-6.

production process (cold-drawing and patenting) increase the tensile strength of prestressing steel. Even though, the prestressing steel is much less prone to rheological phenomena that mild steel, the prestress losses are inevitable for post-tensioned prestressed concrete structures also due to concrete drying shrinkage and creep. The task of design engineers is to minimize these losses and correctly calculate them to plan tendons re-tensioning if needed. Moreover, the tendons subjected to various stress states might be sensitive to fatigue, and therefore, lower their tensile strength over time.

High carbon alloys have sufficient ductility if the ratio between ultimate tensile strength and the yield strength is greater than 1.1[12], but still are usually more brittle[10] than the regular reinforcing steel, which brings an undesired risk of unsignalized failure of the structures strengthened with those materials. The standards[12] greatly limit (by 25 %) the maximum prestressing force to be applied on tendons or wires in respect to the material theoretical strength to minimize the effects of relaxation and ensure quasi-plastic failure. Even thou, the standards require certain quasi-plastic behaviour of wires before rupture[13] with a minimum value of ultimate elongation to ensure minimal safety margin in case of accidental catastrophic load. The brittleness of the steel might be affected not only by its original composition and manufacturing process but also due to environmental conditions and certain strain levels or combination of the two. These aspects were described in detail in the literature review part.

In the Swedish nuclear reactors containments two types of prestressing systems were implemented: the VSL 19 Ø13 mm, 7-wire strands (Forsmark 1&2) and BBRV, 139 Ø6 with individual wires. BBRV, 139 Ø6, individual wires (Ringhals and Forsmark 3) (Table 1). Moreover, two different corrosion protection systems were used. In Forsmark a dry air provided by ventilation system and protection grease cover in Ringhals.

Table 1 Tensioning and corrosion protection systems in respect to the analyzed reactor containments

Reactor	Operation	Type	Tensioning system	Corrosion protection
Forsmark 1	1980	BWR	VSL	Dry air
Forsmark 2	1981	BWR	VSL	Dry air
Forsmark 3	1985	BWR	BBRV	Dry air
Ringhals 2	1975-2019	PWR	BBRV	Grease
Ringhals 3	1981	PWR	BBRV	Grease
Ringhals 4	1983	PWR	BBRV	Grease

[12] Standard 1992-1-1:2005 Eurocode 2: Design of concrete structures – Part 1-1: General rules and rules for buildings. 2005
[13] Standard SS 14 17 57 Stål för spännarmering av betong. 1987

1.3 STATISTICAL ANLYSIS METHODS

The most used statistical analysis method for homogeneous datasets is normal Gaussian distribution characterized with a symmetrical distance from mean value with the results scatter. However, for limited number of measurements a quasi-normal (Student's t-distribution) is used, as the population of samples is not statistically reliable. the first part of the performed data analysis mean values, sample standard deviations and coefficients of variation were calculated to access the statistical reliability of the trends.

For data characterized with normal distribution or quasi-normal (Student's t-distribution) a percentage of results within the dataset can be calculated with a certain probability. For this distribution the estimated mean value is calculated as:

$$\bar{X} = \frac{1}{n}\sum_{i=1}^{n} X_i \qquad \textbf{[Eq 1]}$$

Where X_i is an individual measurement and n is the population size. Whereas the estimated standard deviation S is calculated as follows:

$$\boldsymbol{S = \sqrt{\frac{1}{n-1}\sum_{i=1}^{n}(X_i - \bar{X})^2}} \qquad \textbf{[Eq 2]}$$

Secondly, the reliability of the trends was assessed by confidence intervals (CI). It was referred to each performed test result. The confidence interval is calculated as:

$$\boldsymbol{CI = \bar{X} \pm Z_{\frac{\alpha}{2}} \frac{S}{\sqrt{n-1}}} \qquad \textbf{[Eq 3]}$$

where $\bar{X}$ is the mean value ($\bar{X} = \frac{1}{n}\sum_{i=1}^{n} X_i$ **[Eq 1]**), Z is a value dependent on the desired confidence value level obtained from integration of area under the normal distribution curve (Figure 1) (for CI of 95 % Z = 1.96), the α-value is also dependent on the CI $\alpha = \frac{1-CI}{2}$ (for CI of 95 % α = 0.025), and S is an estimated standard deviation ($\boldsymbol{S = \sqrt{\frac{1}{n-1}\sum_{i=1}^{n}(X_i - \bar{X})^2}}$ [Eq 2).

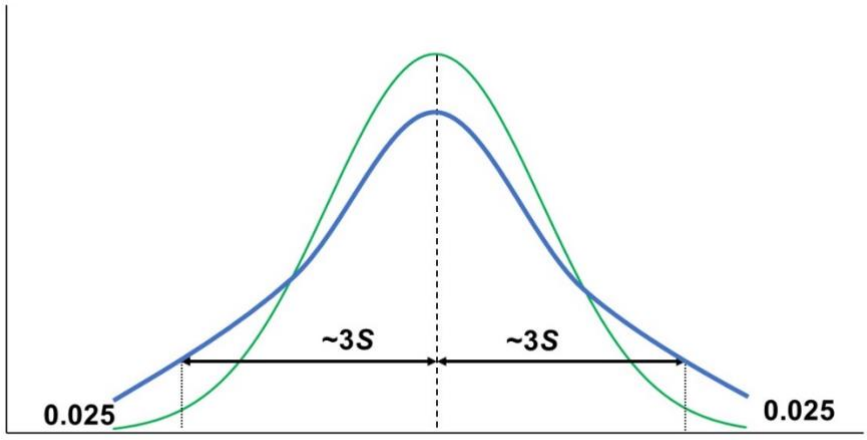

Figure 1 The scheme of Gaussian distribution curve (green) and Student's t-distribution (blue), with marked mean value (dash line) and 95% confidence interval area, within 3 standard deviations of a sample (*S*).

2 Sampling and testing procedures

The strands from two or three different tendons were extracted from containments in Ringhals and Forsmark approximately every 5 years and subjected to uniaxial tensile test and reversed bend test.

2.1 SAMPLING PROCEDURE

Extraction of samples was performed according to the American code Boiler and pressure vessel code ASME, section IWL 2523.2[14] stating that:

1. Each removed wire or strand shall be examined over its entire length for corrosion and mechanical damage. The examination shall determine the location of the most severe corrosion, if any. Strand wires shall be examined for wedge slippage marks.
2. Tension test shall be performed on each removed wire or strand: one at each end, one at mid-length, and one in the location of the most corroded area, if any.

The standards also list the expected information obtained in tensile test as: yield strength, ultimate tensile strength, and ultimate elongation.

The extraction of wires in Ringhals and Forsmark has been performed by the same company over years. From Ringhals extraction reports the requirement for the maximum dragging force during extraction is 30 kN, however on average only 15 kN has been achieved.

After extraction, the wires were cut and prepared for testing and microscopic investigation by Vattenfall R&D lab in Älvkarleby.

2.2 TESTING

The extracted samples were subjected to three types of examination:

1. Uniaxial tensile test according to the Swedish standard SS 11 21 38[15].
2. Reverse bending test according to SS 11 26 22[16]. The test was performed for three types of samples from each wire: in original state, subjected to hydrogen for 4 h and subjected to hydrogen for 24 h.
3. Metallographic examination by means of stereomicroscope.

The original reports were not available to the Authors of this report, but the requested raw data has been extracted for the presented statistical analysis. Therefore, the Authors have assumed that all the standards requirements were followed, the data was not subjected to systematic errors and the observed changes have purely statistical and phenomenological nature.

[14] The American Society of Mechanical Engineers (ASME) Boiler and Pressure Vessel Code, Section XI
[15] Standard SS 11 21 38
[16] Standard SS 11 26 22

3 Statistical data analysis

This chapter presents the statistical analysis of the experimental data from Forsmark and Ringhals. In cases of identified trends, a linear regression lines were derived from the data set. Secondly, a confidence interval of 95 % was calculated. The trends were assessed as statistically meaningful when the average change of the measured material property was at least greater than the measurement confidence interval.

3.1 UNIAXIAL TENSILE TEST

The first and most extensive data set in presented analysis concerns uniaxial tensile test. Depending on the prestressing system used some measured parameters differ. For all wires, the values of ultimate tensile force F_m, ultimate elongation ε_g and modulus of elasticity E were measured. For Forsmark 1&2 where VSL 7-wire strands system was used additionally force at 1 % elongation $F_{1.0}$ was measured, while for Forsmark 3 and Ringhals where BBRW single strand system was applied force at 0.2 % elongation $F_{0.2}$ was registered. For the second case additionally a ratio of $F_{0.2}/F_m$ was calculated. A typical force-strain curve from the tests was depicted at Figure 2.

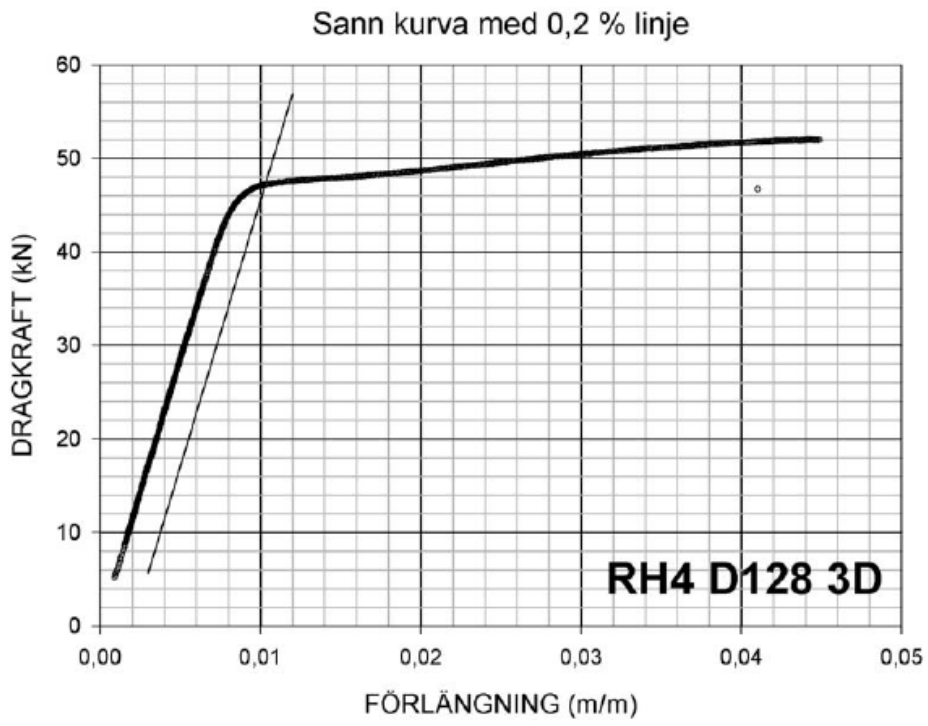

Figure 2 Typical Force (Dragkraft) – strain (Förlägning) curve from Ringhals 4 test in 2010.

3.1.1 Modulus of elasticity E

The results on the modulus of elasticity for all containments together were presented at Figure 3 in function of service life. The results are characterized with a very large scatter varying between 150 GPa and 220 GPa. The scatter is the highest for Forsmark 1&2 where entire strands have been tested (VSL system). The structure of the strands with 7 wires could be one of the main factors causing larger scatters. In other containments the scatters can be related to the wires extraction process. Neither in the whole dataset, nor in individual containments statistically meaningful trends could be identified. Moreover, there are no requirements in the used standards concerning the modulus of elasticity values to be fulfilled.

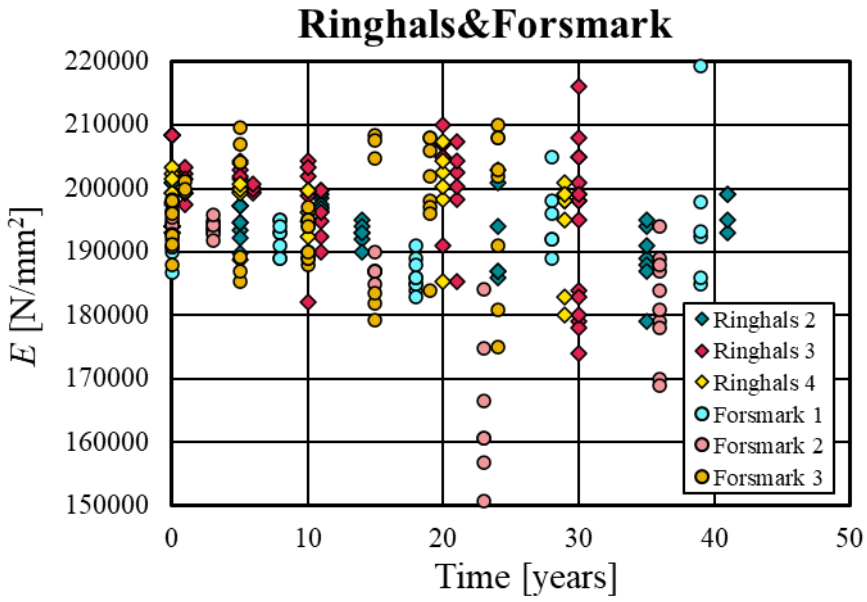

Figure 3 Results of elastic modulus in function of service life for all analyzed containments.

3.1.2 Ultimate tensile strength F_m

The initial difference in the ultimate tensile strength is related to different tendons system with different wires cross-sections. Therefore, the ultimate tensile strength has been compared only within each tendon type. The average coefficient of variation for F_m for all the containments was *COV*=1.9 %, which indicates low variability. However, the weak trends are within the measurement uncertainty and cannot be treated as statistically meaningful. The coefficients of variation for respective containments are presented in Table 2. The *COV* varied between 1.4 % for Ringhals 3 to 2.4 % for Forsmark 2. No clear difference between the variability of VLS and BBRV systems was observed.

Table 2 Coefficient of variation for each containment

Containment	Prestressing system	*Fm*	
		Mean value [kN]	COV [%]
Ringhals 2	BBRV	50.56	2.0
Ringhals 3	BBRV	51.12	1.4
Ringhals 4	BBRV	51.46	2.1
Forsmark 1	VSL	188.40	2.0
Forsmark 2	VSL	187.67	2.4
Forsmark 3	BBRV	50.53	2.1

The minimum requirements for new steel (marked with red dashed lines at Figure 4) were not fulfilled for some individual samples, however the mean values within each testing series where above the required original values apart from Forsmark 2 in 2003, where six out of eight measured values were below the requirement. Secondly, the required ultimate tensile strength was increased between ’86 an ’89. That change resulted in about 40 % of results for Ringhals and Forsmark 3 below the new required values.

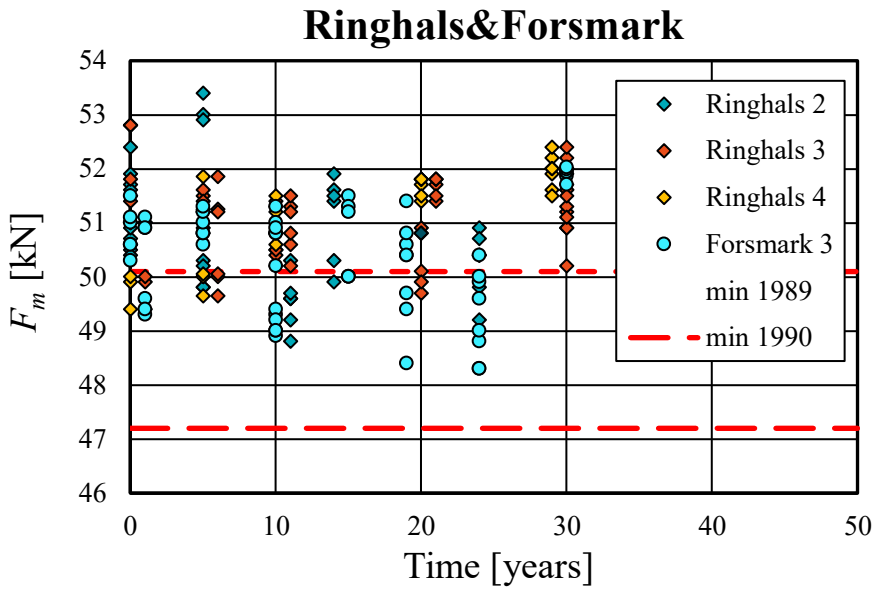

a)

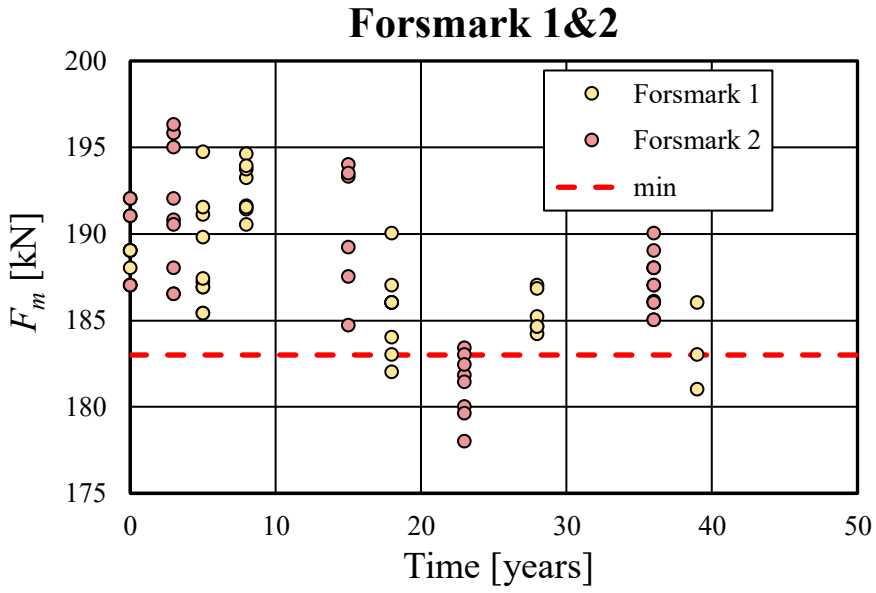

b)

Figure 4 Ultimate tensile strength Fm in function of service life for a) Ringhals and Forsmark 3 (with BBRV single strands system) and b) Forsmark 1&2 (with VSL 7-wire strands). The red dashed line indicates the minimum value required by standard Stål 14 17 57 Stål för spännarmering (fine dashed line from 1973 and large dashed from 1987).

3.1.3 Elastic-plastic ratio $F_{0.2}/F_m$

The ratio of force at 0.2% strain (at the end of linear elastic relation) to ultimate tensile strength expresses the brittleness at failure and therefore is limited in the applied standard to 0.85. The standard requirement was not fulfilled for some individual Forsmark 3 and a few Ringhals tendons, however the mean values were always above the limit. Due to high results scatter no statistically meaningful

trends were identified. Figure 5 presents all the elastic-plastic ratio results in function of service life.

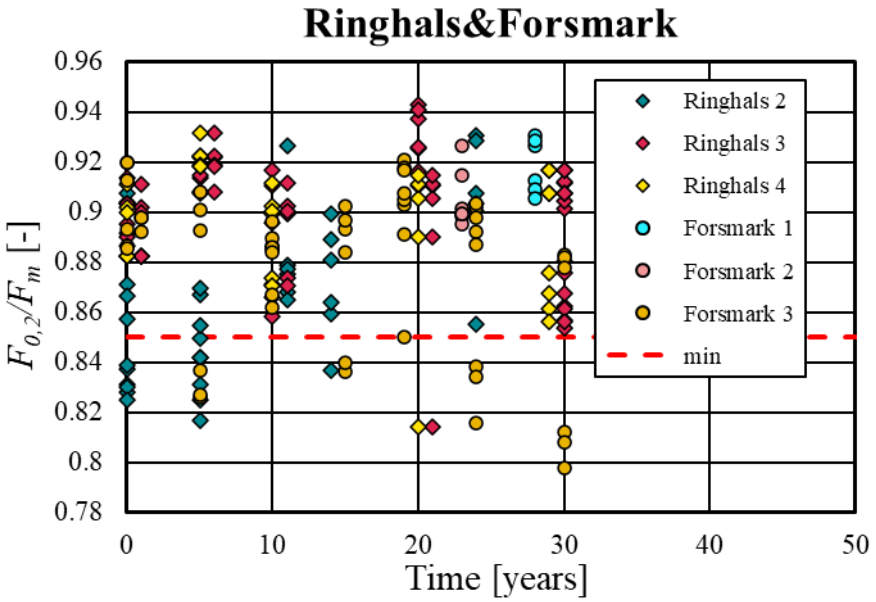

Figure 5 The limit of proportionality in function of service life for all the containments. The red dashed line indicates the minimum value required by standard.

3.1.4 Ultimate elongation ε_g

High carbon content steel, like prestressing steel, are characterized with very high strength and low ductility comparing to regular reinforcing steel. Therefore, the ultimate elongation is one of the crucial properties for hard steel as it expresses the spare deformation after reaching ultimate tensile strength which could be directly related to reliability of the structure and signalized failure required by design standards[17] and structural engineering practice. In the analyzed dataset the decrease of the ultimate elongation value is the most pronounce and clearly significant from statistical perspective (Figure 6). Moreover, the most recently tested samples from Ringhals do not fulfill the standard requirement of minimum 3.5%.

[17] EN-1992-1-1:2005 Eurocode 2: Design of concrete structures – Part 1-1: General rules and rules for buildings. European committee for standardization, Brussels 2005

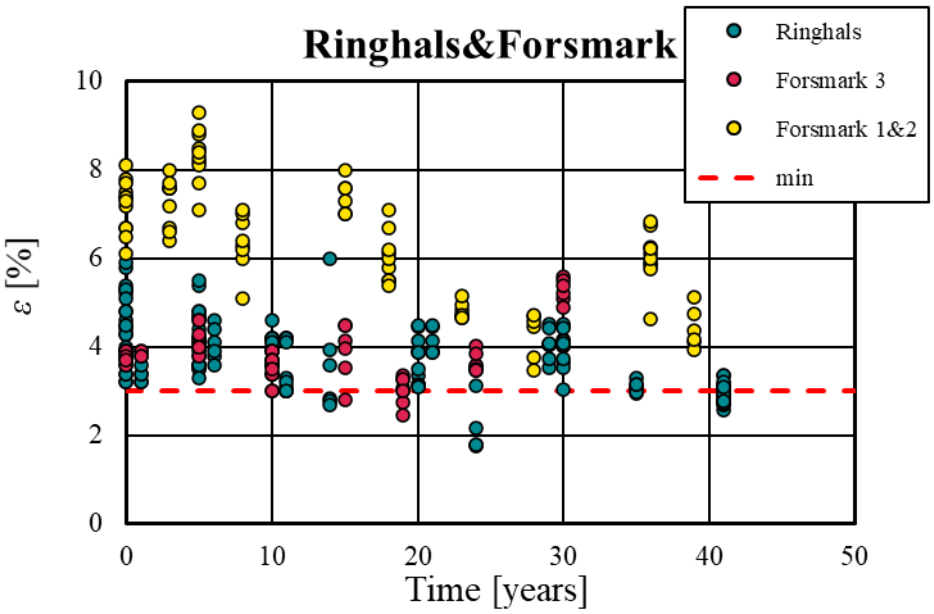

Figure 6 Ultimate elongation ε_g in function of service life for all the analyzed containments. The red dashed line indicates the minimum value required by standard "Stål 17 57. Stål för spännarmering" from 1973

As the observed general trends concerning the decrease of ultimate elongation are clear, the dataset was split into several subgroups (single containments, tendons type, tendons orientation) and analyzed more precisely separately.

Tendons embrittlement by containments

At first the results were split into separate plants. In the Ringhals dataset as a whole a decreasing trend was observed. The average ultimate elongation decreased from 4.6 % in the first tests to nearly 3 % in the latest once (Figure 7) which is below the required by the standard 3.5 %. In Gaussian normal distribution usually more than 95% of results are within ±3 times standard deviation σ from the mean value. This measure was used to analyze the observed trend globally. In case of Ringhals the average standard deviation was equal to σ=0.36 %. Which means that the decrease of the mean value from 4.6 % to 2.9 % (by 1.7 %) is statistically meaningful (higher than 3σ=1.1 %). Moreover, the mean value of the linear regression has crossed the standard minimum requirement of 3.5 % after around 35 years of exploitation.

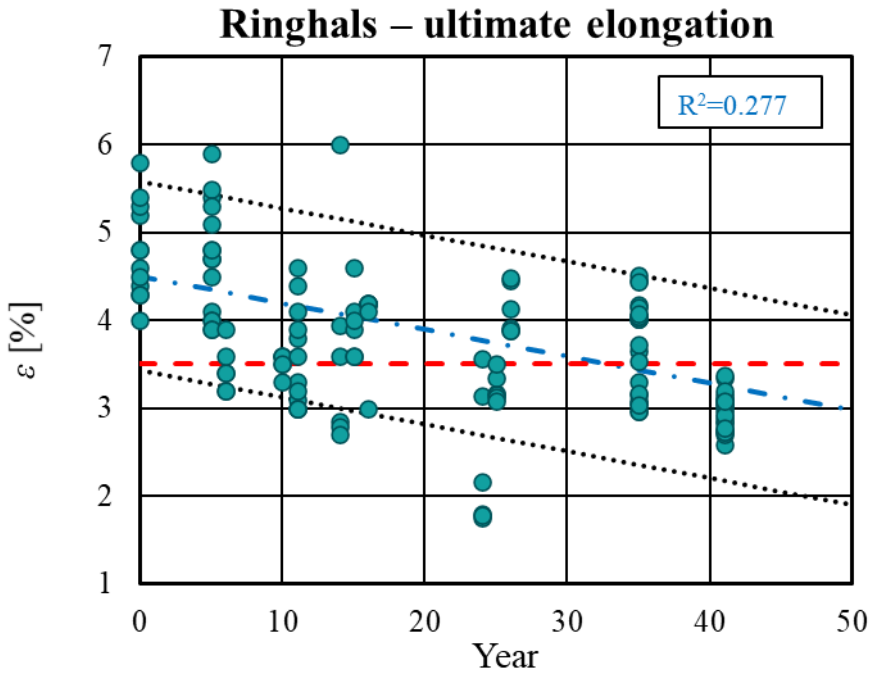

Figure 7 Ultimate elongation in all Ringhals containments in function of service life with dashed blue linear regression line and dotted lines indicating 3 times average standard deviation for the whole dataset. The red dashed line indicates the minimum value required by standard.

Secondly, the data was split into separate containments for more precise analysis. This time also the data dispersion within single tests was considered by means of varying confidence interval CI=95 %, which means that 95 % of results calculated basing on the confidence interval are within the range of CI. The criterium used for determination of statistically meaningful trends used in this report is the ratio of mean value to confidence interval of 95 % greater than one, which means that the probability of the trend is equal to at least 95 %.

Analyzing Ringhals 2 containment the average ultimate elongation has decreased from 4.6 % in 1975 to only 3.0 % in 2016, while the respective confidence intervals were $CI_{95\%}$ = 0.90 % and $CI_{95\%}$ = 0.68 % (Figure 8a). The change of the mean value by 1.6 % is greater than the confidence intervals, which makes the observed trend statistically meaningful. Moreover, the values of the ultimate elongation from 1986 onwards were below the standard minimum requirement of 3.5 %.

For Ringhals 3 the change of the mean value from 4.2 % to 3.6 % (by 0.6 %) is lower than the confidence interval $CI_{95\%}$ = 1.7 % and 0.9 % (Figure 8b), which means that the trend is not statistically meaningful. Therefore, the observed variation may have purely statistical character. Moreover, the confidence interval analysis exhibited that it is statistically probable that the true value is below the standard requirement of 3.5 % for the last measurement in 2016 (lower bound of confidence interval at 2.7 %).

Similarly, for Ringhals 4 the ascending trend of the mean values from 3.7 % in 1981 to 4.2 % in 2010 (change by 0.5 %) falls within the statistical distribution of 95% confidence interval (0.4-0.8 %) (Figure 8c). For Ringhals 4 the lower limit of CL of

95 % is over the standard requirement of 3.5 % for the last measurement from 1990 onwards, which indicated that the true value is higher than requirement.

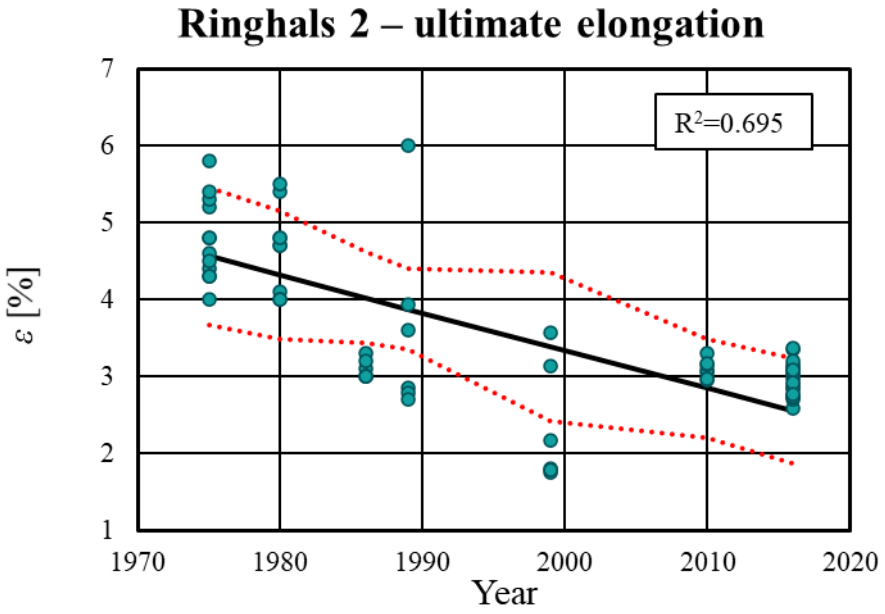

a)

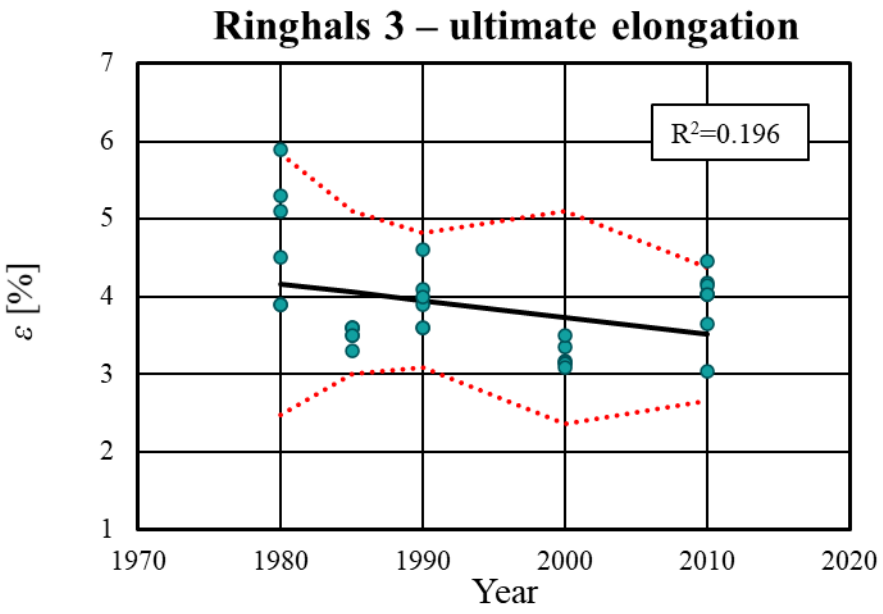

b)

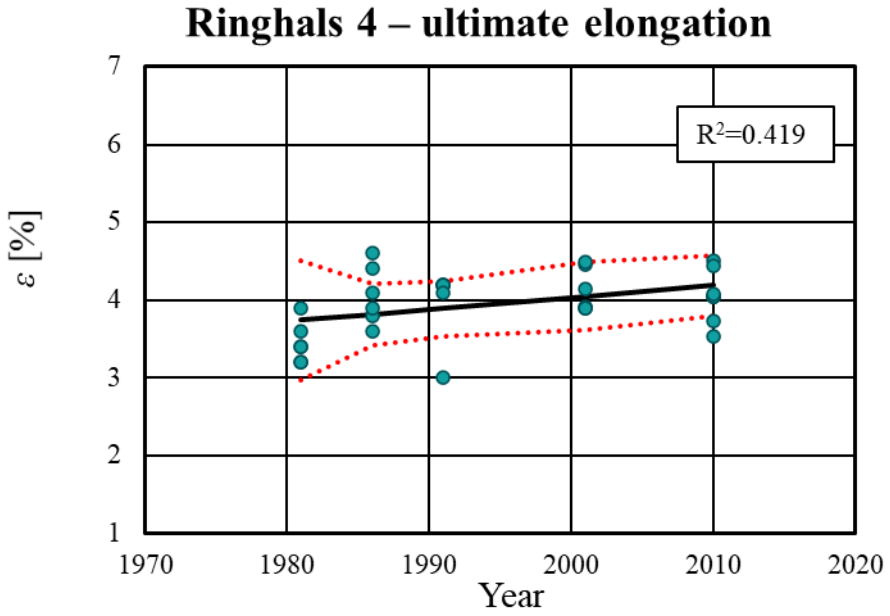

c)

Figure 8 Ultimate elongation in function of testing year for a) Ringhals 2, b) Ringhals 3 and c) Ringhals 4 containment. Black solid line represents linear regression and red dotted lines represent confidence interval of 95%.

The results for Forsmark containments were generally divided into two groups: (1) Forsmark 1&2 where the VSL 7-wire strands system was used and (2) Forsmark 3 where the BBRV single strands system was applied. It is clearly visible that both systems exhibited completely different behavior in terms of ultimate elongation evolution over time (Figure 9). For Forsmark 1&2 a clear decreasing trend from initial value of 7.6 % down to 4.7 % after 40 years occurred. A simplified analysis of 3 times the mean standard deviation for the whole data population indicated with black dashed lines at Figure 9 presents the meaningfulness of the linear trend. Even thou the decrease in ultimate elongation was great (nearly 3 %) it did not exceed the required limit of 3.5 %. However, if the linear trend would be maintained in the future (linear extrapolation indicated by the blue dashed line at Figure 9) within the next 15-20 years the mean value will decrease below the standard requirement. For the BBRV system there is no clear trend. The values measured for Forsmark 3 are partially below the standard requirement.

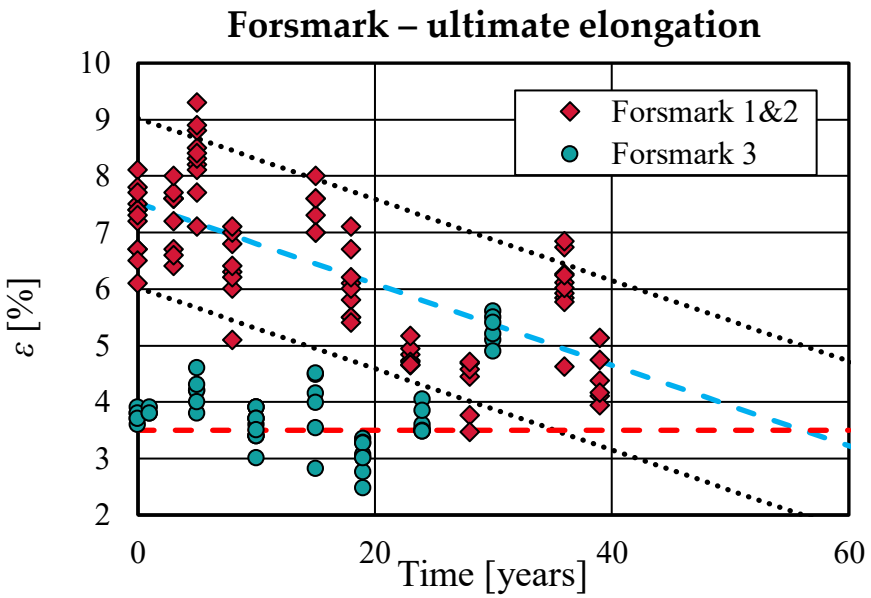

Figure 9 Ultimate elongation in all Forsmark containments in function of service life with dashed blue linear regression line and dotted lines indicating 3 times average standard deviation for the whole dataset. The red dashed line indicates the minimum value required by standard.

The detailed analysis of Forsmark 1&2 including the confidence interval confirms the strong decreasing trend (by 3.5 % For Forsmark 1 and 2.0 % for Forsmark 2) greater than the confidence interval $CI_{95\%}$ = 1.1 and 1.8 % respectively (Figure 10a&b). The confidence interval is also stable over the time changing between 1.1 % and 1.8 %, which indicates stable results scatter related to natural scatters in experimental tests and random distribution of material properties.

The increasing trend observed for Forsmark 3 (from 3.8 % in 1986 to 4.2 % in 2016) falls within the growing confidence interval $CI_{95\%}$ = 0.8-2.1 % (Figure 10c) and is not meaningful from statistical point of view.

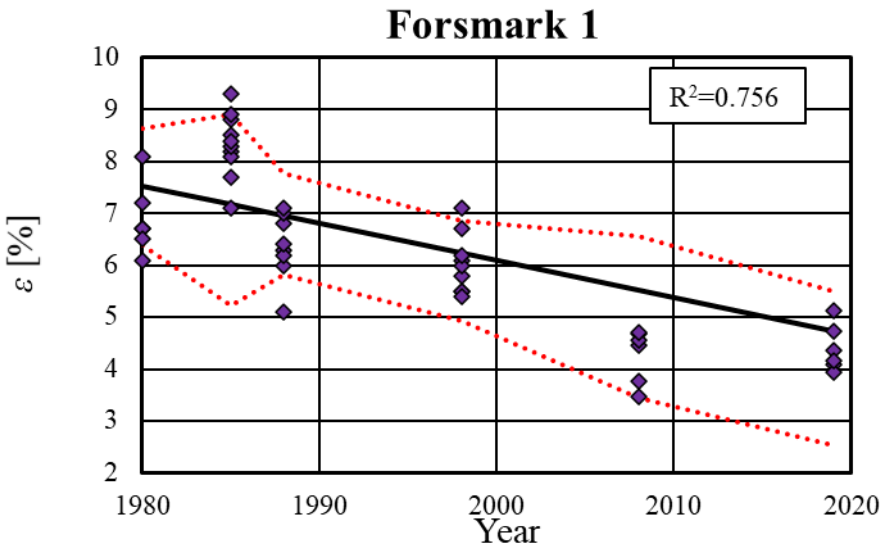
Forsmark 1
R²=0.756
ε [%]
Year
10
9
8
7
6
5
4
3
2
1980
1990
2000
2010
2020

a)

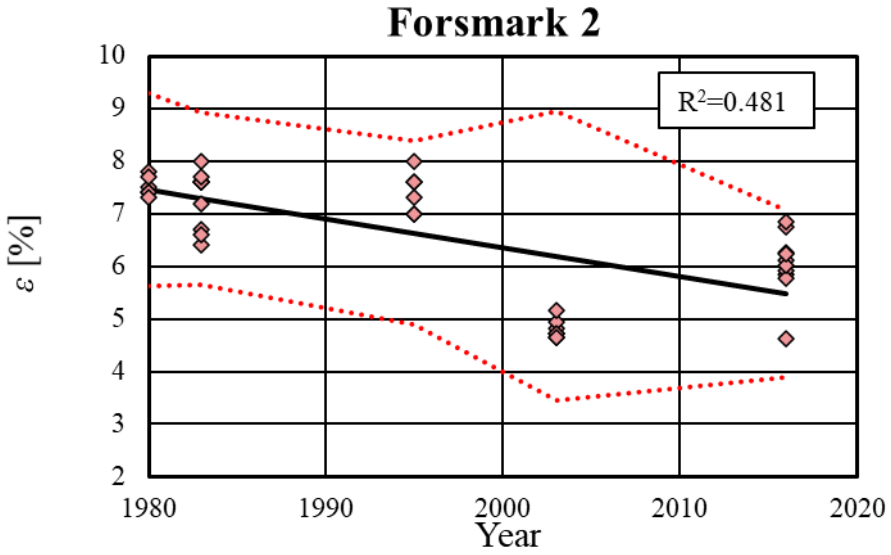
Forsmark 2
R²=0.481
ε [%]
Year
10
9
8
7
6
5
4
3
2
1980
1990
2000
2010
2020

b)

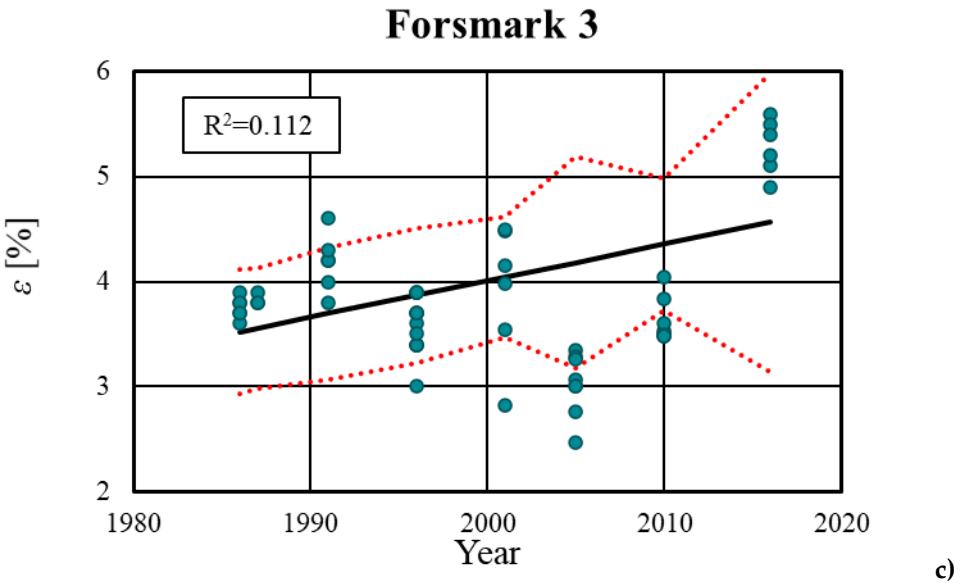

Figure 10 Ultimate elongation in function of testing year for a) Forsmark 1, b) Forsmark 2 and c) Forsmark 3 containment. Black solid line represents linear regression and red dotted lines represent confidence interval of 95%.

Tendons embrittlement by orientation

The tendons were extracted from 3 different orientations/elements in the containments: horizontal, vertical and dome. The results were divided by tendons orientation in the containment to check if it was relevant for the embrittlement. As most of the available results for Forsmark containments were marked only with the number of the tendon without indication of the orientation, only the results for Ringhals were analyzed.

The results for tensile strength did not exhibit statistically meaningful trends both for horizontal and dome tendons (Figure 11a). However, even in analysis of pure linear regression no significant difference in tensile strength was observed, as the horizontal tendons mean value changes between 50.5 MPa and 50.8 MPa, while for dome tendons the mean value changes between 51.4 MPa and 50.5 MPa (Figure 11a). Similarly for ultimate elongation values the linear regressions for horizontal and dome tendons have very similar decreasing characteristic, 4.4 % down to 3.3 % for horizontal tendons, and 4.5 % to 3.0 % for dome.

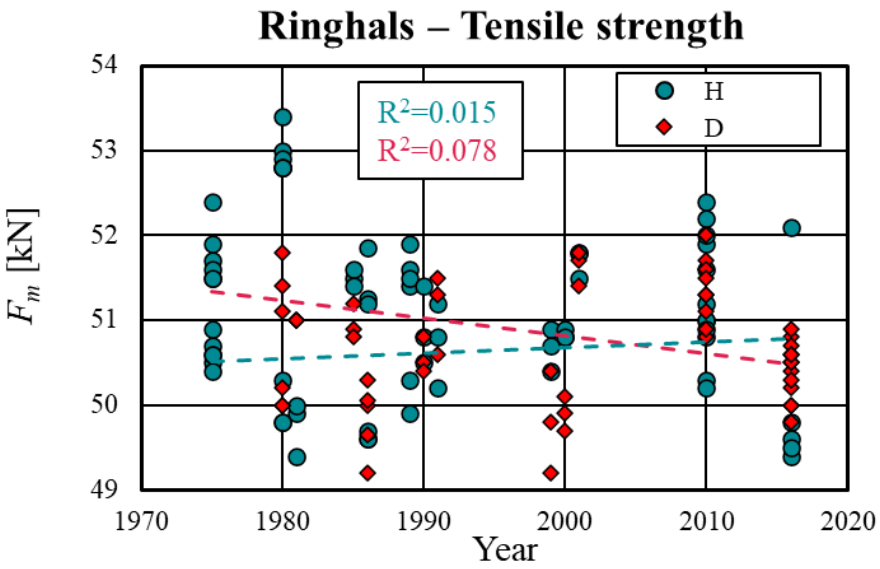

a)

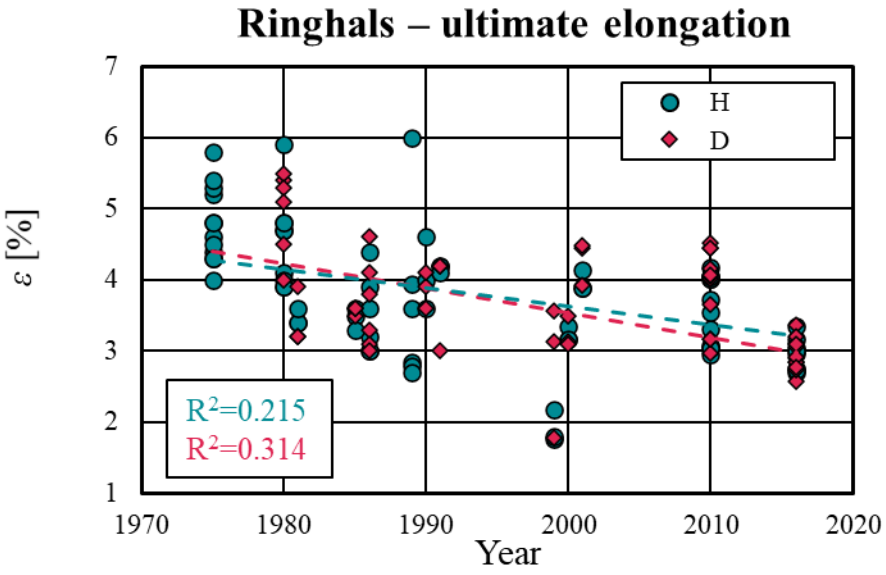

b)

Figure 11 Results for all Ringhals containments divided for wires extracted from horizontal direction (H) and dome (D) a) Tensile strength, b) ultimate elongation in function of testing year. Dashed lines represent linear regression trend.

3.2 REVERSED BEND TEST

The second experimental test performed for extracted strands and wires to evaluate their degradation defined as brittleness in bending was a reversed bend test. In this test the sample is fixed in a grip and bended in two opposite directions. The test result is the bend count at material fracture. The test was performed for samples is threefold state: (1) natural conditions and after hydrogen treatment for (2) 4 hours and (3) 24 hours. The hydrogen treatment intended to simulate the

natural material degradation in an accelerated manner. The hydrogen concentrates in microcracks and causes their growth, thus increasing the material brittleness.

As expected, the hydrogen treatment, especially after 24 hours decreased the maximum bend count (the wire fractured after lower number of bending cycles) (Figure 12). Moreover, the difference between the mean value of bend counts between the wires in original state and after hydrogen treatment was increasing over time (expressed by linear regression lines at Figure 12), which may indicate the material degradation. All the values for wires in original state were over the standard requirement of minimum 3 bend counts.

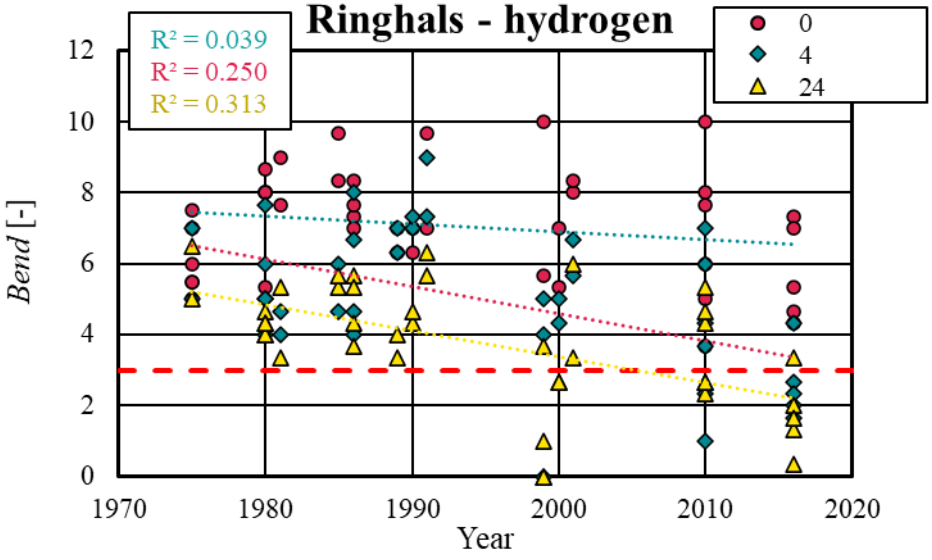

Figure 12 Reversed bend test results for a) all Ringhals containments by time of hydrogen treatment samples in original state marked as 0 (red circles), 4 hours (green diamonds), and 24 hours (yellow triangles) with trend lines in respective colors. The red dashed line indicates the minimum value required by standard.

The trends for 24-hour hydrogen treatment were analyzed in detail using the confidence interval for each separate containment at Figure 13. The confidence interval analysis revealed that the trends for wires without hydrogen treatment were not statistically meaningful (changes of the mean values 1.5, 2.1 and -0.6 for $CI_{95\%}$=1.8, 2.2 and 2.2 respectively for Ringhals 2, 3 and 4). Moreover, all trends indicating slight decrease of brittleness in time for Ringhals 4 were not meaningful (Figure 12c). However, for Ringhals 2 and 3 the identified trends for 4- and 24-hour hydrogen treatment increasing brittleness were statistically meaningful (changes of mean values 4.0, 2.0 with $CI_{95\%}$=1.6 and 1.5 for 4-hours hydrogen treatment and 3.5, 1.8 with $CI_{95\%}$=1.0 and 0.9 for 24-hours hydrogen treatment in Ringhals 2 (Figure 12a) and 3 (Figure 12b) respectively). Moreover, the R^2-values of linear regression lines for Ringhals 2 were increasing with increasing hydrogen treatment time, which means that the variation was decreasing. For Ringhals 3 the R^2-values were stable between 0.45 and 0.50, which indicates fairly good approximation with linear trend for so small dataset.

Comparing the obtained results with the standard requirement of at least 3 bend counts it is clearly visible that also the statistical prediction of 95% results is below the required value of 3 for Ringhals 2. In Ringhals 3, even thou the individual

results were lower than the requirement, the mean value was higher than 3. For Ringhals 4 all results and the confidence intervals were over the required bend count.

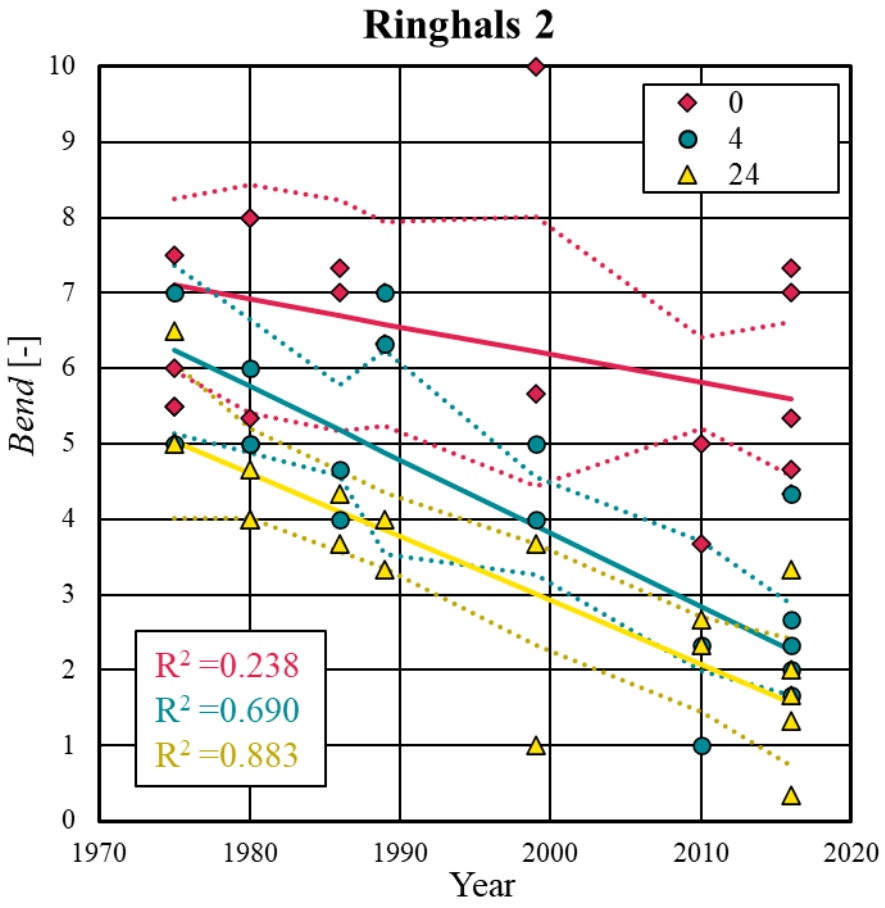

a)

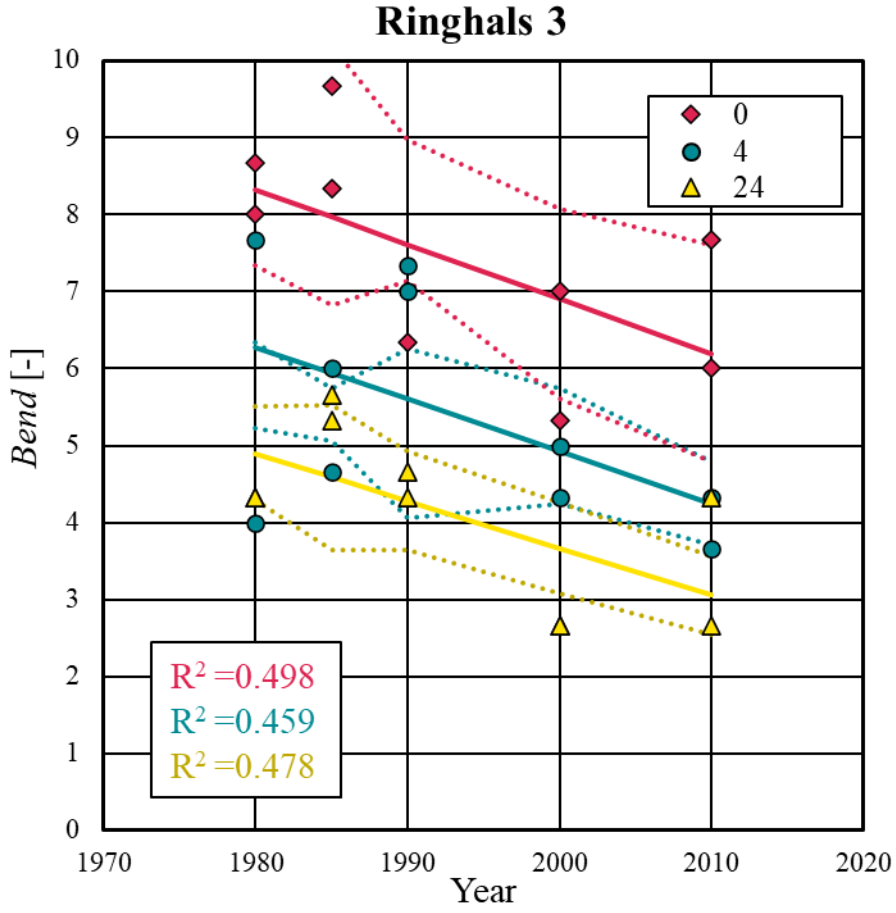
Ringhals 3
Bend [-]
Year
0
4
24
R² =0.498
R² =0.459
R² =0.478
0
1
2
3
4
5
6
7
8
9
10
1970
1980
1990
2000
2010
2020

b)

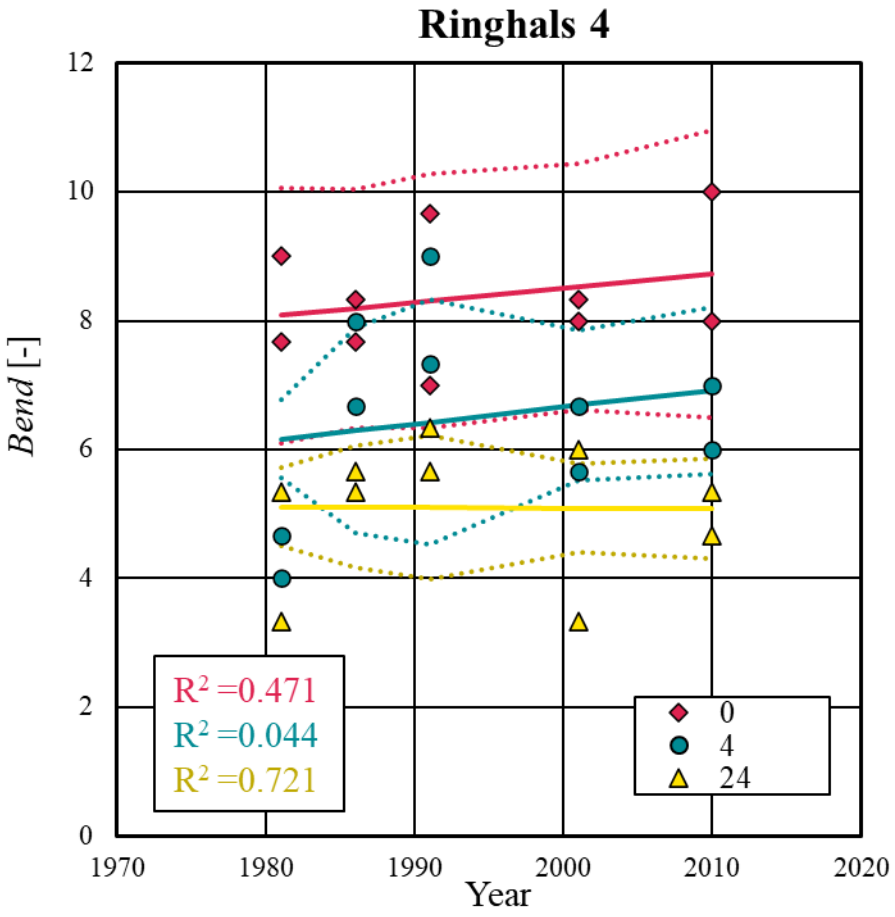

c)

Figure 13 Reversed bend test results for a) Ringhals 2, b) Ringhals 3 and c) Ringhals 4 in original state (red diamonds), after 4 hours (green circles) and 24 hours (yellow triangles) hydrogen treatment with linear regression lines (continues lines) and confidence intervals of 95 % (dotted lines) with respective colors.

4 Literature study on hard steel degradation

This chapter gathers state-of-the-art concerning high carbon content steel and the possible phenomenon causing the observed loss of ductility over long service life and analyses which of them could be a case in the analyzed containments.

4.1 STRESSORS AFFECTING THE PRESTRESSING STEEL

In their report on aging degradation of concrete structures in nuclear power plants, the authors identified the following stressors to cause failures of the prestressing steel tendons[18]:

- corrosion
- elevated temperature
- irradiation
- fatigue
- losses of prestressing forces and end effects

4.1.1 Corrosion

Most corrosion-related failures of prestressing parts are due to localized attacks. The following prestressing steel failures have been identified as caused by localized corrosion: pitting corrosion, stress corrosion cracking and hydrogen embrittlement.

Pitting corrosion

Pitting corrosion is the electrochemical process resulting in material loss of the prestressing tendon surface, reducing its capability to support loads. Pitting corrosion will only occur in the presence of aggressive anionic species[19], and chloride ions are usually the cause. Pitting is considered to be autocatalytic in nature, meaning that once a pit starts to grow, the conditions developed are such that further pit growth is promoted. The anodic and cathodic electrochemical reactions occur separate spatially during pitting (Figure 14). As the pit grows (anode), the dissolved metal ions are confined within the pit due to the restricted geometry. As a result, accumulated metal ions undergo hydrolysis, and a local acidity develops within the pit creating a very aggressive environment.

[18] Do M.J., Chockie A.D, (1994) SKI Report 94: 15 on Aging Degradation of Concrete Structures in Nuclear Power Plants. Battelle Seattle Research Center.
[19] Frankel G. S., (1998) Journal of the Electrochemical Society, Vol. 145, No. 6, 1998, pp. 2186-2198.

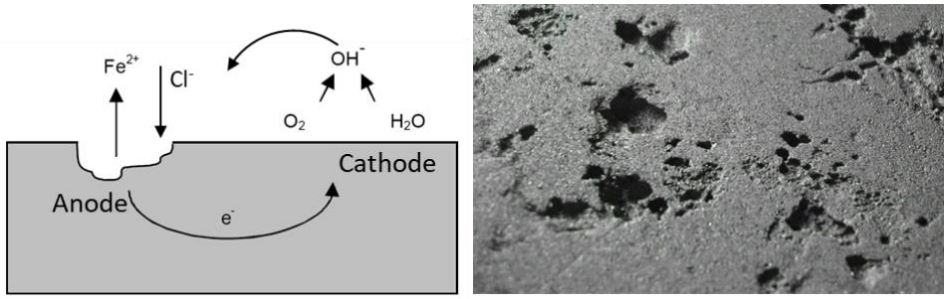

Figure 14 Pitting corrosion, diagram showing the mechanism and photo (from www.abfad.co.uk/editorial/pitting-corrosion-and-storage-tank-failure) showing actual damage.

Stress corrosion cracking

Stress corrosion cracking (SCC) refers to cracking caused by the simultaneous presence of tensile stress and a specific corrosive medium[23]. There is no unified mechanism for SCC. However, there are three important conditions that must be present simultaneously to produce SCC: a susceptible metal, a critical environment and tensile stress. Each metal has a specific critical environment. The specific environments which cause SCC for High-strength steel are[21]:

- Seawater
- Chloride solutions
- Solutions containing H_2S
- NO_3^- solutions

This corrodent species can be present in small concentration to initiate SCC.

During SCC, the metal is virtually unattacked over most of the surface while fine cracks progress through it. This cracking phenomenon has serious consequences since it can occur at stresses within the range of typical design stress[23].

Hydrogen embrittlement

Hydrogen embrittlement (HE) is a corrosive process that occurs when hydrogen atoms enter the metal lattice and reduce its ductility. There are many sources of Hydrogen Embrittlement[20], however they can be divided into two categories based on how the hydrogen is introduced into the metal, Internal Hydrogen Embrittlement (IHE) and Hydrogen Environmental Embrittlement (HEE).

The first category is from the preexisting hydrogen already present within the metal from creation and the second category is hydrogen introduced from the environment the metal is placed in. Examples of IHE include processes such as casting, surface cleaning, pickling, electroplating, welding, and heat treatments. Examples of HEE include general corrosion from exposure to the environment or through misapplication of various protection measures.

[20] Lee J.A., (2016) Hydrogen Embrittlement NASA/TM—2016–218602, Huntsville, Alabama.

Figure 15 shows the three conditions that must be met to cause HE failure in high-strength steel: material type that is susceptible to hydrogen damage, tensile stress (typically from an externally applied load) and hydrogen.

The actual mechanism by which HE occurs is not completely understood and several mechanisms has been suggested[21]. However, what happens in general is that when stresses are applied on steel the hydrogen tends to migrate to stress concentration points (local microcracks), where the created pressure develops the pre-existing micro-damages.

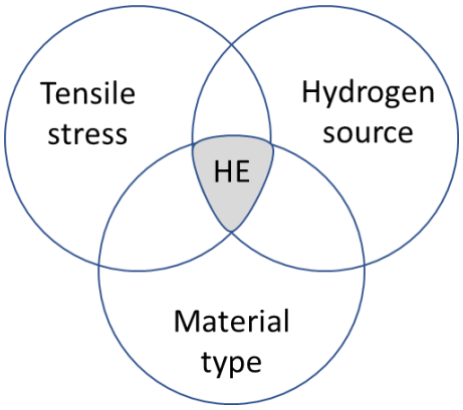

Figure 15 The three conditions that must be met for hydrogen embrittlement (HE) failure to occur. Stress and hydrogen are triggers, whereas material susceptibility is the fundamental requirement for HE to occur.

It can often be difficult to distinguish between SCC and HE, but these are two different phenomena. In general, HE is considered as a cathodic mechanism and SCC as an anodic mechanism. The SCC is a dissolution mechanism of removing materials at the crack tip through a corrosion process, and the environments that cause SCC are usually aqueous in nature, such as by contact with condensed layers of moisture or by immersion in a bulk liquid solution[20].

Reported corrosion failures

To protect against corrosion, the ducts containing the post-tensioned tendons are filled with organic corrosion inhibitors or air ventilated with dry air. However, failures of the prestressing steel tendons have been reported despite the corrosion inhibition measures[22].

At the Joseph M. Farley nuclear power plant (PWR reactor) about 8 years (1985) after tensioning fracture at the anchor block for several vertical tenson cables was discovered. Similar damages were discovered ones again at the same plant in 2012. It was found that hydrogen embrittlement of the steel material in the anchor block caused the failure. Several factors are believed to have contributed, such as free water in the grease/wax injection, high hardness in the steel material and high stress levels in the anchorage. The free water at anchorages is assumed to have

[21] McCafferty E., (2010) Introduction to corrosion science, Springer, New York.
[22] Andersson P., (2016) SSM Report 2016:13 Spännarmerade betongkonstruktioner vid kärntekniska anläggningar. Scanscot Technolgy AB, Lund.

accumulated from poorly sealed upper tension cable hoods that are exposed to outdoor climate.

At Calvert Cliff's nuclear power plant (PWR reactor) about 20 years (1997) after tensioning corrosion and wire breakage was discovered. It was found that these failures were caused by water and air penetration due to insufficient initial filling of grease just behind the anchor block.

In Sweden, there is one reported case of durability related problems regarding tension cables. At Forsmark 3, one year after operation started in 1986 breakage of horizontal tension cables was discovered. The possible reason for this was assumed to be corrosion caused by water from the construction period.

From practical standpoint, most pitting failures are caused by chloride and chloride-containing ions[23]. So, theoretically for reactor containments (PWR) that are not built-in, there is a risk of chloride-initiated reinforcement corrosion due to airborne pollutants and sea salt. Most likely to occur round the anchor block.

Further, as the tension cables are highly stressed both hydrogen embrittlement and stress corrosion cracking are two possible degradation mechanisms.

4.1.2 Elevated temperature

Elevated temperature can be potentially harmful to properties of prestressing tendons. Thermal damage to prestressing steels occurs when the steel is exposed to temperature approaching 200°C for extended periods[24]. Studies on the climatic condition in the Swedish reactor containments have shown that the temperatures on the containment walls varied between 20 to 50 °C during operation[24].

4.1.3 Irradiation

Irradiation by neutron fluence can produce changes in mechanical properties such as the yield strength and reduction of ductility, increasing the risk of brittle fracture[18]. However, research under the SAG program (established I 1987 by the United States Nuclear Regulatory Commission to gather and document the operational experience of concrete structures) indicated that irradiation is not detrimental to the reinforcing steel. But the researchers recommended that addition research should be conducted to evaluate in more detail the possible impact of irradiation on the reinforcing steel.

[23] Fontana M.G.,(1987) Corrosion Engineering, Third ED.
[24] Oxfall M., (2016) Climatic conditions inside nuclear reactor containments, ENERGIFORSK

5 New experimental results

The new experimental program was proposed as a validation method of the trends identified with the statistical data analysis. The tests concerned testing wires extracted during the project and some unused original tendons to verify if the long-term stress or environmental exposure affected the material. Additionally chemical and microstructure analysis were performed to confirm the material structure and link it to mechanical results.

The samples as described in Table 3 were extracted and prepared by Vattenfall. The same samples sets were sent to RISE and to the Vattenfall lab for parallel testing.

Table 3 Wires samples marking as received

Strand	Marking	Wire
Forsmark Nya	F Nya	1 2 3
Forsmark 3 Vertikal	F3 V	1 2 M
Forsmark 3 Bassäng	F3 B	1 2 M
Ringhals 3	R3 D	Ände 1 Ände 2 Mitt
Ringhals 3	R3 H	Ände 1 Ände 2 Mitt
Ringhals 4	R4 D	Ände 1 Ände 2 Mitt
Ringhals 4	R4 H	Ände 1 Ände 2 Mitt

5.1 MECHANICAL TESTS

5.1.1 Samples and methods

The uniaxial tensile test has been performed parallelly at RISE facilities in Borås and in Vattenfall lab in Älvkarleby. The wires diameter 6 mm, approximately 2 m long, from seven different 7-wire strands were delivered to RISE for testing (Figure 16). Three wires were taken from each strand. The received samples with marking according to Table 3 were cut to obtain samples with length of 500 mm.

Figure 16 Wires delivered to RISE for testing with original marking

The original standard (SS 11 21 38) for testing the tensile strength and ultimate elongation has never been used at RISE before. The used standards for this kind of tests are SS-EN ISO 15630-1:2019 and SS-EN ISO 6892-1:2019 B. There is a slight difference in the way the ultimate elongation (gränstöjning) δ_g is derived. In the old standard the elongation is measured across the fracture as a difference of elongations at a distance of $Lo \geq 120$ mm and $Lo/2 \geq 60$ mm (Figure 17a), while in the new standards the elongation is measured in the part of the specimen under elastic deformation only at a distance of at least 50 mm from the fracture (Figure 17b). The different measurment strategy should not affect the results as both results concern the part of the specimen under elastic elongation only.

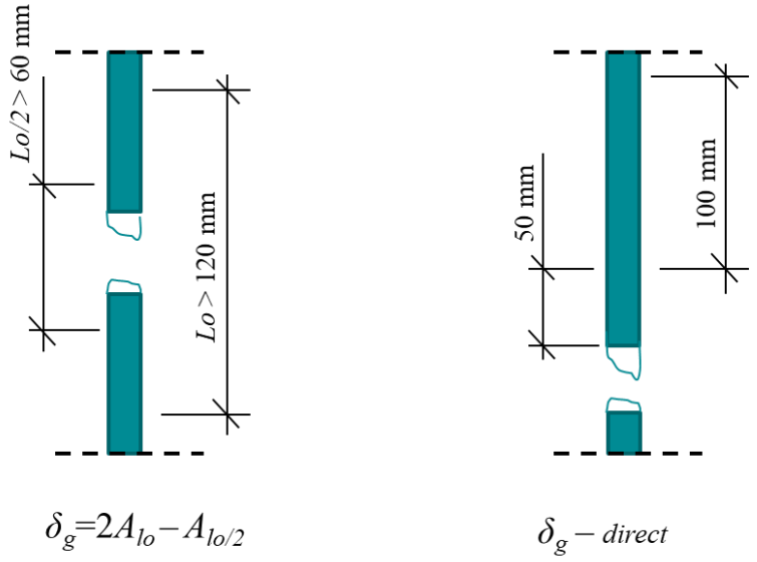

Figure 17 The difference of the ultimate elongation measurement between standards a) SS 11 21 38 and b) SS-EN ISO 15630-1:2019 and SS-EN ISO 6892-1:2019 B.

The second difference between both standards lies in determining the proof strength. According to the old standard the paper print-out from the test result was used and the parallel line to the secant elastic modulus line between 10 % and 70 % of the minimum required force was transferred with a ruler to the 0.2%-limit. In the new standard it is done digitally with the E-modulus line derived using "least

squares fit method" on the elastic part of the curve and transferred to the 0.2%-limit. The difference between both methods should be insignificant.

The tensile tests at RISE were performed according to SS-EN ISO 15630-1:2019 and SS-EN ISO 6892-1:2019 B (Figure 18).

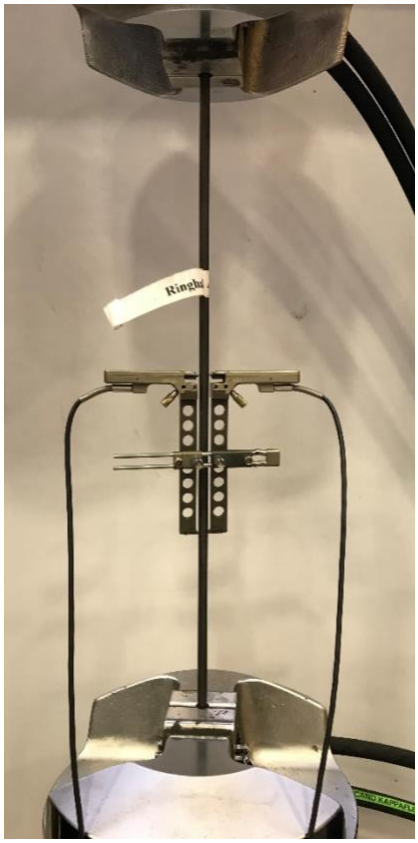

Figure 18 Mounting of the wire in the testing machine with visible strain measuring system.

All samples were tested 9th and 10th of March 2021.

The total calculated measurement uncertainty for the measured values is given in appendix 1. Reported uncertainty corresponds to an approximate 95 % confidence interval around the measured value. The interval has been calculated in accordance with EA-4/16[25], which is normally accomplished by quadratic addition of the actual standard uncertainties and multiplication of the resulting combined standard uncertainty by the coverage factor k=2.

The measurements uncertainties were given as:

Measurement uncertainty - proof strength:	*< 1,5 %*
Measurement uncertainty - tensile strength:	*< 1,1 %*
Measurement uncertainty - stress ratio:	*< 3 %*
Measurement uncertainty - elongation at maximum force:	*< 7 % of given value*

[25] EA-4/16 EA guidelines on the expression of uncertainty in quantitative testing

5.1.2 Results obtained by RISE

The results were presented by containment in the tables below (Table 4 -

Table 7). The measured proof strength and tensile strength were characterized with very low scatter within each wire (*COV*< 0.9 %). The ultimate elongation was characterized with higher variation of up to *COV*=11 %.

Table 4 Tensile test results for unused Forsmark wires

Tensile test

Specimen marking	Diameter D mm	Cross-section S_0 mm^2	Proof strength $R_{p0.2}$ N/mm^2	Tensile-strength R_m N/mm^2	Stress ratio $R_m/R_{p0.2}$	Elongation at maximum force A_{gt} (ε_g) %
F Nya 1	6,01	28,4	1643	1845	1,12	5,5
F Nya 2	6,00	28,3	1650	1849	1,12	5,7
F Nya 3	6,00	28,3	1638	1848	1,13	5,0

Table 5 Tensile test results for used Forsmark 3 wires

Specimen marking	Diameter D mm	Cross-section S_0 mm^2	Proof strength $R_{p0.2}$ N/mm^2	Tensile-strength R_m N/mm^2	Stress ratio $R_m/R_{p0.2}$	Elongation at maximum force A_{gt} (ε_g) %
	6.02	28.5	1577	1821	1.15	5.5
F3 V	6.02	28.5	1583	1816	1.15	5.3
	6.02	28.5	1585	1822	1.15	5.5
	6.02	28.5	1612	1819	1.13	5.2
F3 B	6.01	28.4	1636	1831	1.12	5.1
	6.01	28.4	1636	1829	1.12	5.2

Table 6 Tensile test results for Ringhals 3 wires

Specimen marking	Diameter D mm	Cross-section S_0 mm^2	Proof strength $R_{p0.2}$ N/mm^2	Tensile-strength R_m N/mm^2	Stress ratio $R_m/R_{p0.2}$	Elongation at maximum force A_{gt} (ε_g) %	
	6.00	28.3	1629	1785	1.10	4.3	*
R3 A	6.00	28.3	1615	1784	1.10	4.3	*
	6.01	28.4	1625	1789	1.10	5.2	
	6.01	28.4	1578	1819	1.15	5.1	
R3 B	6.01	28.4	1554	1826	1.18	4.4	
	6.00	28.3	1586	1821	1.15	5.3	

Table 7 Tensile test results for Ringhals 4 wires

Specimen marking	Diameter D mm	Cross-section S_0 mm^2	Proof strength $R_{p0.2}$ N/mm^2	Tensile-strength R_m N/mm^2	Stress ratio $R_m/R_{p0.2}$	Elongation at maximum force A_{gt} (ε_g) %	
	6.05	28.8	1703	1882	1.11	5.2	
R4 D	6.05	28.8	1676	1852	1.11	4.1	
	6.05	28.8	1678	1862	1.11	4.7	
	6.01	28.4	1688	1866	1.11	5.2	
R4 H	6.01	28.4	1621	1784	1.10	4.3	*
	6.01	28.4	1682	1867	1.11	4.7	

* Samples that failed in grip

The ultimate tensile strength measured by RISE for Ringhals and Forsmark 3 was higher than all historical results (Figure 19). The strength of used and unused tendons from Forsmark the same apart from differences falling within the uncertainty of the measurement (Figure 19b). The mean value changed within the confidence interval – no strength degradation was observed. The results scatters for Forsmark wires were much lower than in historical data (*COV*=0.2 % to *COV*=1.5 %). The result from 2016 for Forsmark 3 has also been obtained by RISE and falls within a linear trend between unused and used wire. This confirms the lack of long-term changes in tensile strength. All measurements from RISE are over the SIS standard requirement of F_m=51.1 kN.

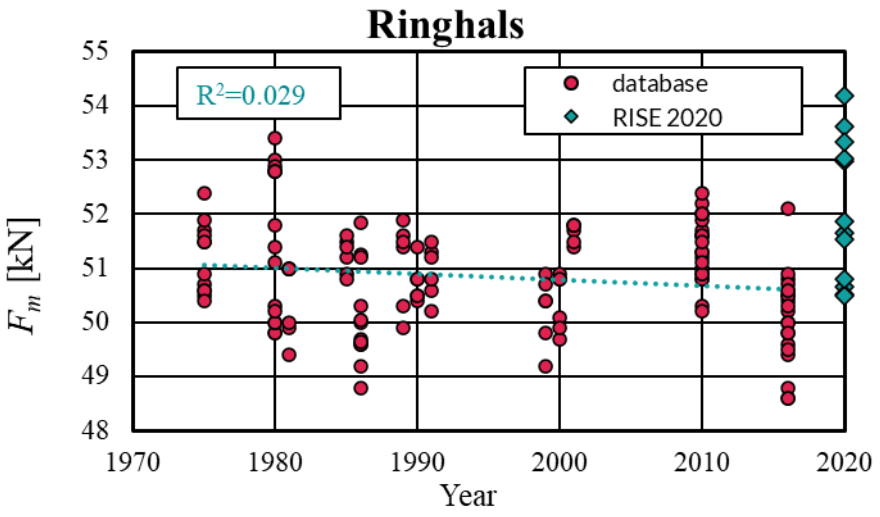

a)

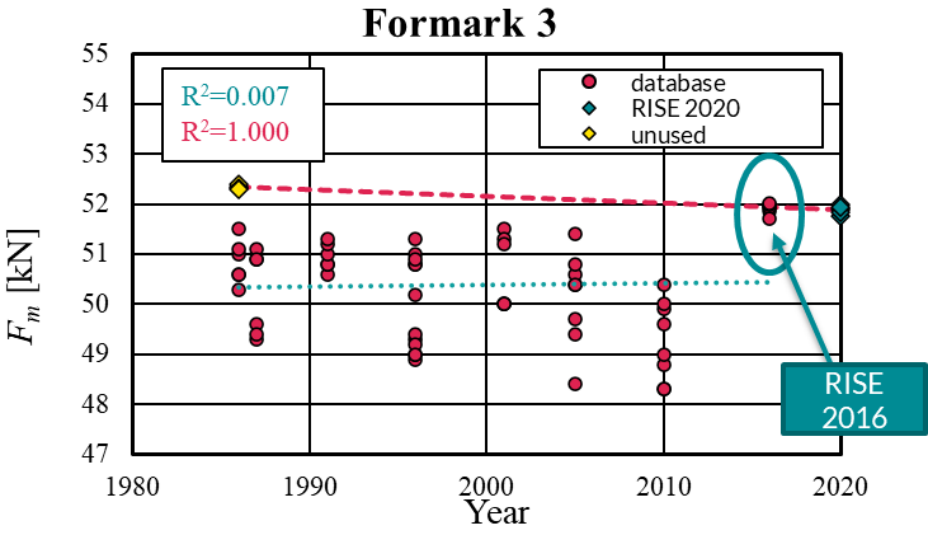

b)

Figure 19 The results of maximum tensile force for a) Ringhals and b) Forsmark 3 in historical database (red circles), from the tests performed within the project on used (green diamonds) and unused wires (yellow diamonds). The red dashed line indicates linear regression line for unused tendons and new tests by RISE only, while the dotted green line indicates linear regression for the historical database only.

The force at 0.2 % elastic limit measured by RISE falls within the scatters of data from historical measurements (Figure 20). The trends fall within the uncertainty of the measurement and therefore are statistically non-meaningful. There was no meaningful change in the elastic limit between the used and unused samples – no material degradation (Figure 20b).

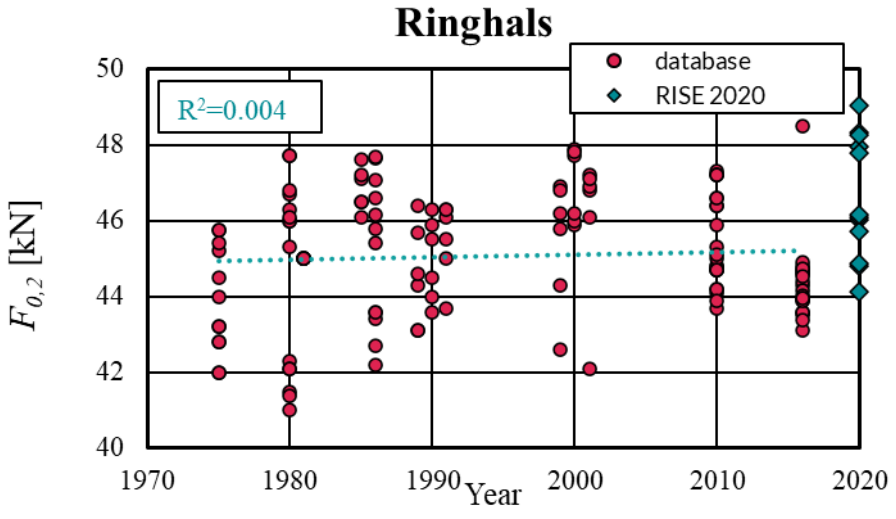

a)

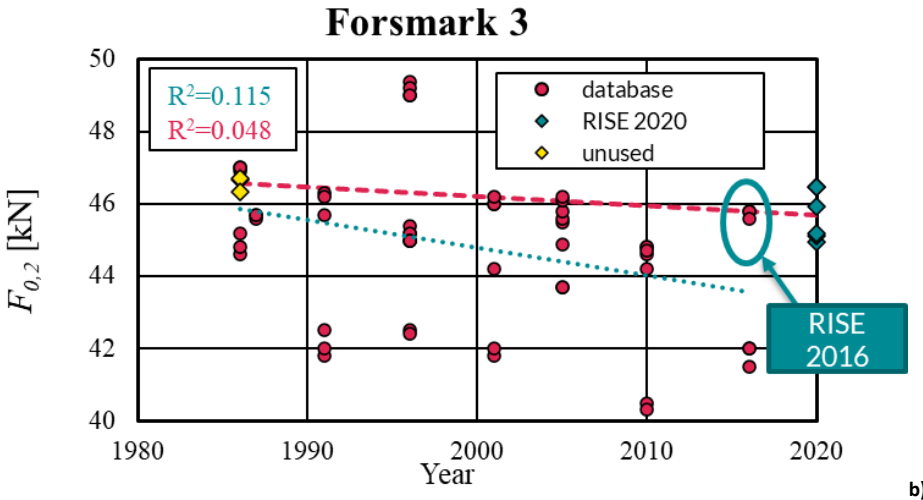

b)

Figure 20 The results of force at 0,2 % strain for a) Ringhals and b) Forsmark 3 in historical database (red circles), from the tests performed within the project on used (green diamonds) and unused wires (yellow diamonds). The red dashed line indicates linear regression line for unused tendons and new tests by RISE only, while the dotted green line indicates linear regression for the historical database only.

The measured values of ultimate elongation are contradictory to the identified trend for all Ringhals containments. The new values fulfill the SIS standard requirement of 3.5 %. The mean value obtained by RISE is the same as for the first registered measurement in 1975 (Figure 21a). The new results for Forsmark 3 were higher by 50 % in comparison with historical data. This increases significantly the confidence interval and therefore make the overall trend statistically nonmeaningful (Figure 21b). The results obtained for unused wires indicate lack of material degradation in comparison with the new results. The results obtained by RISE in 2016 are in line with the lack of material degradation between original and aged material.

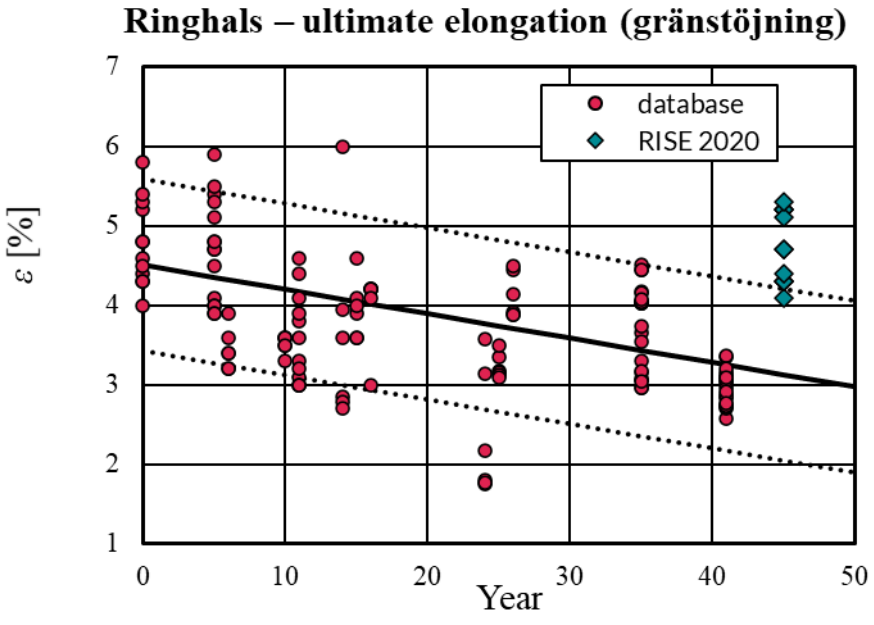

a)

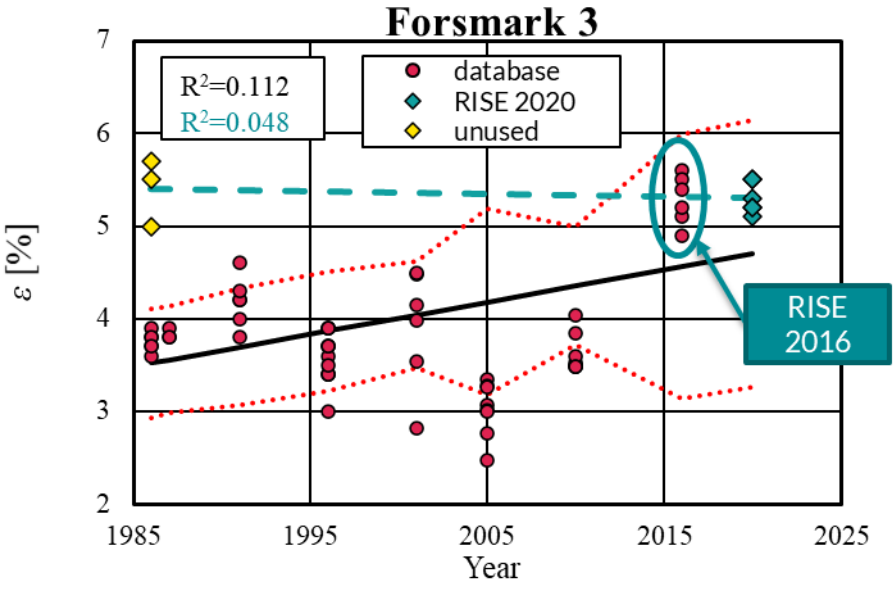

b)

Figure 21 The results of ultimate elongation for a) Ringhals and b) Forsmark 3 in historical database (red circles), from the tests performed within the project on used (green diamonds) and unused wires (yellow diamonds). The green dashed line indicates linear regression line for unused tendons and new tests by RISE only, the continues black lines are linear regression lines for the database only, while the red and black dotted lines indicate confidence interval for all Forsmark 3 and three standard deviations for Ringhals samples.

5.1.3 Results obtained by Vattenfall

The same set of samples was parallelly tested by Vattenfall Älvkarleby lab to cross-check the obtained results and capture eventual discrepancies due to the testing procedures, used machines or human errors. The differences between the mean values for the same wires tested by RISE and Vattenfall were calculated in percent and presented in Table 8. For maximum tensile force and force at 0.2 % strain the maximum difference was 3.8 %, which is double of the value of the test uncertainty (1.5 % for proof strength), which means that the differences might have purely statistical origin related to method uncertainty and natural material heterogeneity. Larger differences were observed for the ultimate elongation values where the maximum discrepancy was equal to 20.2 % for the first Ringhals 3 wire, which is 3 times higher than the RISE test uncertainty (7 % for ultimate elongation). It was caused by high scatter of the individual results within the samples from the same wire tested by RISE (COV 11.3 %), however it was not the highest scatter observed. It could be related to minor random difference in the material structure between the RISE and Vattenfall samples.

Table 8 The differences between the mean values for the same wires tested by RISE and Vattenfall

Containment	$F_{0,2}$ (kN)	F_{max} (kN)	ε_g (%)	$F_{0,2}$ /F_{max}
Ringhals 3	1.5%	-2.0%	-20.2%	3.6%
Ringhals 3	1.8%	3.8%	-6.3%	-1.9%
Ringhals 4	1.4%	1.7%	-17.4%	-0.3%
Ringhals 4	2.9%	3.8%	-2.8%	-0.9%
Forsmark 3	-1.8%	-0.3%	-3.7%	-1.5%
Forsmark 3	-0.5%	0.4%	-5.8%	-0.9%

The coefficients of variation for tests performed by RISE and Vattenfall were presented in Table 9. The level of results variation was very similar for all the derived values and varied between 0.6 % and 0.9 % apart from ultimate elongation, where *COV* was equal to 7.6 % and 6.4 % for RISE and Vattenfall respectively. Comparable variation of the results indicates that the tests uncertainty was similar independently on the machine, personnel and testing procedure.

Table 9 The coefficients of variation for the same wires tested by RISE and Vattenfall

Containment	*COV* $F_{0,2}$		*COV* F_{max}		*COV* ε_g		*COV* $F_{0,2}$ /F_{maX}	
	RISE	**Vatt.**	**RISE**	**Vatt.**	**RISE**	**Vatt.**	**RISE**	**Vatt.**
Ringhals 3	0.5%	1.8%	0.4%	1.1%	11.3%	2.6%	0.4%	0.5%
Ringhals 3	0.9%	0.5%	0.3%	0.7%	9.6%	12.1%	1.2%	0.9%
Ringhals 4	2.2%	0.2%	2.6%	0.8%	9.5%	5.6%	0.4%	2.2%
Ringhals 4	0.9%	0.2%	0.8%	0.3%	11.8%	13.0%	0.2%	0.9%
Forsmark 3	0.6%	0.2%	0.2%	0.2%	1.1%	2.2%	0.5%	0.6%
Forsmark 3	0.3%	1.8%	0.2%	1.1%	2.1%	2.6%	0.3%	0.3%
Mean values	0.9%	0.8%	0.7%	0.7%	7.6%	6.4%	0.5%	0.6%

5.1.4 Conclusions

- The new results did not exhibit any degradation in ultimate elongation,
- The results obtained at RISE are slightly higher than the majority of historical results,
- No meaningful difference exceeding the uncertainty of the method was observed between used and un-prestressed wires,
- The results obtained independently by RISE and Vattenfall had very similar mean values and results scatter, which indicates that the used methodology was consistent,
- The source of embrittlement in reverse bend test after hydrogen treatment remains unclear and could be further investigated.

5.2 CHEMICAL ANALYSIS

5.2.1 Samples and method

From the ends of wire samples received (Table 3) for mechanical tests longitudinal sections were cut out for chemical analysis of the steel. The samples were tested for the weight proportion of elements (Al, Si, P, S, Ca, Ti, V, Cr, Mn, Co, Ni, Cu, Zr, Nb, Mo, Sn, Sb, Ta and W) with X-ray fluorescens technique (Figure 22) with internal method SP1494. The method is based on a semi-quantitative analysis of the surface layer. The samples surface was grinded before the analysis. The carbon content was determined on steel samples with IR detection of formed CO_2 by combustion in oxygen in high frequency induction furnace, method SP0653. The test was conducted on the 8th of April 2021.

Figure 22 The testing setup for X-ray fluorescens measurements of elements content in steel.

5.2.2 Results

The results were presented separately for Forsmark (Table 10) and Ringhals (Table 11) samples in comparison with the requirements by the standard SS 14 17 57[Error! Bookmark not defined.]. The values exceeding the standard requirement were highlighted with red colour.

For both new, unused wires and used wires from Forsmark 3 the standard values of Phosphonium and Sulphur were exceeded. In new samples and in the wire centre higher Phosphorus content than in the end sample was detected this may come from anti-corrosion coating or from lubricating in cold drawing process. The coal content is high for both unused and used wires as expected for hard steel.

Table 10 Results of steel chemical analysis for wires from Forsmark with comparison to standard SS 14 17 57 requirements. The presented results are % of samples mass.

Element	Forsmark ny	Forsmark 3 Vertikal mitten	Forsmark 3 Bassäng mitten	Standard SS 14 17 57[26]
Carbon, C	0,76	0,80	0,76	-
Aluminium, Al	ca. 0,28	ca. 0,19	ca. 0,13	-
Silicon, Si	ca. 0,28	ca. 0,33	ca. 0,34	-
Phosphorus, P	**ca. 0,83**	**ca. 1,6**	**ca. 1,1**	x < 0,040
Sulfur, S,	**ca. 0,063**	**ca. 0,21**	**ca. 0,097**	x < 0,040
Calcium, Ca	ca. 0,071	ca. 0,29	ca. 0,12	-
Titanium, Ti	< 0,01	< 0,01	ca. < 0,01	-
Vanadium, V	< 0,01	< 0,01	ca. < 0,01	-
Chromium, Cr	ca. 0,029	ca. 0,036	ca. 0,032	-
Manganium, Mn	ca. 0,69	ca. 0,67	ca. 0,73	-
Cobalt, Co	< 0,01	< 0,01	ca. < 0,01	-
Nickel, Ni	ca. 0,054	ca. 0,078	ca. 0,054	-
Copper, Cu	ca. 0,025	ca. 0,14	ca. 0,019	-
Zirkonium, Zr	< 0,01	< 0,01	ca. < 0,01	-
Niobium, Nb	< 0,01	< 0,01	ca. < 0,01	-
Molybdenium, Mo	< 0,01	< 0,01	ca. < 0,01	-
Tin, Sn	< 0,01	< 0,01	ca. < 0,01	-
Antimonium, Sb	< 0,01	< 0,01	ca. < 0,01	-
Tantalum, Ta	< 0,01	< 0,01	ca. < 0,01	-
Volframium, W	< 0,01	< 0,01	ca. < 0,01	-
Iron, Fe	Rest	Rest	Rest	-

Similarly, as for Forsmark the coal level was high and stable (between 0.78 and 0.94 %) for all samples. The Phosphorus content was detected in relatively high concentrations (0.21-0.74 %) exceeding the standard requirement. Some higher

[26] SS 14 17 57 Ståhl för spännarmering av betong

Sulphur concentrations were also found in Ringhals samples which may also come from the corrosion protection applied at the steel production stage.

Table 11 Results of steel chemical analysis for wires from Ringhals with comparison to standard SS 14 17 57 requirements. The presented results are % of samples mass.

Element	Ringhals 4 D45 ände 1	Ringhals 4 H18 ände 1	Ringhals 3 H46 ände 1	R3 D59	Standard SS 14 17 57[27]
Carbon, C	0,84	0,80	0,78	0,78	-
Aluminium, Al	ca. 0,075	ca. 0,51	ca. 0,32	ca. 0,29	-
Silicon, Si	**ca. 0,33**	**ca. 0,26**	**ca. 0,20**	**ca. 0,27**	x < 0,040
Phosphorus, P	**ca. 0,74**	**ca. 0,38**	**ca. 0,21**	**ca. 0,29**	x < 0,040
Sulfur, S	ca. 0,037	ca. 0,031	ca. 0, 26	ca. 0,020	-
Calcium, Ca	ca. 0,17	ca. 0,048	ca. 0,028	ca. 0,030	-
Titanium, Ti	< 0,01	< 0,01	< 0,01	< 0,01	-
Vanadium, V	ca. 0,030	< 0,01	< 0,01	< 0,01	-
Chromium, Cr	ca. 0,25	ca. 0,022	ca. 0,020	ca. 0,027	-
Manganium, Mn	ca. 0,72	ca. 0,74	ca. 0,67	ca. 0,70	-
Cobalt, Co	< 0,01	< 0,01	< 0,01	< 0,01	-
Nickel, Ni	ca. 0,040	ca. 0,026	ca. 0,031	ca. 0,035	-
Copper, Cu	ca. 0,019	< 0,01	ca. 0,013	ca. 0,028	-
Zirkonium, Zr	< 0,01	< 0,01	< 0,01	< 0,01	-
Niobium, Nb	< 0,01	< 0,01	< 0,01	< 0,01	-
Molybdenium, Mo	< 0,01	< 0,01	< 0,01	< 0,01	-
Tin, Sn	< 0,01	< 0,01	< 0,01	< 0,01	-
Antimonium, Sb	< 0,01	< 0,01	< 0,01	< 0,01	-
Tantalum, Ta	< 0,01	< 0,01	< 0,01	< 0,01	-
Volframium, W	< 0,01	< 0,01	< 0,01	< 0,01	-
Iron, Fe	Rest	Rest	Rest	Rest	-

5.3 MICROCSOPIC ANALYSIS WITH SEM AND EDS

5.3.1 Theoretical background

Hydrogen embrittlement of a steel material can be caused by exposing the material to environmental conditions that either induces stress corrosion cracking (SCC) or are rich in hydrogen[28]. In some cases, the surface finishing of steel can cause hydrogen embrittlement due to hydrogen evolution during the surface treatment, for instance plating can be such an operation[29]. In hydrogen rich environments the diffusion to grain boundaries will weaken the carbon steel, thus the effect of hydrogen

[27] SS 14 17 57 Ståhl för spännarmering av betong

[28] D. A. Jones, Principles and prevention of Corrosion, Second Edi. Upper Saddle River: Prentice Hall, 1996.

[29] S. P. Lynch, "Hydrogen embrittlement (HE) phenomena and mechanisms," in Stress corrosion cracking: Theory and practice, Elsevier Ltd, 2011, pp. 90–130.

embrittlement will be most notable near the surface[30]. This can in some cases be visible as brittle fractures in the material, via trans granular and intergranular cracking on the microscopic level. There can also be more subtle differences on the fracture mechanism, although this cannot be resolved using a SEM[29].

5.3.2 SEM investigation of samples

The samples were delivered after mechanical testing, marked with sample names. The sample names are summarised in Table 12 below. The sample chosen for microscopical analysis are marked in green.

Table 12 First batch of samples received after the mechanical tests.

Samples			
Ringhals 3	**Ringhals 4**	**Forsmark 3**	**Forsmark**
H Ände 1	D Ände 1	V #1	Nya 1
H Ände 2	D Ände 2	V #2	Nya 2
H Mitt	D mitten	V mitten	Nya 3
D Ände 1	Ringhals 4 H Ände 2	B #1	Nya 1 omprov
D Ände 2	Ringhals 4 H mitten	B #2	
D mitten		B mitten	

For investigation of the fracture surface the samples were partially embedded in epoxy resin (EpoFix, Struers, Denmark). To ensure grounding of the samples to the microscope the bottom part of the epoxy embedded sample was ground down using SiC paper to expose the metallic tendon. No subsequent coating of the samples was performed.
The investigation of the samples was performed using a Zeiss Supra 40VP Scanning Electron Microscope (SEM). The fractures were studied using the second electron imaging.
Only the marked sample in Table 1 was subjected to this kind of investigation. As no significant difference was seen after investigating the samples marked in green, and no significant difference was seen in the mechanical data, it was decided that no new data would emerge from the rest of the samples.

5.3.3 Investigation of corrosion indicators

The samples were investigated using an Oxford Instruments X-Max 80 Electron Dispersive X-ray spectroscopy (EDX) detector, coupled to the microscope mentioned above. Samples investigated with EDX are underlined in Table 12. The investigation was carried out on both the surface of the tendons, and on cross sections. The cross sections were prepared by embedding the samples in a hot mounting resin (DuroFast, Struers, Denmark) and polishing the sample to a 1 μm finish using SiC paper and diamond suspension.

[30] T. Depover, E. Wallaert, and K. Verbeken, "Fractographic analysis of the role of hydrogen diffusion on the hydrogen embrittlement susceptibility of DP steel," Mater. Sci. Eng. A, vol. 649, pp. 201–208, Jan. 2016.

5.3.4 Results

Fracture surface

In Figures 23-25 an overview of the fracture surfaces after mechanical testing can be seen. Figure 23 shows samples marked Forsmark Nya 1, 2 and 3 shown seen as rows A, B and C in the figure. Some radial cracks can be seen in the sample. The same can be seen in Figures 24 and 25 which show Forsmark 3 V and Ringhals 3 D samples, respectively. For Figure 24, rows A, B and C corresponds to V #1, V #2 and V mitten and in Figure 25 rows A, B and C corresponds to Ände 1, Ände 2 and mitten.

In Figures 26-27 example micrographs at higher magnifications of the fracture surfaces is shown. All examined surfaces show a ductal fracture morphology. No discernible difference could be seen between the samples.

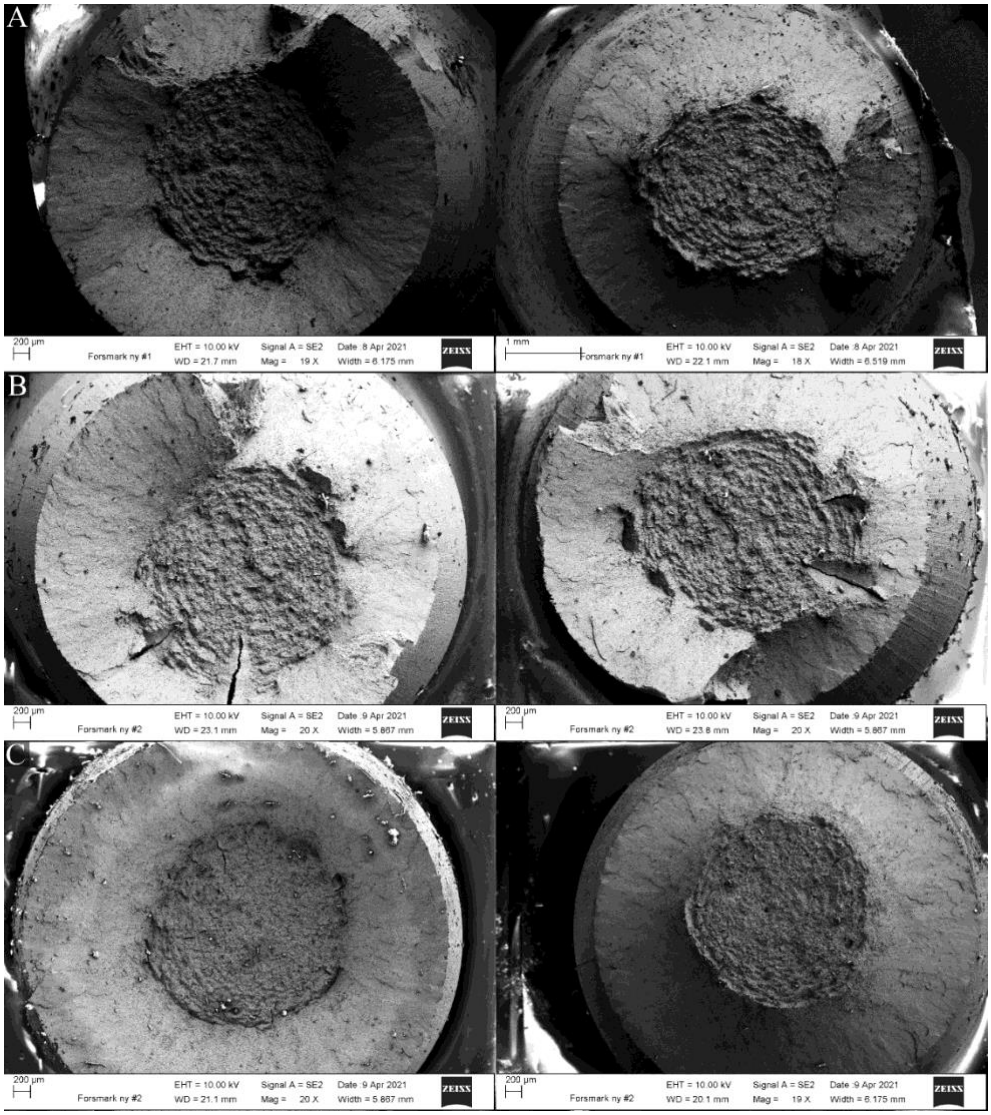

Figure 23 Overview of the fracture surface on sample Forsmark Nya 1, 2 and 3 (seen in rows A, B and C respectively).

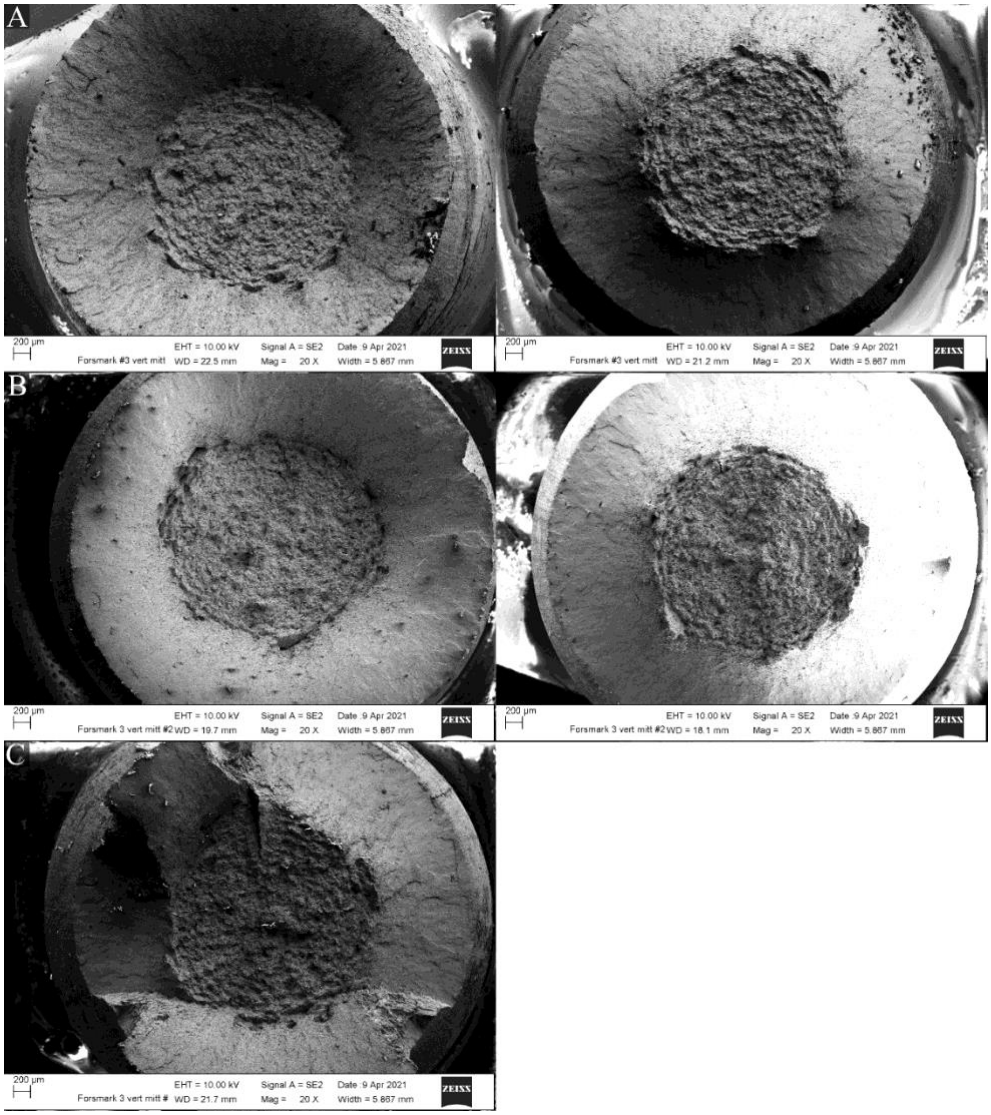

Figure 24 Overview micrographs of sample Forsmark 3 V #1, #2 and mitten (seen in rows A, B and C respectively).

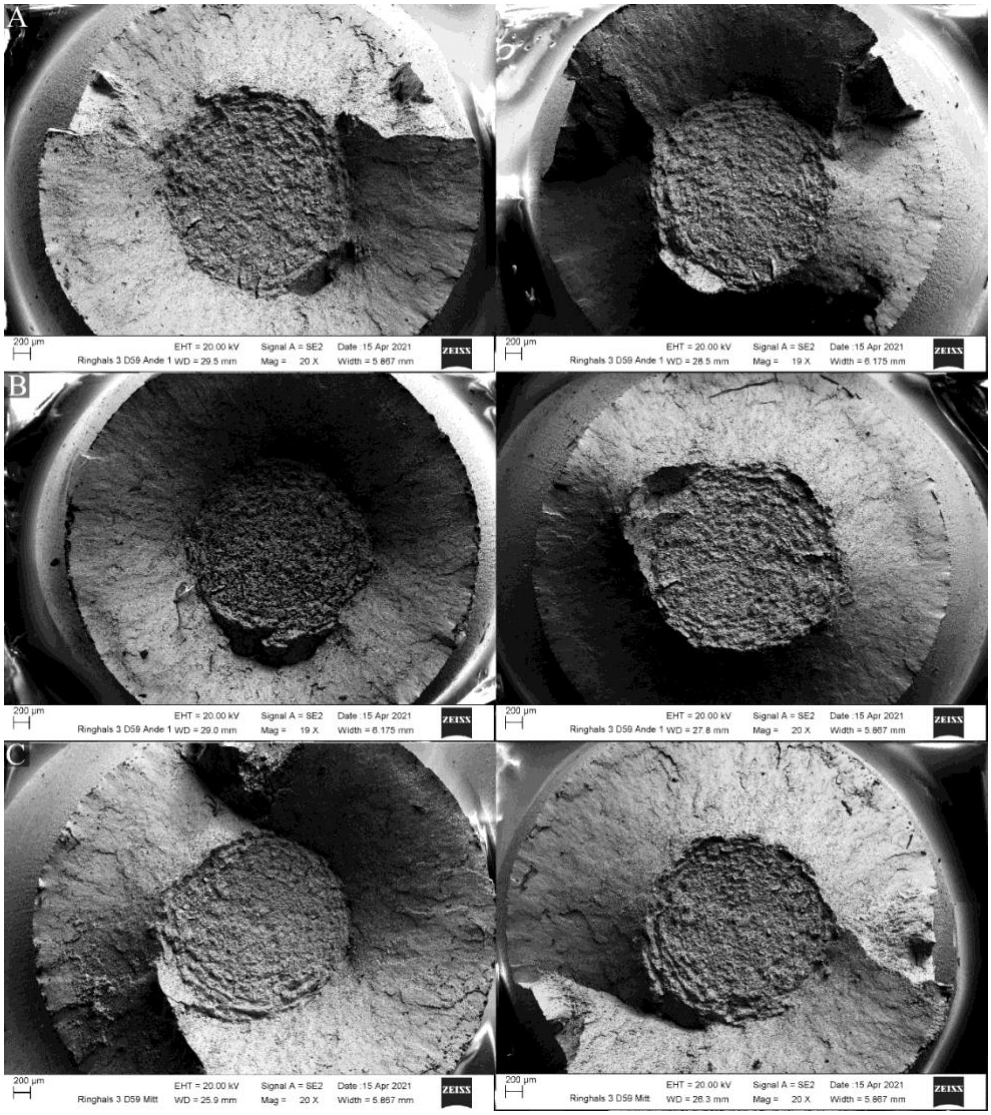

Figure 25 Overview micrographs of the samples Ringhals 3 D Ände 1, Ände 2 and mitten (seen in rows A, B and C respectively).

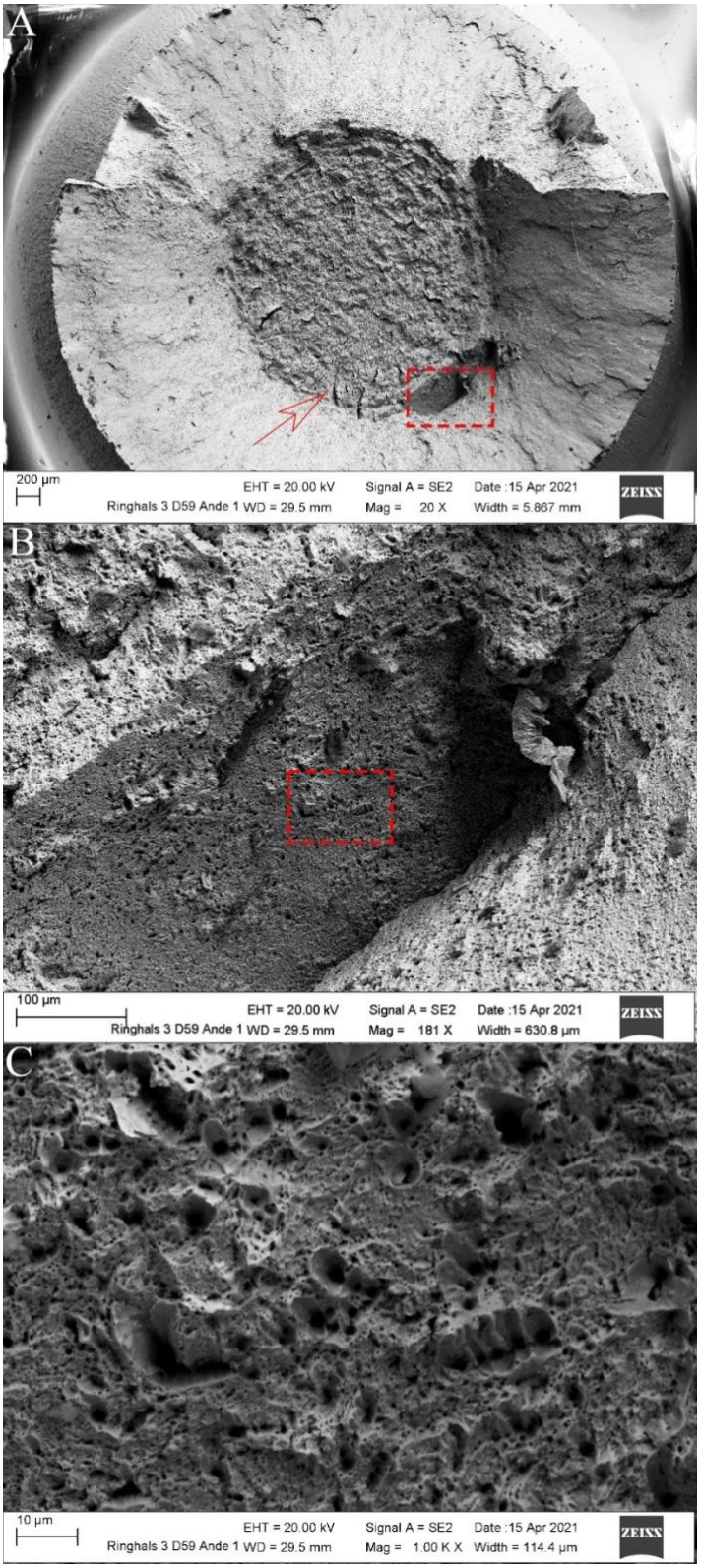

Figure 26 Micrographs of increasing magnification of the fracture surface on Ringhals 3 D Ände 1.

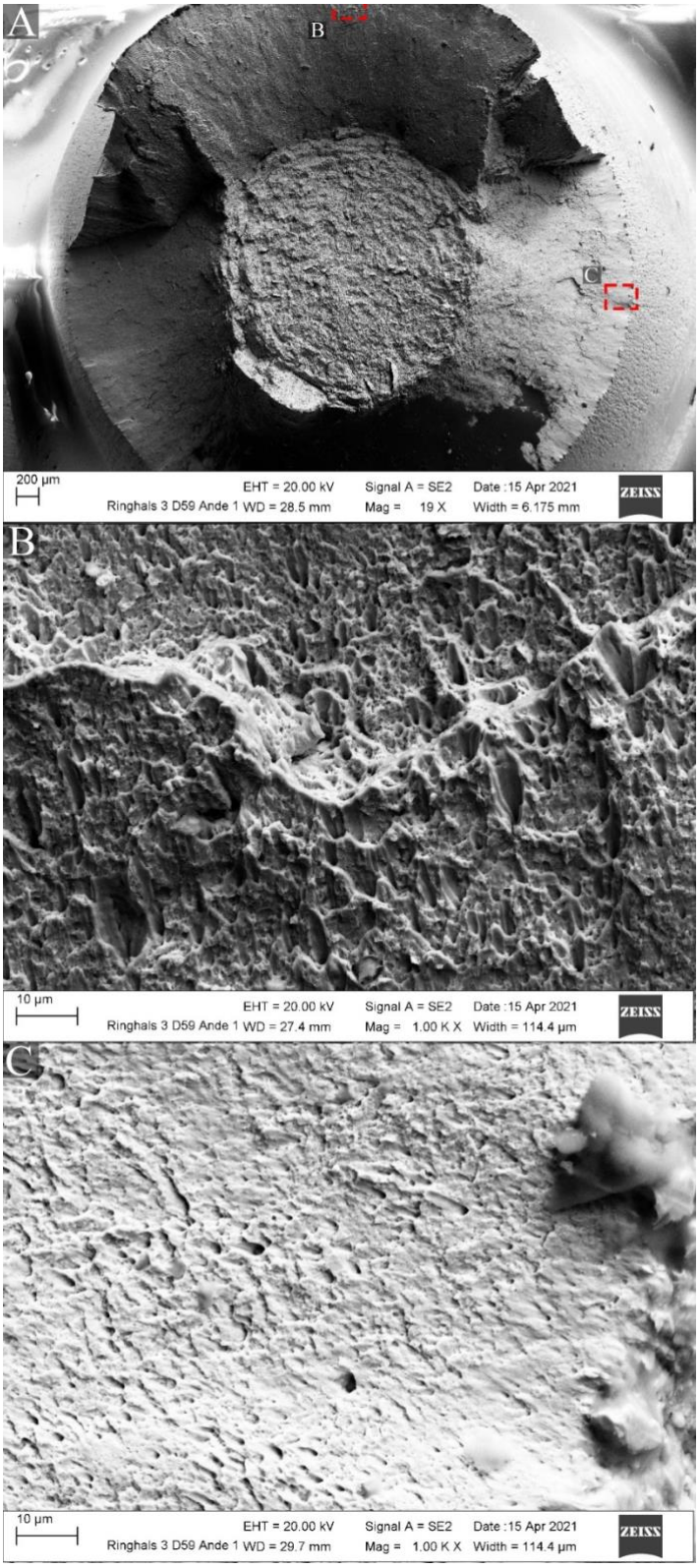

Figure 27 Example of micrographs of sample Ringhals 3 D Ände 1 at higher magnification.

5.3.5 Cross sections and EDX analysis of same

In Figures 28-30 micrographs of some of the no discernible differences that could be seen between the unexposed, Forsmark Nya 1, see Figure 28, samples, and the samples from Frosmark 3 and Ringhals 3. Seen Figures 29 and 30. Most of the entire surface is covered with a thin layer rich in Phosphor, Zinc and Oxygen. This surface is consistent with zinc phosphate layers. This is true of all samples. Both the exposed and "new" samples show a few surface defects, seen as pits or even small cracks. They are seen on all samples and are in the range of 10-50 μm. It can be seen in the figures below that they too are filled what is consistent with a phosphate layer. As the same characteristics can be seen on all samples both the ones that were subjected to long term exposure and those that are unexposed, it seems unlikely that this would be an ongoing degradation process.

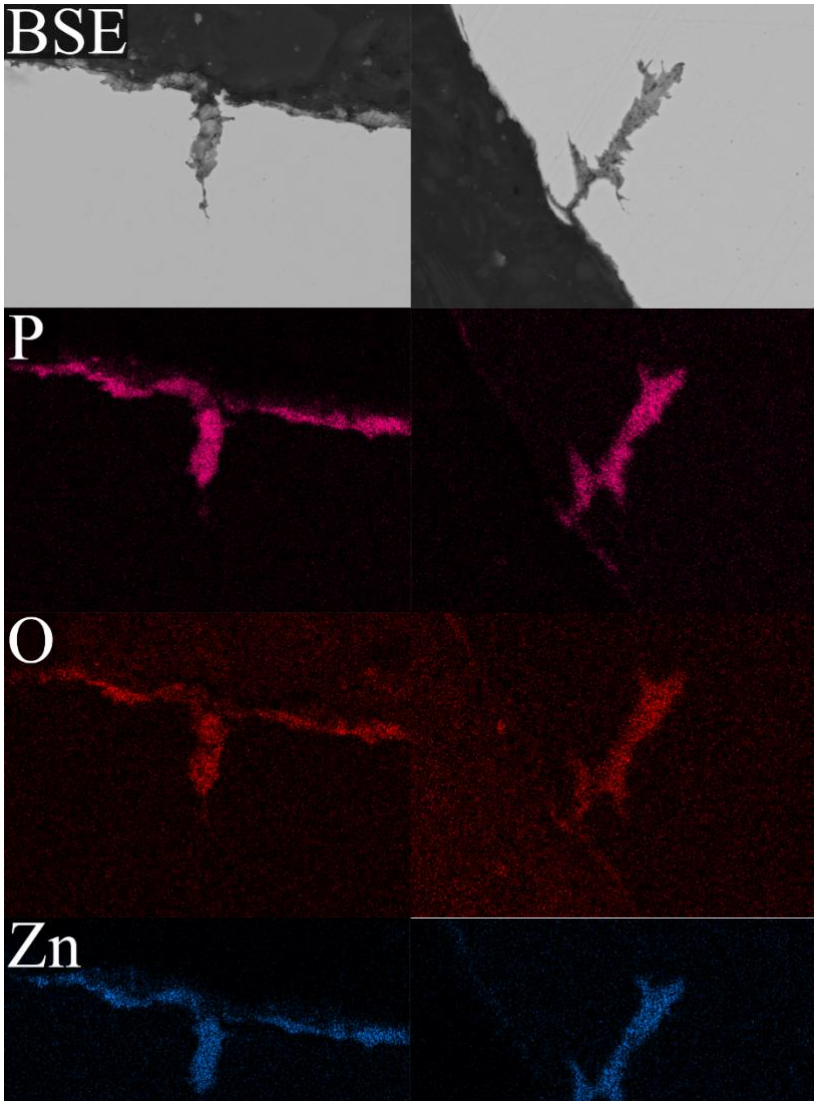

Figure 28 EDS mapping of the cross section over the surface of Forsmark Nya 1. Top row shows a back Scattered Electron image and the lower rows show P, O and Zn elemental maps. Intensity of the colour in the elemental maps correspond to a higher signal from that element.

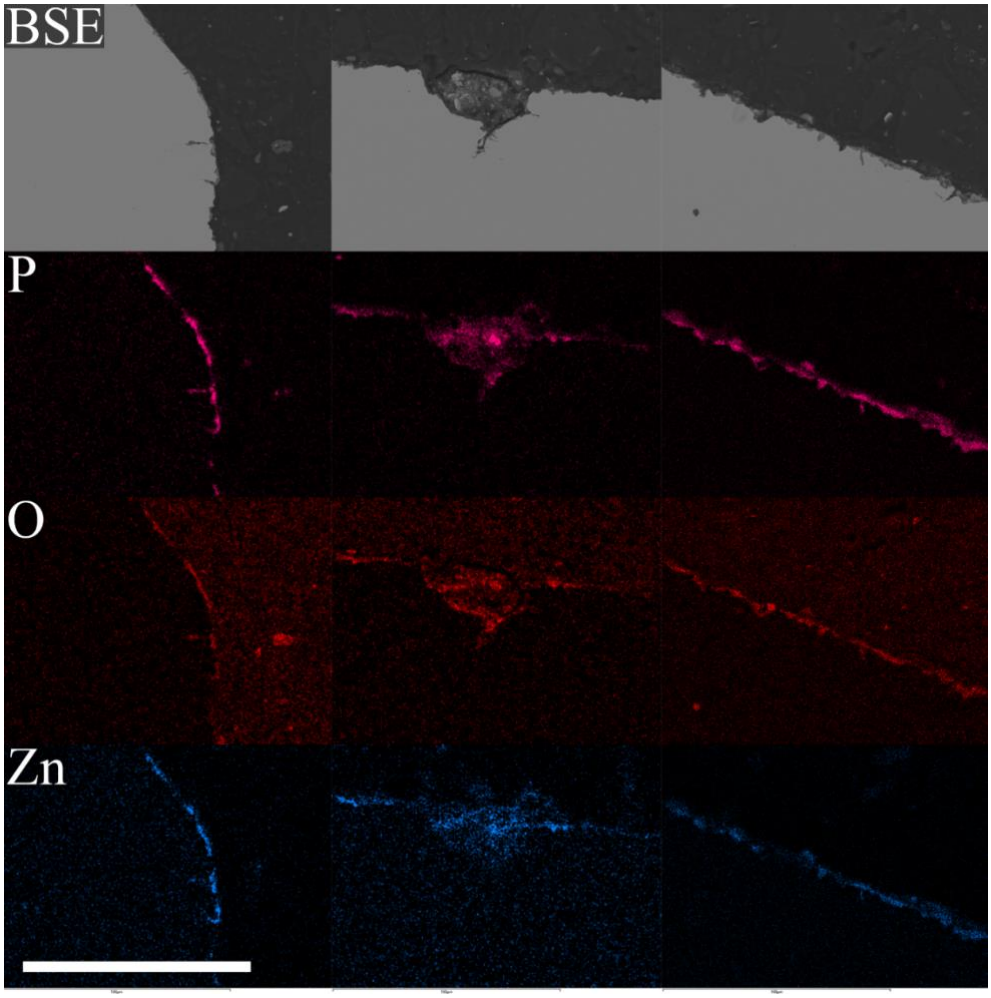

Figure 29 EDS mapping of the cross section over the surface of Forsmark 3 V #1. Top row shows a back Scattered Electron image and the lower rows show P, O and Zn elemental maps. Intensity of the colour in the elemental maps correspond to a higher signal from that element.

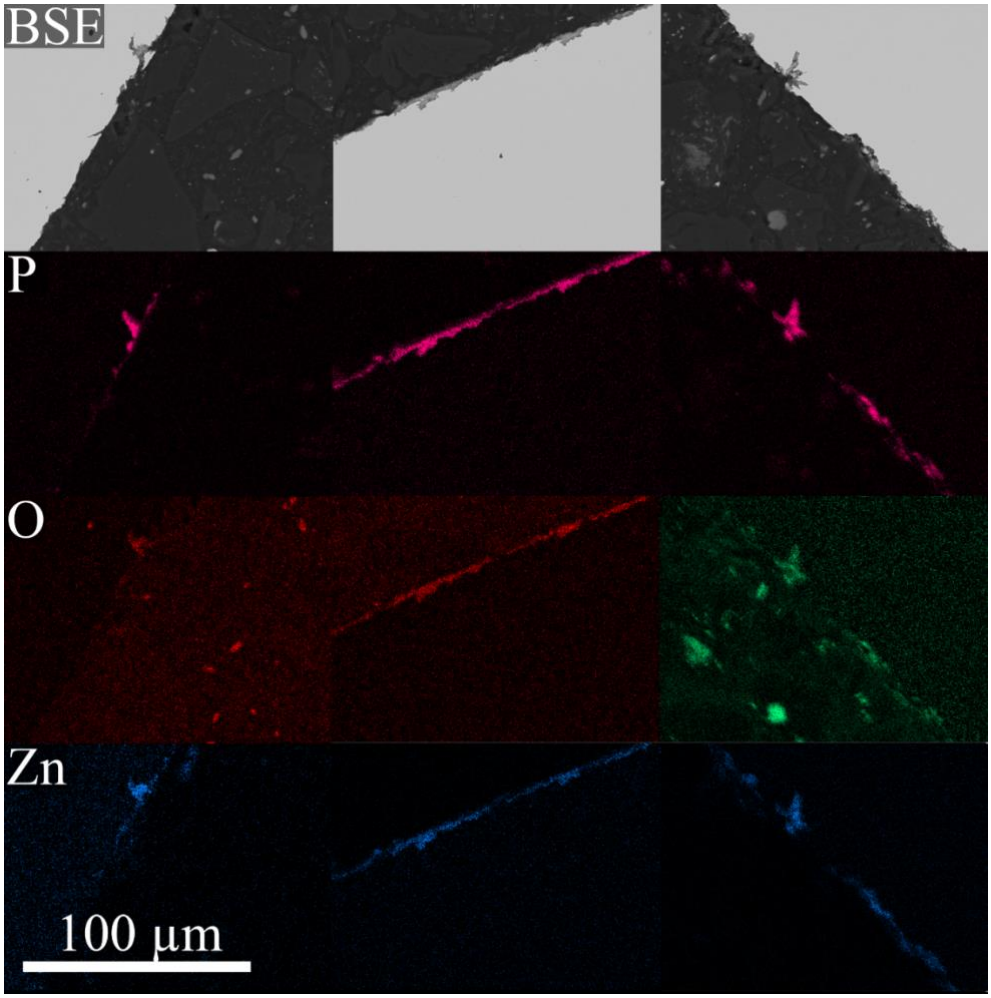

Figure 30 EDS mapping of the cross section over the surface of Ringhals 3 D mitten. Top row shows a back Scattered Electron image and the lower rows show P, O and Zn elemental maps. Intensity of the colour in the elemental maps correspond to a higher signal from that element.

5.3.6 Analysis after hydrogen exposure and bend test

After bend test according to SS 11 26 22 a clear difference in appearance of the fractured surface can be seen. SEM imaging of the fractured surface from three samples, R4D 10B, R4H 3B exposed for 24h in H_2 and R4D 12B exposed for 24h in H_2. In the upper area of each figure an overview micrograph of the sample can be seen. The fracture area extends outside the frame of the overview image. On the right of the overview a photograph of the samples can be seen taken from above and from the side. The unexposed sample showed a significantly shorter fracture surface compared to the exposed samples. They showed a long and thin fracture, bending outward.
For sample R4D 10B all areas show a ductile fracture. Both the crack initiation area (A in Figure 31) and in the central and bed area (B and C in Figure 31). Multiple bends during the test initiated cracks at different hights in the sample, which can be clearly seen in the overview.
The exposed samples R4H 3B and R4D 12B in Figure 32 and Figure 32 show similar fracture morphology. At the crack initiation site (A in the Figures) a remarkably different appearance can be seen. This area has been subjected to repeating collisions

during the test, which resulted in smearing of the surface. However, it appears that there are areas consistent with a brittle fracture with trans granular cracking.
In the central area the fracture is ductile in all samples, see site B in Figures 32-33. The lack of brittleness in the central part could be explained with the limited diffusion of hydrogen into the central part of the sample.
On the long thin fracture surface, see area C in Figures 32-33 a significantly more brittle appearance can be seen. This area is characterized by long brittle decohesion of the grains in the material as marked with the green arrows in the figures below. In between the decohesion events, a ductile fracture surface can be seen. Further features in this area, which seems to exhibit a more of a peeling force on the material, a steplike morphology can be seen. It is most clearly seen in figure 10 marked with a red arrow and can also be seen in the low magnification image (with the 120 μm scale bar). These features are present on all the hydrogen exposed samples.

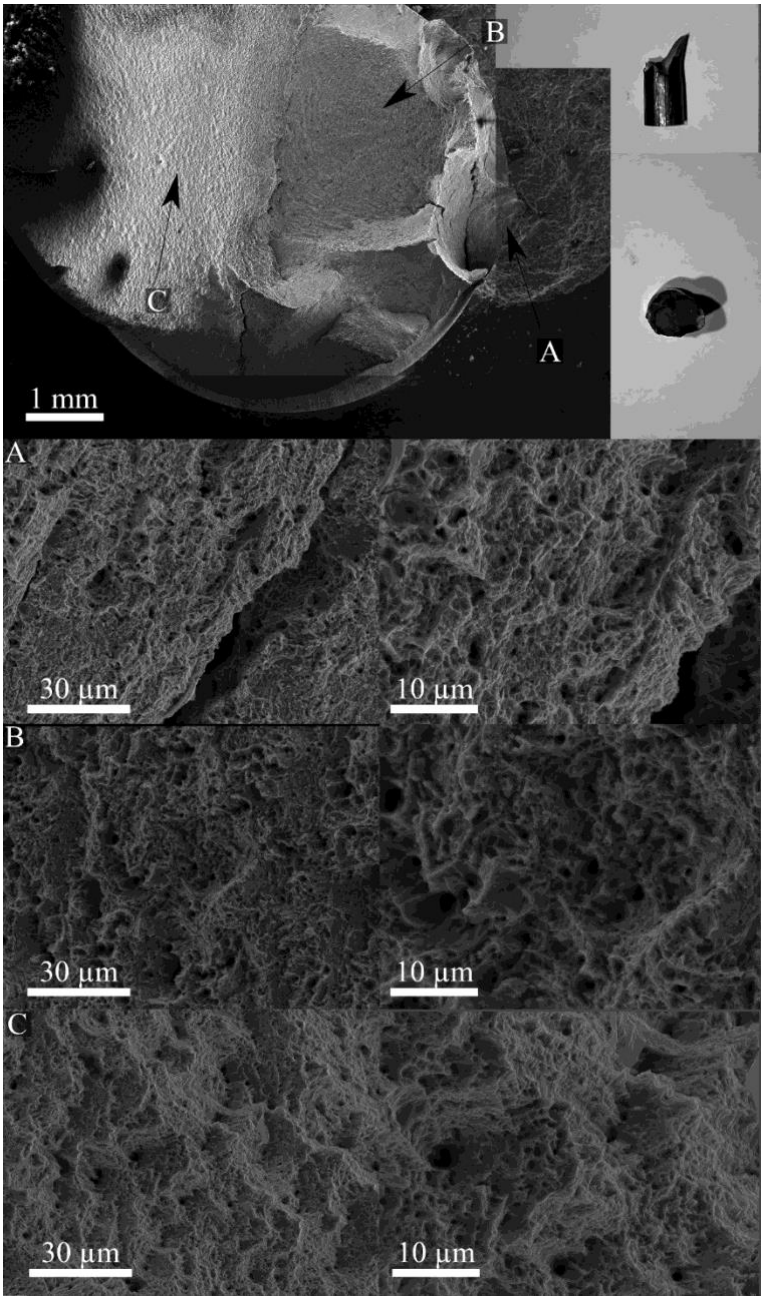

Figure 31 Unexposed R4D 10B sample. Fracture surface imaged at different magnifications, corresponding areas in the overview micrograph. For reference two photographs from different angles of the sample is shown to the right of the overview.

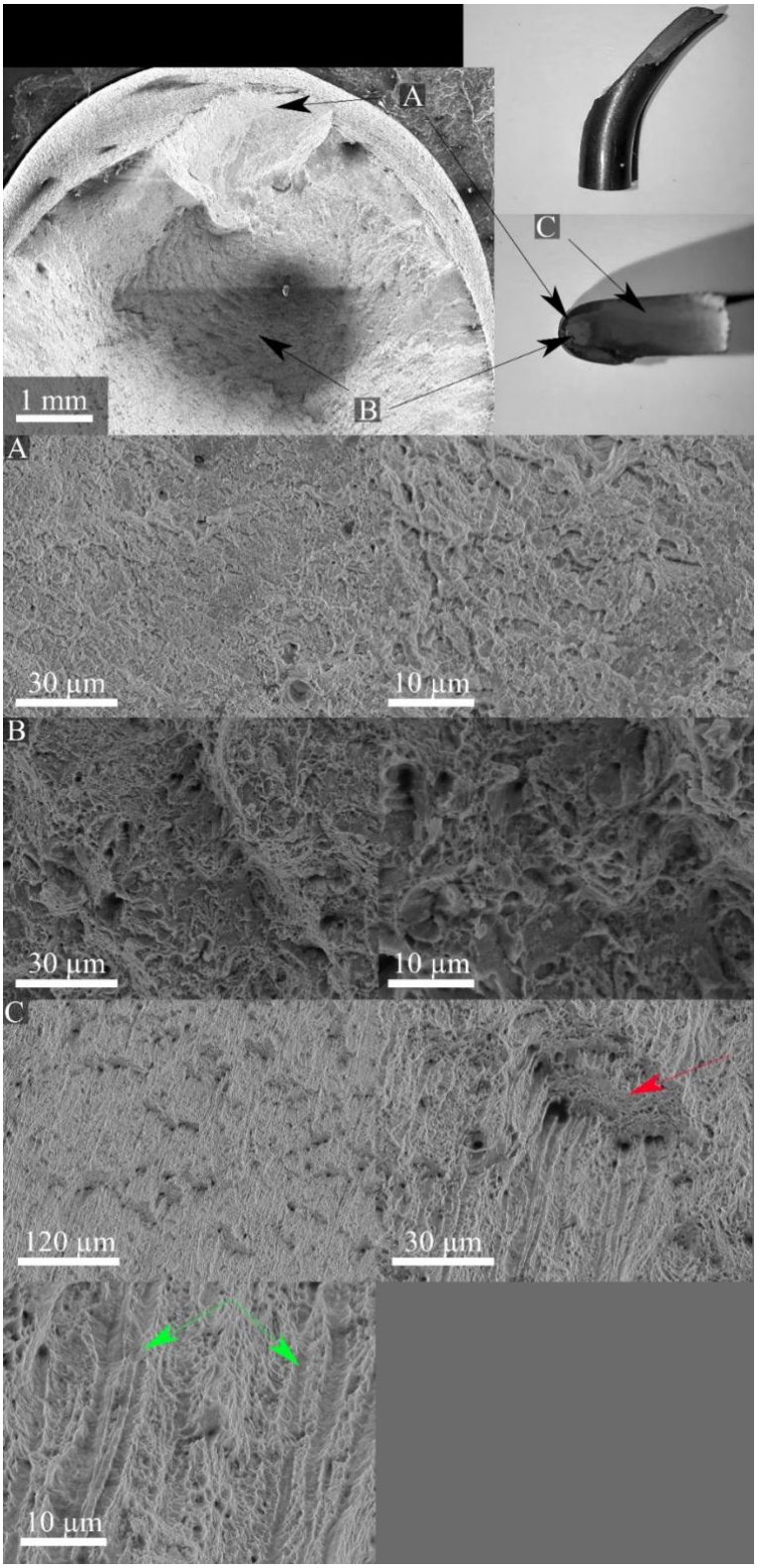

Figure 32 R4H 3B 24h H_2 sample. Fracture surface imaged at different magnifications, corresponding areas in the overview micrograph. For reference two photographs from different angles of the sample is shown to the right of the overview.

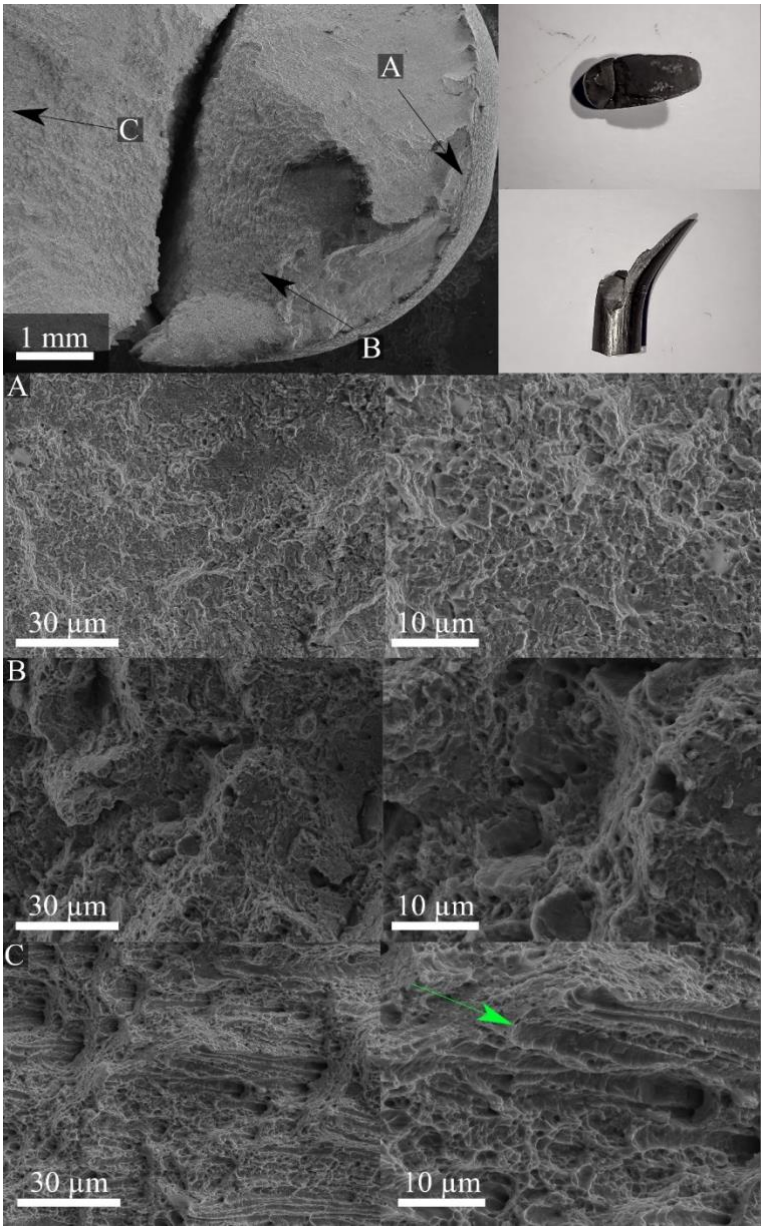

Figure 33 R4D 12B 24h H_2 sample. Fracture surface imaged at different magnifications, corresponding areas in the overview micrograph. For reference two photographs from different angles of the sample is shown to the right of the overview.

Conclusion

For the tensile test, no visible difference could be seen between the samples, either between the different sites or whether the samples were exposed or not. All samples had ductile fractures. This was also consistent with the mechanical data. Neither could any ongoing degradation process be seen. All samples showed similar morphology and chemistry on the surface.

For the samples subjected to the bending test, a clear difference between exposed and unexposed samples could be seen. A fracture morphology at the initiation site, that is consistent with a brittle fracture could be seen in the initiation site. No such appearance could be seen in the unexposed sample, where ductile fractures were present across the entire fracture area.

In the “peeling” area a decohesion of grain could be seen, consistent with a brittle fracture, as well as a step morphology. The centre of the hydrogen exposed samples showed a ductile fracture appearance. This is consistent with a diffusion mechanism of hydrogen into the material, embrittling the outer most volume of the sample.

6 Conclusions and future research

The following conclusion can be drawn from the statistical analysis of the database, experimental campaign of used and unused wires and literature review concerning durability and corrosion mechanisms of hard steel under long-term stress:

1. The analyzed database is characterized with high variability which implicates high uncertainty of the observed trends. Only for a few containments the trends for ultimate elongation were statistically meaningful (the change of mean value was greater than the confidence interval of 95 %. Also, for the reversed bending test the identified trends were statistically meaningful by the same criteria.

2. The only clear, statistically meaningful trends were observed for ultimate elongation. The most pronounce decrease of ductility was observed for Forsmark 1&2 where VSL 19 Ø13 mm, 7-wire strands were applied, and tendons are placed in dry air corrosion protection.

3. The new mechanical results obtained within the project did not confirm the material degradation suggested by trends identified by statistical analysis concerning tensile strength and ultimate elongation. The observed statistically meaningful trends probably have deterministic nature related to either samples damage at extraction, different testing procedure or malfunction of used equipment that was not reported.

4. The chemical analysis did not indicate any clear differences in steel composition between the containments and between the new and aged material. The carbon content was stable between the containments, as well as between the used and unused wires. Sulfur and Phosphorus content was significantly higher than the standard requirement. The S and P origin is probably remaining from anti-corrosion protection. Some minor Aluminum remains from production stage were also found.

5. The microscopic analysis of the fracture surfaces from uniaxial tensile test and cross-sections neither have exhibited direct signs of hydrogen embrittlement, nor has identified any significant corrosion.

6. No significant differences were identified in the microscopic investigation between the new and prestressed samples. Both type of samples showed surface defects (microcracks) and aluminum inclusions originated probably during manufacturing.

7. The detected material surface defects observed by EDS may be one of the reasons of high results scatter in mechanical tests. Moreover, microcracks could be responsible for the embrittlement observed in revers bend test.

8. For the samples subjected to the reversed bending test, a clear difference between exposed and unexposed samples could be seen. A fracture morphology at the initiation site, that is consistent with a brittle fracture could be seen in the initiation site. No such appearance could be seen in

the unexposed sample, where ductile fractures were present across the entire fracture area.

Basing on the obtained data the following further research directions are suggested:

1. The large discrepancies between the historical and newly obtained results bring the question of the testing procedures, machines, and data processing reliability. To ensure the repeatability and certainty of the obtained results in the future a series of round-robin tests with an accredited lab could be helpful.
2. The question of increased embrittlement over time in the reversed bend test remains unsolved due to lack of new results confirming or excluding the identified trends. This matter could be investigated in subsequent projects for instance by fracture surfaces SEM analysis of unused and used wires to investigate if the surface microcracks are propagating further under hydrogen treatment for used wires than for unused once.
3. The decreasing trend of ultimate elongation was the strongest Forsmark 1 and Forsmark 2, where no samples were experimentally tested within this project. In the subsequent research similar testing could be performed for wires extracted from those containments which had different wires (VSL 19 Ø13 mm, 7-wire strands).

7 Appendix 1 – raw data used for the statistical analysis

7.1 RINGHALS 2 – TENSILE TEST

1975								
	Sample nr	Kabel nr	distance from "skalle"	Elastic modulus	Ultimate tensile force	Ultimate elongation	$F_{0,2}$	$F_{0,2}/F_m$
				[N/mm^2]	[kN]	[%]	[kN]	[-]
Ringhals 2	1	H 57 (lubricated)	2	194000	51.5	4.8	42.8	0.83
	2		3	194000	51.7	4.6	42.8	0.83
	3		31	194000	51.6	4.8	43.2	0.84
	4		38	194000	51.5	4.4	43.2	0.84
	5		59	194000	50.7	4.5	45.2	0.89
	6		60	194000	50.5	4.0	44.0	0.87
	Avg.		-	**194000**	**51.4**	**4.6**	**43.4**	**0.85**
	COV		-	**0.0%**	**1.0%**	**6.5%**	**2.1%**	**3.0%**
	7	H 194 (nongrouted)	2	193000	50.6	5.2	42.0	0.83
	8		3	193000	50.9	5.3	42.0	0.83
	9		32	201000	51.9	5.8	44.5	0.86
	10		39	201000	52.4	5.4	45.4	0.87
	11		59	194000	50.6	4.3	45.8	0.90
	12		60	194000	50.4	4.3	45.8	0.91
	Avg.		-	**163667**	**42.7**	**4.3**	**36.6**	**0.72**
	COV		-	**2.4%**	**1.9%**	**14.2%**	**4.9%**	**4.9%**
requirements SIS				-	48.1	3.00		0.85

1980								
	Sample nr	Kbel nr	distance from "skalle"	Elastic modulus	Ultimate tensile force	Ultimate elongation	$F_{0,2}$	$F_{0,2}/F_m$
				[N/mm^2]	[kN]	[%]	[kN]	[-]
Ringhals 2	1	H 190 (nongrouted)	End	193500	50.3	4.8	41.5	0.83
	2		Mid	189800	49.8	4.7	41.4	0.83
	3		End	194700	49.8	4.7	42.3	0.85
	Avg.		-	**192667**	**50.0**	**4.7**	**41.7**	**0.84**
	COV		-	**1.3%**	**0.6%**	**1.2%**	**1.2%**	**1.5%**
	4	H 198 (lubricated)	End	194700	53.0	4.8	45.3	0.85
	5		Mid	197300	53.4	4.1	46.3	0.87
	6		End	197300	52.9	4.0	46.0	0.87
	Avg.		-	**196433**	**53.1**	**4.3**	**45.9**	**0.86**
	COV		-	**0.8%**	**0.5%**	**10.1%**	**1.1%**	**0.9%**
	7	D 23 (lubricated)	End	188700	50.0	5.4	42.1	0.84
	8		Mid	197300	50.0	4.0	42.1	0.84
	9		End	192300	50.2	5.5	41.0	0.82
	Avg.		-	**192767**	**50.1**	**5.0**	**41.7**	**0.83**
	COV		-	**2.2%**	**0.2%**	**16.9%**	**1.5%**	**1.8%**
requirements SIS				-	47.2	3.0	-	0.85

1986								
	Sample nr	Kbel nr	Position	Elastic modulus	Ultimate tensile force	Ultimate elongation	$F_{0,2}$	$F_{0,2}/F_m$
				[N/mm^2]	[kN]	[%]	[kN]	[-]
Ringhals 2	1	D 57 (dom)	End	198470	50.3	3.3	46.6	0.93
	2		Mid	199150	49.2	3.1	42.7	0.87
	3		End	197130	48.8	3.0	42.2	0.86
	Avg.		-	**198250**	**49.4**	**3.1**	**43.8**	**0.89**
	COV		-	**0.5%**	**1.6%**	**4.9%**	**5.5%**	**3.9%**
	4	H 192 (lhorizontal)	End	196470	49.6	3.0	43.6	0.88
	5		Mid	197470	49.6	3.0	43.4	0.88
	6		End	196800	49.7	3.2	43.6	0.88
	Avg.		-	**196913**	**49.6**	**3.1**	**43.5**	**0.88**
	COV		-	**0.3%**	**0.1%**	**3.8%**	**0.3%**	**0.2%**
requirements SIS				-	47.2	3.0	-	0.85

1989								
	Sample nr	Kbel nr	Position	Elastic modulus	Ultimate tensile force	Ultimate elongation	$F_{0,2}$	$F_{0,2}/F_m$
				[N/mm^2]	[kN]	[%]	[kN]	[-]
Ringhals 2	1	H 117	End	195000	51.6	2.9	46.4	0.90
	2		Mid	193000	50.3	2.8	44.3	0.88
	3		End	194000	51.4	2.7	45.7	0.89
	Avg.		-	**194000**	**51.1**	**2.8**	**45.5**	**0.89**
	COV		-	**0.5%**	**1.4%**	**2.7%**	**2.4%**	**1.0%**
	4	H 122	End	192000	51.9	6.0	44.6	0.86
	5		Mid	190000	51.5	3.6	43.1	0.84
	6		End	193000	49.9	3.9	43.1	0.86
	Avg.		-	**191667**	**51.1**	**4.5**	**43.6**	**0.85**
	COV		-	**0.8%**	**2.1%**	**28.8%**	**2.0%**	**1.7%**
requirements SIS				-	50.1	3.5	-	0.85

1999								
	Sample nr	**Kbel nr**	**Position**	**Elastic modulus**	**Ultimate tensile force**	**Ultimate elongation**	**$F_{0,2}$**	**$F_{0,2}/F_m$**
				[N/mm^2]	**[kN]**	**[%]**	**[kN]**	**[-]**
Ringhals 2	1	H 111	End	194000	50.9	2.17	46.2	0.91
	2		Mid	186000	50.4	1.76	46.9	0.93
	3		End	201000	50.7	1.80	45.8	0.90
	Avg.		-	**193667**	**50.7**	**1.9**	**46.3**	**0.91**
	COV		-	**3.9%**	**0.5%**	**11.8%**	**1.2%**	**1.6%**
	4	D 56	End	203000	49.2	3.14	44.3	0.90
	5		Mid	187000	50.4	1.78	46.8	0.93
	6		End	187000	49.8	3.57	42.6	0.86
	Avg.		-	**192333**	**49.8**	**2.8**	**44.6**	**0.89**
	COV		-	**4.8%**	**1.2%**	**33.0%**	**4.7%**	**4.1%**
requirements SIS				-	50.1	3.5	-	0.85

2010								
	Sample nr	**Kbel nr**	**Position**	**Elastic modulus**	**Ultimate tensile force**	**Ultimate elongation**	**$F_{0,2}$**	**$F_{0,2}/F_m$**
				[N/mm^2]	**[kN]**	**[%]**	**[kN]**	**[-]**
Ringhals 2	1	H 109	End	179000	50.3	2.96	44.1	0.88
	2		Mid	194000	50.8	3.06	44.8	0.88
	3		Mid	189000	51.0	3.08	44.7	0.88
	4		End	188000	51.0	3.31	44.8	0.88
	Avg.		-	**190333**	**50.9**	**3.2**	**44.8**	**0.88**
	COV		-	**1.7%**	**0.2%**	**4.4%**	**0.1%**	**0.3%**
	5	D 79	End	187000	50.8	2.97	44.7	0.88
	6		Mid	191000	51.3	3.16	45.3	0.88
	7		End	195000	51.6	3.17	45.0	0.87
	Avg.		-	**191000**	**51.2**	**3.1**	**45.0**	**0.88**
	COV		-	**2.1%**	**0.8%**	**3.6%**	**0.7%**	**0.6%**
requirements SIS				-	50.1	3.5	-	0.85

2016								
	Sample nr	Kbel nr	Position	Elastic modulus [N/mm^2]	Ultimate tensile [kN]	Ultimate elongation [%]	$F_{0,2}$ [kN]	$F_{0,2}/F_m$ [-]
Ringhals 2	1	D 79	End	193000	50.8	3.10	44.6	0.88
	2		Mid	199000	50.2	2.84	44.3	0.88
	3		Mid	195000	50.0	2.58	44.8	0.90
	4		End	199000	50.4	2.89	44.4	0.88
	Avg.		-	**196500**	**50.4**	**2.9**	**44.5**	**0.88**
	COV		-	**1.5%**	**0.7%**	**7.5%**	**0.5%**	**0.9%**
	5	H193	End	192000	48.8	2.76	43.5	0.89
	6		Mid	190000	48.6	2.70	43.6	0.90
	7		Mid	198000	48.6	2.97	43.1	0.89
	8		End	208000	52.1	3.16	48.5	0.93
	Avg.		-	**197000**	**49.5**	**2.9**	**44.7**	**0.90**
	COV		-	**4.1%**	**3.5%**	**7.2%**	**5.7%**	**2.2%**
	9	H109	End	196000	49.4	3.04	43.9	0.89
	10		Mid	190000	49.6	3.01	44.2	0.89
	11		Mid	194000	49.8	3.35	44.0	0.88
	12		End	193000	49.5	2.73	44.9	0.91
	Avg.		-	**193250**	**49.6**	**3.0**	**44.2**	**0.89**
	COV		-	**1.3%**	**0.3%**	**8.4%**	**1.0%**	**1.1%**
	13	D 70	End	192000	50.5	2.85	44.7	0.89
	14		Mid	196000	50.9	3.37	44.6	0.88
	15		Mid	197000	50.7	3.12	44.8	0.88
	16		End	197000	50.6	3.06	44.5	0.88
	Avg.		-	**195500**	**50.7**	**3.1**	**44.6**	**0.88**
	COV		-	**1.2%**	**0.3%**	**6.9%**	**0.2%**	**0.4%**
	17	V 109	End	170000	50.0	2.74	43.6	0.87
	18		Mid	172000	50.5	2.92	44.0	0.87
	19		Mid	167000	50.6	3.20	43.9	0.87
	20		Mid	171000	50.3	3.09	43.4	0.86
	21		End	172000	49.8	2.77	44.0	0.88
	Avg.		-	**170400**	**50.2**	**2.9**	**43.8**	**0.87**
	COV		-	**1.2%**	**0.7%**	**6.8%**	**0.6%**	**0.9%**
requirements SIS				-	50.1	3.5	-	0.85

7.2 RINGHALS 2 – REVERSED BEND TEST

		1975						
		Sample nr	Hydrogene treatment time	Distance from "skalle"	Min	Max	Average	Fodran enl
			[h]	[-]	[-]	[-]	[-]	[-]
H 57	Ringhals 2	1	0	4	6	9	7.5	5.0
		2	0	32	6	8	7.0	-
		3	4	33	6	8	7.0	-
		4	24	34	5	8	6.5	
		5	0	61	4	6	5.5	-
H 194		6	0	4	5	7	6.0	-
		7	0	33	2	7	5.0	
		8	4	34	3	6	5.0	
		9	24	35	3	6	5.0	
		10	0	61	4	7	5.5	

		1980						
		Sample nr	Hydrogene treatment time	End	Mid	End	Average	Fodran enl
			[h]	[-]	[-]	[-]	[-]	[-]
H190	Ringhals 2	1	0	7	8	9	8.0	5.0
		2	4	6	6	6	6.0	-
		3	24	4	6	4	4.7	-
H 198		4	0	6	4	6	5.3	5.0
		5	4	4	6	5	5.0	-
		6	24	5	5	2	4.0	-
D 23		7	0	6	9	9	8.0	5.0
		8	4	5	6	4	5.0	-
		9	24	4	4	4	4.0	-

		1986						
		Sample nr	Hydrogene treatment time	End	Mid	End	Average	Fodran enl
			[h]	[-]	[-]	[-]	[-]	[-]
D 57	Ringhals 2	1	0	10	6	6	7.3	5.0
		2	4	8	2	4	4.7	-
		3	24	4	5	2	3.7	-
H 192		4	0	6	9	6	7.0	5.0
		5	4	4	6	2	4.0	-
		6	24	2	4	7	4.3	-

	1989							
		Sample nr	Hydrogene treatment time	End	Mid	End	Average	Fodran enl
			[h]	[-]	[-]	[-]	[-]	[-]
H 117	Ringhals 2	1	0	7	7	7	7.0	5.0
		2	4	7	7	5	6.3	-
		3	24	2	4	4	3.3	-
H 122		4	0	7	6	6	6.3	5.0
		5	4	8	6	7	7.0	-
		6	24	4	6	2	4.0	-

	1999							
		Sample nr	Hydrogene treatment time	End	Mid	End	Average	Fodran enl
			[h]	[-]	[-]	[-]	[-]	[-]
H 111	Ringhals 2	1	0	6	4	7	5.7	4.0
		2	4	5	5	5	5.0	-
		3	24	3	0	0	1.0	-
D 56		4	0	10	11	9	10.0	4.0
		5	4	3	5	4	4.0	-
		6	24	3	4	4	3.7	-

	2010							
		Sample nr	Hydrogene treatment time	End	Mid	End	Average	Fodran enl
			[h]	[-]	[-]	[-]	[-]	[-]
H 109	Ringhals 2	1	0	5	4	6	5.0	4.0
		2	4	2	3	2	2.3	-
		3	24	2	3	3	2.7	-
D 79		4	0	5	4	2	3.7	4.0
		5	4	0	2	1	1.0	-
		6	24	2	2	3	2.3	-

	2016							
		Sample nr	Hydrogene treatment time	End	Mid	End	Average	Fodran enl
			[h]	[-]	[-]	[-]	[-]	[-]
H 193	Ringhals 2	1	0	7	7	8	7.3	4.0
		2	4	4	3	6	4.3	-
		3	24	4	2	4	3.3	-
D 79		4	0	4	6	4	4.7	4.0
		5	4	1	2	2	1.7	-
		6	24	1	0	0	0.3	-
H 109		7	0	7	7	7	7.0	4.0
		8	4	2	2	2	2.0	-
		9	24	2	2	2	2.0	-
V 109		10	0	5	6	5	5.3	4.0
		11	4	4	2	2	2.7	-
		12	24	0	2	2	1.3	-
D 70		13	0	4	5	4	4.3	4.0
		14	4	0	3	4	2.3	-
		15	24	3	2	0	1.7	-

7.3 RINGHALS 3 – TENSILE TEST

1980								
	Sample nr	Kabel nr	Location	Elastic modulus	Ultimate tensile force	Ultimate elongation	$F_{0,2}$	$F_{0,2}/F_m$
				[N/mm^2]	[kN]	[%]	[kN]	[-]
Ringhals 3	1	D 115	End	208400	51.4	5.3	46.0	0.89
	2		Mid	208400	51.1	4.5	46.7	0.91
	3		End	208400	51.8	5.1	46.1	0.89
	Avg.		-	**208400**	**51.4**	**5.0**	**46.3**	**0.90**
	COV		-	**0.0%**	**0.7%**	**8.4%**	**0.8%**	**1.4%**
	4	H 202	End	208400	52.8	3.9	47.7	0.90
	5		Mid	208400	52.8	3.9	47.7	0.90
	6		End	197800	52.8	5.9	46.8	0.89
	Avg.		-	**204866.7**	**52.8**	**4.6**	**47.4**	**0.90**
	COV		-	**3.0%**	**0.0%**	**25.3%**	**1.1%**	**1.1%**
requirements SIS				-	50.1	3.50		0.85

1985								
	Sample nr	Kabel nr	Location	Elastic modulus	Ultimate tensile force	Ultimate elongation	$F_{0,2}$	$F_{0,2}/F_m$
				[N/mm^2]	[kN]	[%]	[kN]	[-]
Ringhals 3	1	D 25	End	202950	50.9	3.5	46.5	0.91
	2		Mid	204010	50.8	3.6	46.1	0.91
	3		End	204370	51.2	3.6	46.5	0.91
	Avg.		-	**203776.7**	**51.0**	**3.6**	**46.4**	**0.91**
	COV		-	**0.4%**	**0.4%**	**1.6%**	**0.5%**	**0.4%**
	4	H 198	End	199830	51.5	3.6	47.1	0.91
	5		Mid	201550	51.6	3.5	47.6	0.92
	6		End	201900	51.4	3.3	47.2	0.92
	Avg.		-	**201093.3**	**51.5**	**3.5**	**47.3**	**0.92**
	COV		-	**0.6%**	**0.2%**	**4.4%**	**0.6%**	**0.4%**
requirements SIS				-	50.1	3.50		0.85

1990								
	Sample nr	Kabel nr	Location	Elastic modulus	Ultimate tensile force	Ultimate elongation	$F_{0,2}$	$F_{0,2}/F_m$
				[N/mm^2]	[kN]	[%]	[kN]	[-]
Ringhals 3	1	D 51	End	204400	50.5	3.9	46.3	0.92
	2		Mid	201900	50.8	4.1	45.5	0.90
	3		End	203400	50.4	3.6	45.9	0.91
	Avg.		-	**203233.3**	**50.6**	**3.9**	**45.9**	**0.91**
	COV		-	**0.6%**	**0.4%**	**6.5%**	**0.9%**	**1.2%**
	4	H 117	End	190100	50.5	3.6	44.0	0.87
	5		Mid	198800	50.8	4	43.6	0.86
	6		End	182100	51.4	4.6	44.5	0.87
	Avg.		-	**190333.3**	**50.9**	**4.1**	**44.0**	**0.87**
	COV		-	**4.4%**	**0.9%**	**12.4%**	**1.0%**	**0.8%**
requirements SIS				-	50.1	3.50		0.85

2000								
	Sample nr	Kabel nr	Location	Elastic modulus	Ultimate tensile force	Ultimate elongation	$F_{0,2}$	$F_{0,2}/F_m$
				[N/mm^2]	[kN]	[%]	[kN]	[-]
Ringhals 3	1	H 68	End	191000	50.8	3.17	47.9	0.94
	2		Mid	205000	50.9	3.35	47.7	0.94
	3		End	210000	50.8	3.16	47.8	0.94
	Avg.		-	**202000**	**50.8**	**3.2**	**47.8**	**0.94**
	COV		-	**4.9%**	**0.1%**	**3.3%**	**0.2%**	**0.3%**
	4	D 119	End	207000	50.1	3.50	45.9	0.92
	5		Mid	207000	49.7	3.13	46.0	0.93
	6		End	205000	49.9	3.09	46.2	0.93
	Avg.		-	**206333.3**	**49.9**	**3.2**	**46.0**	**0.92**
	COV		-	**0.6%**	**0.4%**	**7.0%**	**0.3%**	**0.6%**
requirements SIS				-	50.1	3.50		0.85

2010								
	Sample nr	Kabel nr	Location	Elastic modulus	Ultimate tensile force	Ultimate elongation	$F_{0,2}$	$F_{0,2}/F_m$
				[N/mm^2]	[kN]	[%]	[kN]	[-]
Ringhals 3	1	H 114	End	179000	51.6	4.18	44.2	0.86
	2		Mid	178000	50.2	3.04	44.2	0.88
	3		Mid	174000	51.2	4.02	43.7	0.85
	4		End	184000	50.9	4.02	43.9	0.86
	Avg.		-	**178750**	**51.0**	**3.8**	**44.0**	**0.86**
	COV		-	**2.3%**	**1.2%**	**13.7%**	**0.6%**	**1.4%**
	5	D 41	End	205000	50.9	3.65	46.4	0.91
	6		Mid	216000	51.7	4.45	46.6	0.90
	7		Mid	208000	51.3	4.15	46.4	0.90
	8		End	205000	51.1	4.02	46.6	0.91
	Avg.		-	**208500**	**51.3**	**4.1**	**46.5**	**0.91**
	COV		-	**2.5%**	**0.7%**	**8.1%**	**0.2%**	**0.6%**
requirements SIS				-	50.1	3.50		0.85

RISE 2021								
	Sample nr	Kabel nr	Location	Elastic modulus	Ultimate tensile force	Ultimate elongation	$F_{0,2}$	$F_{0,2}/F_m$
				[N/mm^2]	[kN]	[%]	[kN]	[-]
Ringhals 3	1	H 46	**End**		**50.5**	**4.3**	**46.1**	**0.91**
	2		**End**		**50.5**	**4.3**	**45.7**	**0.85**
	3		Mid		50.8	5.2	46.2	0.86
	Avg.		-		**50.6**	**4.6**	**46.0**	**0.88**
	COV		-		**0.4%**	**11.3%**	**0.5%**	**3.6%**
	4	D 59	End		51.7	5.1	44.8	0.87
	5		End		51.9	4.4	44.1	0.85
	6		Mid		51.5	5.3	44.9	0.87
	Avg.		-		**51.7**	**4.9**	**44.6**	**0.86**
	COV		-		**0.3%**	**9.6%**	**0.9%**	**1.2%**
requirements SIS				-	50.1	3.50		0.85

7.4 RINGHALS 3 – REVERSED BEND TEST

	1980							
		Sample nr	Hydrogene treatment time	End	Mid	End	Average	Fodranenl
			[h]	[-]	[-]	[-]	[-]	[-]
D 115	Ringhals 3	1	0	8	8	8	8.0	5.0
		2	4	8	8	7	7.7	-
		3	24	5	4	4	4.3	-
H 202		4	0	9	9	8	8.7	5.0
		5	4	4	4	4	4.0	-
		6	24	6	3	4	4.3	-

	1985							
		Sample nr	Hydrogene treatment time	End	Mid	End	Average	Fodranenl
			[h]	[-]	[-]	[-]	[-]	[-]
D 25	Ringhals 3	1	0	8	9	8	8.3	5.0
		2	4	5	8	5	6.0	-
		3	24	4	6	6	5.3	-
H 198		4	0	11	10	8	9.7	5.0
		5	4	5	4	5	4.7	-
		6	24	6	6	5	5.7	-

		1990						
		Sample nr	Hydrogene treatment time	End	Mid	End	Average	Fodran enl
			[h]	[-]	[-]	[-]	[-]	[-]
D 51	Ringhals 3	1	0	6	6	7	6.3	5.0
		2	4	7	7	7	7.0	-
		3	24	4	4	5	4.3	-
H 117		4	0	5	7	9	7.0	5.0
		5	4	7	7	8	7.3	-
		6	24	5	4	5	4.7	-

		2000						
		Sample nr	Hydrogene treatment time	End	Mid	End	Average	Fodran enl
			[h]	[-]	[-]	[-]	[-]	[-]
D 68	Ringhals 3	1	0	6	3	7	5.3	5.0
		2	4	4	5	6	5.0	-
		3	24	2	4	2	2.7	-
H 119		4	0	6	8	7	7.0	5.0
		5	4	5	4	4	4.3	-
		6	24	2	4	2	2.7	-

		2010						
		Sample nr	Hydrogene treatment time	End	Mid	End	Average	Fodran enl
			[h]	[-]	[-]	[-]	[-]	[-]
H 114	Ringhals 3	1	0	6	8	4	6.0	4.0
		2	4	3	5	3	3.7	-
		3	24	2	4	2	2.7	-
D 41		4	0	7	8	8	7.7	4.0
		5	4	4	5	4	4.3	-
		6	24	5	4	4	4.3	-

7.5 RINGHALS 4 – TENSILE TEST

1981								
	Sample nr	Kabel nr	Location	Elastic modulus	Ultimate tensile force	Ultimate elongation	$F_{0,2}$	$F_{0,2}/F_m$
				[N/mm^2]	[kN]	[%]	[kN]	[-]
Ringhals 4	1	D 115	End	197470	51.0	3.9	45.0	0.88
	2		Mid	199320	51.0	3.2	45.0	0.88
	3		End	199320	51.0	3.2	45.0	0.88
	Avg.		**-**	**198703**	**51.0**	**3.4**	**45.0**	**0.88**
	COV		**-**	**0.5%**	**0.0%**	**11.8%**	**0.0%**	**0.0%**
	4	H 202	End	202260	49.9	3.4	45.0	0.90
	5		Mid	203300	49.4	3.4	45.0	0.91
	6		End	201550	50.0	3.6	45.0	0.90
	Avg.		**-**	**202370**	**49.8**	**3.5**	**45.0**	**0.90**
	COV		**-**	**0.4%**	**0.6%**	**3.3%**	**0.0%**	**0.6%**
requirements SIS				-	47.2	3.00		0.85

1986								
	Sample nr	Kabel nr	Location	Elastic modulus	Ultimate tensile force	Ultimate elongation	$F_{0,2}$	$F_{0,2}/F_m$
				[N/mm^2]	[kN]	[%]	[kN]	[-]
Ringhals 4	1	D 26	End	200200	49.7	3.8	45.8	0.92
	2		Mid	199500	50.0	4.6	45.4	0.91
	3		End	200000	50.1	4.1	46.2	0.92
	Avg.		**-**	**199900**	**49.9**	**4.2**	**45.8**	**0.92**
	COV		**-**	**0.2%**	**0.4%**	**9.7%**	**0.8%**	**0.9%**
	4	H 198	End	199200	51.9	4.4	47.6	0.92
	5		Mid	200000	51.3	3.9	47.1	0.92
	6		End	200800	51.2	3.6	47.7	0.93
	Avg.		**-**	**200000**	**51.4**	**4.0**	**47.5**	**0.92**
	COV		**-**	**0.4%**	**0.7%**	**10.2%**	**0.7%**	**0.8%**
requirements SIS				-	47.2	3.00		0.85

1991								
	Sample nr	Kabel nr	Location	Elastic modulus	Ultimate tensile force	Ultimate elongation	$F_{0,2}$	$F_{0,2}/F_m$
				[N/mm^2]	[kN]	[%]	[kN]	[-]
Ringhals 4	1	D 26	End	199800	50.6	4.2	45.5	0.90
	2		Mid	199800	51.3	4.2	46.3	0.90
	3		End	194800	51.5	**3.0**	45.0	0.87
	Avg.		-	**198133**	**51.1**	**3.8**	**45.6**	**0.89**
	COV		-	**1.5%**	**0.9%**	**18.2%**	**1.4%**	**1.8%**
	4	H 198	End	190100	50.2	4.2	43.7	0.87
	5		Mid	192400	51.2	4.2	46.1	0.90
	6		End	196200	50.8	4.1	46.3	0.91
	Avg.		-	**192900**	**50.7**	**4.2**	**45.4**	**0.89**
	COV		-	**1.6%**	**1.0%**	**1.4%**	**3.2%**	**2.4%**
requirements SIS				-	47.2	3.00		0.85

2001								
	Sample nr	Kabel nr	Location	Elastic modulus	Ultimate tensile force	Ultimate elongation	$F_{0,2}$	$F_{0,2}/F_m$
				[N/mm^2]	[kN]	[%]	[kN]	[-]
Ringhals 4	1	D 120	End	185300	51.7	4.5	42.1	0.81
	2		Mid	198200	51.8	4.5	46.1	0.89
	3		End	207300	51.4	3.9	46.8	0.91
	Avg.		-	**196933**	**51.6**	**4.3**	**45.0**	**0.87**
	COV		-	**5.6%**	**0.4%**	**7.4%**	**5.6%**	**5.8%**
	4	H 60	End	202600	51.8	3.9	46.9	0.91
	5		Mid	204400	51.8	4.1	47.2	0.91
	6		End	200300	51.5	3.9	47.1	0.91
	Avg.		-	**202433**	**51.7**	**4.0**	**47.1**	**0.91**
	COV		-	**1.0%**	**0.3%**	**3.6%**	**0.3%**	**0.5%**
requirements SIS				-	47.2	3.50		0.85

2010								
	Sample nr	**Kabel nr**	**Location**	**Elastic modulus**	**Ultimate tensile force**	**Ultimate elongation**	**$F_{0,2}$**	**$F_{0,2}/F_m$**
				[N/mm^2]	**[kN]**	**[%]**	**[kN]**	**[-]**
Ringhals 4	1	H 71	End	195000	51.9	3.5	44.7	0.86
	2		Mid	180000	52.0	4.1	45.1	0.87
	3		MId	198000	52.2	4.1	44.7	0.86
	4		End	183000	52.4	3.7	45.9	0.88
	Avg.		**-**	**189000**	**52.1**	**3.8**	**45.1**	**0.87**
	COV		**-**	**4.7%**	**0.4%**	**6.6%**	**1.3%**	**1.0%**
	5	D 128	End	199000	51.6	4.1	47.3	0.92
	6		Mid	198000	52.0	4.5	47.2	0.91
	7		Mid	201000	52.0	4.4	47.2	0.91
	8		End	199000	51.5	4.1	47.2	0.92
	Avg.		**-**	**199250**	**51.8**	**4.3**	**47.2**	**0.91**
	COV		**-**	**0.6%**	**0.5%**	**5.7%**	**0.1%**	**0.6%**
requirements SIS				-	50.1	3.50		0.85

RISE 2021								
	Sample nr	**Kabel nr**	**Location**	**Elastic modulus**	**Ultimate tensile force**	**Ultimate elongation**	**$F_{0,2}$**	**$F_{0,2}/F_m$**
				[N/mm^2]	**[kN]**	**[%]**	**[kN]**	**[-]**
Ringhals 4	1	H 18	End		53.0	5.2	47.9	0.90
	2		Mid		53.0	4.7	47.8	0.90
	3		**End**		**50.7**	**4.3**	**46.0**	**0.91**
	Avg.		**-**		**52.2**	**4.7**	**47.2**	**0.90**
	COV		**-**		**2.6%**	**9.5%**	**2.2%**	**0.4%**
	4	D 45	End		54.2	5.2	49.0	0.90
	5		Mid		53.6	4.7	48.3	0.90
	6		End		53.3	4.1	48.3	0.90
	Avg.		**-**		**53.7**	**4.7**	**48.5**	**0.90**
	COV		**-**		**0.8%**	**11.8%**	**0.9%**	**0.2%**
requirements SIS				-	50.1	3.50		0.85

7.6 RINGHALS 4 – REVERSED BEND TEST

		1981						
		Sample nr	Hydrogene treatment time	End	Mid	End	Average	Fodran enl
			[h]	[-]	[-]	[-]	[-]	[-]
D 115	Ringhals 4	1	0	9	8	10	9.0	5.0
		2	4	4	5	5	4.7	-
		3	24	6	4	6	5.3	-
H 202		4	0	8	7	8	7.7	5.0
		5	4	5	3	4	4.0	-
		6	24	3	2	5	3.3	-

		1986						
		Sample nr	Hydrogene treatment time	End	Mid	End	Average	Fodran enl
			[h]	[-]	[-]	[-]	[-]	[-]
D 26	Ringhals 4	1	0	8	8	9	8.3	5.0
		2	4	8	8	8	8.0	-
		3	24	6	6	5	5.7	-
H 198		4	0	9	8	6	7.7	5.0
		5	4	6	6	8	6.7	-
		6	24	6	5	5	5.3	-

		1991						
		Sample nr	Hydrogene treatment time	End	Mid	End	Average	Fodran enl
			[h]	[-]	[-]	[-]	[-]	[-]
D 79	Ringhals 4	1	0	10	9	10	9.7	5.0
		2	4	9	9	9	9.0	-
		3	24	6	5	6	5.7	-
H 112		4	0	6	6	9	7.0	5.0
		5	4	7	7	8	7.3	-
		6	24	5	6	8	6.3	-

	2001							
		Sample nr	Hydrogene treatment time	End	Mid	End	Average	Fodran enl
			[h]	[-]	[-]	[-]	[-]	[-]
D 120	Ringhals 4	1	0	8	8	8	8.0	4.0
		2	4	7	7	6	6.7	-
		3	24	6	6	6	6.0	-
H 60		4	0	8	9	8	8.3	4.0
		5	4	6	5	6	5.7	-
		6	24	4	4	2	3.3	-

	2010							
		Sample nr	Hydrogene treatment time	End	Mid	End	Average	Fodran enl
			[h]	[-]	[-]	[-]	[-]	[-]
D 128	Ringhals 4	1	0	8	8	8	8.0	4.0
		2	4	8	6	7	7.0	-
		3	24	4	6	4	4.7	-
H 71		4	0	12	10	8	10.0	4.0
		5	4	8	6	4	6.0	-
		6	24	5	4	7	5.3	-

7.7 FORSMARK 1 – TENSILE TEST

1980						
	Sample nr	Area	Force at 1% elongation	Elastic modulus	Ultimate tensile force	Ultimate elongation
		[mm^2]	[kN]	[N/mm^2]	[kN]	[%]
Forsmark 1	1	99.1	173	196200	188	6.1
	2	99.2	172	194400	189	7.2
	3	99.2	170	186700	189	6.7
	4	99.6	166	192000	189	8.1
	5	99.6	171	190000	189	6.7
	6	99.8	174	194800	191	6.5
	Avg.	**99.4**	**171**	**192350**	**189**	**6.9**
	COV	**0.3%**	**1.7%**	**1.8%**	**0.5%**	**10.1%**
Forsmark 2	7	99.7	174	198300	192	7.8
	8	99.6	172	194200	192	7.5
	9	97.5	167	190900	187	7.4
	10	98.6	168	190800	187	7.4
	11	99.2	172	195500	191	7.3
	12	98.6	168	192900	187	7.7
	Avg.	**98.9**	**170**	**193767**	**189**	**7.5**
	COV	**0.8%**	**1.7%**	**1.5%**	**1.4%**	**2.6%**
requirements SIS		100^{-2}_{+4}	min 156	-	183	3.5

1985						
	Sample nr	Area	Force at 1% elongation	Elastic modulus	Ultimate tensile force	Ultimate elongation
		[mm^2]	[kN]	[N/mm^2]	[kN]	[%]
Forsmark 1	1	99.6	165.3	-	191.1	8.2
	2	99.8	165.9	-	194.7	9.3
	3	99.7	169.2	-	189.8	7.7
	4	99.7	165.1	-	191.5	8.5
	5	98.7	159.9	-	185.4	8.1
	6	98.5	166.8	-	187.2	8.8
	7	99.5	166.3	-	186.9	8.3
	8	99.3	164.4	-	186.9	8.9
	9	99.2	162.6	-	187.4	8.4
	10	99.1	167.6	-	185.4	7.1
	Avg.	**99.3**	**165**		**189**	**8.3**
	COV	**0.4%**	**1.6%**		**1.6%**	**7.5%**
requirements SIS		100^{-2}_{+4}	min 156	-	183	3.5

1988						
	Sample nr	**Area**	**Force at 1% elongation**	**Elastic modulus**	**Ultimate tensile force**	**Ultimate elongation**
		[mm²]	**[kN]**	**[N/mm²]**	**[kN]**	**[%]**
Forsmark 1	1	99.4	174.8	193000	193.2	5.1
	2	99.3	174.2	193000	191.6	6.0
	3	99.4	171.6	189000	194.6	6.8
	4	99.5	173.0	195000	193.7	6.3
	5	99.4	170.8	189000	193.9	6.2
	6	99.5	170.5	195000	191.4	7.0
	7	99.6	171.6	194000	191.5	7.1
	8	99.5	170.5	191000	190.5	6.4
	Avg.	**99.5**	**172**	**192375**	**193**	**6.4**
	COV	**0.1%**	**1.0%**	**1.3%**	**0.8%**	**10.1%**
requirements SIS		100^{-2}_{+4}	min 156	-	183	3.5

1998						
	Sample nr	**Area**	**Force at 1% elongation**	**Elastic modulus**	**Ultimate tensile force**	**Ultimate elongation**
		[mm²]	**[kN]**	**[N/mm²]**	**[kN]**	**[%]**
Forsmark 1	1	99.8	170	185000	186	6.1
	2	99.9	170	184000	186	7.1
	3	100.1	174	185000	190	5.8
	4	99.5	168	186000	183	6.0
	5	99.8	167	189000	182	5.5
	6	99.5	171	186000	186	5.5
	7	99.7	165	188000	186	6.7
	8	99.0	163	183000	184	5.4
	9	99.7	168	191000	187	6.2
	Avg.	**99.7**	**168**	**186333**	**186**	**6.0**
	COV	**0.3%**	**1.9%**	**1.4%**	**1.3%**	**9.5%**
requirements SIS		100^{-2}_{+4}	min 156	-	183	3.5

2008							
	Sample nr	Area	Force at 1% elongation	Elastic modulus	Ultimate tensile force	Ultimate elongation	$F_{0,2}$
		[mm^2]	[kN]	[N/mm^2]	[kN]	[%]	[kN]
Forsmark 1	P5		169.1	196000	187.0	4.7	170.7
	P6		171.4	198000	186.8	3.8	173.1
	P8		170.2	205000	184.2	3.5	171.4
	P9		165.1	189000	185.2	4.5	168.4
	P10		164.5	192000	184.6	4.6	167.1
	P11		168.0	192000	184.6	4.7	171.4
	Avg.		**168**	**195333**	**185**	**4.3**	**170.4**
	COV		**1.6%**	**2.9%**	**0.7%**	**12.3%**	**1.3%**
requirements SIS		100^{-2}_{+4}	min 156	-	183	3.5	

7.8 FORSMARK 2 – TENSILE TEST

1980						
	Sample nr	Area	Force at 1% elongation	Elastic modulus	Ultimate tensile force	Ultimate elongation
		[mm^2]	[kN]	[N/mm^2]	[kN]	[%]
Forsmark 1	1	99.1	173	196200	188	6.1
	2	99.2	172	194400	189	7.2
	3	99.2	170	186700	189	6.7
	4	99.6	166	192000	189	8.1
	5	99.6	171	190000	189	6.7
	6	99.8	174	194800	191	6.5
	Avg.	**99.4**	**171**	**192350**	**189**	**6.9**
	COV	**0.3%**	**1.7%**	**1.8%**	**0.5%**	**10.1%**
Forsmark 2	7	99.7	174	198300	192	7.8
	8	99.6	172	194200	192	7.5
	9	97.5	167	190900	187	7.4
	10	98.6	168	190800	187	7.4
	11	99.2	172	195500	191	7.3
	12	98.6	168	192900	187	7.7
	Avg.	**98.9**	**170**	**193767**	**189**	**7.5**
	COV	**0.8%**	**1.7%**	**1.5%**	**1.4%**	**2.6%**
requirements SIS		100^{-2}_{+4}	min 156	-	183	3.5

1983						
	Sample nr	**Area**	**Force at 1% elongation**	**Elastic modulus**	**Ultimate tensile force**	**Ultimate elongation**
		[mm^2]	**[kN]**	**[N/mm^2]**	**[kN]**	**[%]**
Forsmark 2	1	99.9	170.6	194800	190.8	6.4
	2	100.0	170.3	193700	192.0	7.2
	3	100.0	170.3	194600	190.5	6.7
	4	99.3	166.2	193100	188.0	7.6
	5	99.2	165.3	193700	186.5	7.6
	6	99.3	165.2	192800	186.5	7.6
	7	99.6	170.0	194300	195.8	7.7
	8	99.6	171.3	195800	196.3	8.0
	9	99.6	169.0	191800	195.0	6.6
	Avg.	**99.6**	**169**	**193844**	**191**	**7.3**
	COV	**0.3%**	**1.4%**	**0.6%**	**2.0%**	**7.8%**
requirements SIS		100^{-2}_{+4}	min 156	-	183	3.5

1995						
	Sample nr	**Area**	**Force at 1% elongation**	**Elastic modulus**	**Ultimate tensile force**	**Ultimate elongation**
		[mm^2]	**[kN]**	**[N/mm^2]**	**[kN]**	**[%]**
Forsmark 2	1	98.8	165.5	187000	184.7	7.0
	2	99.7	169.0	187000	189.2	7.6
	3	98.5	167.2	187000	187.5	7.3
	4	99.6	170.0	185000	193.3	7.6
	5	99.6	171.5	187000	194.0	8.0
	6	99.7	172.2	190000	193.5	7.0
	Avg.	**99.3**	**169**	**187167**	**190**	**7.4**
	COV	**0.5%**	**1.5%**	**0.9%**	**2.0%**	**5.3%**
requirements SIS		100^{-2}_{+4}	min 156	-	183	3.5

2003							
	Sample nr	**Area**	**Force at 1% elongation**	**Elastic modulus**	**Ultimate tensile force**	**Ultimate elongation**	**$F_{0,2}$**
		[mm²]	**[kN]**	**[N/mm²]**	**[kN]**	**[%]**	**[kN]**
Forsmark 2	1		161.2	184100	183.4	4.73	164.70
	8		158.8	174800	183.0	4.65	164.90
	2		154.0	166600	181.8	4.83	162.70
	3		152.0	156900	182.4	4.94	164.00
	5		145.9	160700	180.0	4.71	161.90
	6		156.7	160600	181.4	4.66	165.90
	7		150.5	150700	178.0	5.17	164.90
	8		-	-	179.6	-	-
	Avg.		**152**	**159100**	**181**	**4.9**	**163.9**
	COV		**2.7%**	**3.7%**	**0.9%**	**4.2%**	**1.0%**
requirements SIS		100^{-2}_{+4}	min 156	-	183	3.5	

2016							
	Sample nr	**Area**	**Force at 1% elongation**	**Elastic modulus**	**Ultimate tensile force**	**Ultimate elongation**	**$F_{0,2}$**
		[mm²]	**[kN]**	**[N/mm²]**	**[kN]**	**[%]**	**[kN]**
Forsmark 2	5		159.1	170000	185.0	5.84	164.0
	7		164.2	194000	186.0	5.92	165.6
	9		164.7	187000	188.0	6.74	167.7
	6		161.7	189000	185.0	6.11	163.7
	Ingjutning			släppte	187.0	-	-
	8		161.7	188000	188.0	6.26	164.4
	12		157.1	179000	188.0	5.77	161.5
	13		160.2	181000	186.1	4.62	164.2
	11			-	190.0	-	177.8
	3		162.0	169000	187.0	6.01	166.3
	10		162.5	178000	189.0	6.84	167.8
	4		162.8	184000	186.0	6.24	166.2
	Avg.		**162**	**181900**	**187**	**6.0**	**166.3**
	COV		**1.4%**	**4.5%**	**0.8%**	**10.1%**	**2.6%**
requirements SIS		100^{-2}_{+4}	min 156	-	183	3.5	

7.9 FORSMARK 3 – TENSILE TEST

1986						
	Sample nr	Elastic modulus	Ultimate tensile force	Ultimate elongation	$F_{0,2}$	$F_{0,2}/F_m$
		[N/mm^2]	[kN]	[%]	[kN]	[-]
Forsmark 3	1	192700	50.3	3.7	44.6	0.89
	2	191200	50.6	3.8	44.8	0.89
	3	188000	50.6	3.9	45.2	0.89
	4	196500	51.0	3.6	46.9	0.92
	5	196100	51.5	3.8	47.0	0.91
	6	198000	51.1	3.7	47.0	0.92
	Avg.	**193750**	**50.9**	**3.8**	**45.9**	**0.90**
	COV	**2.0%**	**0.9%**	**2.8%**	**2.5%**	**1.8%**
requirements SIS		-	47.2	3.0		0.85

1987						
	Sample nr	Elastic modulus	Ultimate tensile force	Ultimate elongation	$F_{0,2}$	$F_{0,2}/F_m$
		[N/mm^2]	[kN]	[%]	[kN]	[-]
Forsmark 3	1	199600	50.9	3.80	45.7	0.90
	2	201100	51.1	3.90	45.6	0.89
	3	199900	50.9	3.80	45.7	0.90
	4	-	49.3	-	-	-
	5	-	49.6	-	-	-
	6	-	49.4	-	-	-
	Avg.	**200200**	**50.2**	**3.8**	**45.7**	**0.90**
	COV	**0.4%**	**1.7%**	**1.5%**	**0.1%**	**0.4%**
requirements SIS		-	47.2	3.0		0.85

1991						
	Sample nr	Elastic modulus	Ultimate tensile force	Ultimate elongation	$F_{0,2}$	$F_{0,2}/F_m$
		[N/mm^2]	[kN]	[%]	[kN]	[-]
Forsmark 3	1	185300	50.6	4.20	41.8	0.83
	2	189100	50.8	4.20	42.0	0.83
	3	186900	50.8	3.80	42.5	0.84
	4	209600	51.0	4.00	46.3	0.91
	5	204100	51.2	4.30	45.7	0.89
	6	207000	51.3	4.60	46.2	0.90
	Avg.	**197000**	**51.0**	**4.2**	**44.1**	**0.87**
	COV	**5.6%**	**0.5%**	**6.5%**	**5.0%**	**4.5%**
requirements SIS		-	47.2	3.0		0.85

1996						
	Sample nr	Elastic modulus	Ultimate tensile force	Ultimate elongation	$F_{0,2}$	$F_{0,2}/F_m$
		[N/mm^2]	[kN]	[%]	[kN]	[-]
Forsmark 3	1	195000	51.0	3.40	45.2	0.89
	2	194000	51.3	3.90	45.4	0.88
	3	195000	50.8	3.70	45.2	0.89
	4	197000	50.8	3.90	45.0	0.89
	5	195000	50.9	3.90	45.0	0.88
	6	194000	50.2	3.60	45.0	0.90
	7	189000	49.3	3.00	42.5	0.86
	8	188000	48.9	3.40	42.4	0.87
	9	190000	49.0	3.70	49.0	1.00
	10	189000	49.4	3.70	49.4	1.00
	11	189000	49.2	3.40	49.2	1.00
	12	190000	49.0	3.50	49.0	1.00
	Avg.	**192083**	**50.0**	**3.6**	**46.0**	**0.92**
	COV	**1.7%**	**1.9%**	**7.5%**	**5.5%**	**6.4%**
requirements SIS		-	47.2	3.0		0.85

2001						
	Sample nr	**Elastic modulus**	**Ultimate tensile force**	**Ultimate elongation**	**$F_{0,2}$**	**$F_{0,2}/F_m$**
		[N/mm^2]	**[kN]**	**[%]**	**[kN]**	**[-]**
Forsmark 3	1	208300	51.5	4.48	46.0	0.89
	2	204800	51.3	4.50	46.0	0.90
	3	207600	51.2	4.15	46.2	0.90
	4	179300	50.0	2.82	44.2	0.88
	5	181900	50.0	3.98	41.8	0.84
	6	183600	50.0	3.54	42.0	0.84
	Avg.	**194250**	**50.7**	**3.9**	**44.4**	**0.88**
	COV	**7.2%**	**1.5%**	**16.4%**	**4.6%**	**3.4%**
requirements SIS		-	50.1	3.5		0.85

2005						
	Sample nr	**Elastic modulus**	**Ultimate tensile force**	**Ultimate elongation**	**$F_{0,2}$**	**$F_{0,2}/F_m$**
		[N/mm^2]	**[kN]**	**[%]**	**[kN]**	**[-]**
Forsmark 3	1	198000	49.4	3.07	45.5	0.92
	2	197000	49.7	3.35	45.6	0.92
	3	208000	48.4	2.47	43.7	0.90
	4	196000	51.4	3.01	43.7	0.85
	5	släppte	-	-	-	-
	6	184000	50.4	2.76	44.9	0.89
	7	206000	50.6	3.28	45.8	0.91
	8	202000	50.8	3.26	46.1	0.91
	9	208000	50.4	3.00	46.2	0.92
	Avg.	**199875**	**50.1**	**3.0**	**45.2**	**0.90**
	COV	**4.0%**	**1.9%**	**9.7%**	**2.2%**	**2.5%**
requirements SIS		-	50.1	3.5		0.85

2010						
	Sample nr	**Elastic modulus**	**Ultimate tensile force**	**Ultimate elongation**	**$F_{0,2}$**	**$F_{0,2}/F_m$**
		[N/mm^2]	**[kN]**	**[%]**	**[kN]**	**[-]**
Forsmark 3	1	175000	48.8	3.53	39.8	0.82
	2	181000	48.3	3.48	40.5	0.84
	3	191000	48.3	3.50	40.3	0.83
	4	202000	49.0	4.04	44.2	0.90
	5	203000	49.6	3.60	44.8	0.90
	6	210000	49.9	3.49	44.8	0.90
	7	208000	50.0	3.48	44.6	0.89
	8	208000	50.4	3.84	44.7	0.89
	Avg.	**197250**	**49.3**	**3.6**	**43.0**	**0.87**
	COV	**6.8%**	**1.6%**	**5.8%**	**5.4%**	**4.1%**
requirements SIS		-	50.1	3.5		0.85

2016						
	Sample nr	**Elastic modulus**	**Ultimate tensile force**	**Ultimate elongation**	**$F_{0,2}$**	**$F_{0,2}/F_m$**
		[N/mm^2]	**[kN]**	**[%]**	**[kN]**	**[-]**
Forsmark 3	1	-	51.9	5.10	45.8	0.88
	2	-	51.9	5.20	45.8	0.88
	3	-	51.9	4.90	45.6	0.88
	4	-	51.7	5.60	42.0	0.81
	5	-	52.0	5.50	42.0	0.81
	6	-	51.7	5.40	41.5	0.80
	Avg.		**51.9**	**5.3**	**43.8**	**0.84**
	COV		**0.2%**	**5.0%**	**4.9%**	**4.8%**
requirements SIS		-	50.1	3.5		0.85

7.10 FORSMARK 3 – REVERSED BEND TEST

1986							
	Sample nr	Hydrogene treatment time	End	Mid	End	Avegage	Fodran enl
		[h]	[-]	[-]	[-]	[-]	[-]
Forsmark 3	1	0	11	11	10	10.7	5.0
	2	4	7	8	7	7.3	-
	3	24	4	4	4	4.0	-
	4	0	10	10	10	10.0	5.0
	5	4	7	8	5	6.7	-
	6	24	5	3	7	5.0	-

1987							
	Sample nr	Hydrogene treatment time	End	Mid	End	Avegage	Fodran enl
		[h]	[-]	[-]	[-]	[-]	[-]
Forsmark 3	1	0	10	10	10	10.0	5.0
	2	4	9	7	9	8.3	-
	3	24	9	9	9	9.0	-
	4	0	14	13	12	13.0	5.0
	5	4	12	8	9	9.7	-
	6	24	7	4	8	6.3	-

1991							
	Sample nr	Hydrogene treatment time	End	Mid	End	Avegage	Fodran enl
		[h]	[-]	[-]	[-]	[-]	[-]
Forsmark 3	1	0	9	9	9	9.0	5.0
	2	4	7	8	8	7.7	-
	3	24	7	4	5	5.3	-
	4	0	8	8	8	8.0	5.0
	5	4	8	7	8	7.7	-
	6	24	5	4	6	5.0	-

1996							
	Sample nr	Hydrogene treatment time	0 hours	4 hours	24 hours		
		[h]	[-]	[-]	[-]		
Forsmark 3	1		9	5	7		
	2		9	7	5		
	3		8	6	5		
	4		10	5	4		
	5		9	5	6		
	6		8	5	5		
	Avg.		8.8	5.5	5.3	5.0	
	7		13	7	5		
	8		9	6	5		
	9		8	6	4		
	10		8	5	5		
	11		10	5	4		
	12		10	7	5		
	Avg.		9.7	6.0	4.7	5.0	

2001							
	Sample nr	Hydrogene treatment time	End	Mid	End	Avegage	Fodran enl
		[h]	[-]	[-]	[-]	[-]	[-]
Forsmark 3	1	0	10	11	11	10.7	4.0
	2	4	7	7	7	7.0	-
	3	24	3	5	6	4.7	-
	4	0	10	10	11	10.3	4.0
	5	4	4	5	4	4.3	-
	6	24	2	3	4	3.0	-

2005							
	Sample nr	Hydrogene treatment time	End	Mid	End	Avegage	Fodran enl
		[h]	[-]	[-]	[-]	[-]	[-]
Forsmark 3	1	0	4	4	4	4.0	4.0
	2	4	3	3	2	2.7	-
	3	24	3	1	2	2.0	-
	4	0	4	5	5	4.7	4.0
	5	4	2	2	2	2.0	-
	6	24	1	1	2	1.3	-
	7	0	4	4	5	4.3	4.0
	8	4	3	3	3	3.0	-
	9	24	2	2	2	2.0	-

2010							
	Sample nr	Hydrogene treatment time	End	Mid	End	Avegage	Fodran enl
		[h]	[-]	[-]	[-]	[-]	[-]
Forsmark 3	1	0	11	9	11	10.3	4.0
	2	4	7	8	9	7.9	-
	3	24	4	5	7	5.3	-
	4	0	10	10	10	10.0	4.0
	5	4	6	6	6	6.0	-
	6	24	4	3	6	4.3	-

2016		
	Sample nr	0 hours
		[-]
Forsmark 3	1	10
	2	6
	3	7
	Avg.	7.3
	4	7
	5	9
	6	7
	Avg.	7.4

ANALYSIS OF LONG-TERM DURABILITY OF PRESTRESSED TENDONS IN SWEDISH NUCLEAR REACTOR CONTAINMENTS

The project analysed a unique database gathered over 40 years of destructive testing of prestressing tendons performed within interval technical evaluations in Swedish nuclear reactors containments. The statistical methods based on confidence interval were used to evaluate the meaningfulness of the observed trends in material embrittlement. A literature study concerning possible phenomena behind the material degradation was performed. In the second stage of the project experiments on mechanical performance, chemical composition and the microscopic analysis of selected wires was performed to validate the findings of statistical analysis. The new results did not confirm the trends observed in the historical data in uniaxial tensile test. The chemical and microscopic analysis did not indicate any material degradation. The fracture of new tests had typically ductile character, however the samples treated with hydrogen subjected to reversed bend test exhibited embrittlement on the surface. The project is concluded with reflection on the used testing methods and possible procedures to ensure reliability of the experimental results in the future, as well as, possible further research in the steel embrittlement.

A new step in energy research

The research company Energiforsk initiates, coordinates, and conducts energy research and analyses, as well as communicates knowledge in favor of a robust and sustainable energy system. We are a politically neutral limited company that reinvests our profit in more research. Our owners are industry organisations Swedenergy and the Swedish Gas Association, the Swedish TSO Svenska kraftnät, and the gas and energy company Nordion Energi.

Energiforsk